



NUMERICAL STUDY OF THE EFFECTS OF GEOMETRIC PARAMETERS ON  
PERFORMANCE OF SOLAR CHIMNEY POWER PLANTS

OSAMA SABBAR NSAIF NSAIF

SEPTEMBER, 2019

NUMERICAL STUDY OF THE EFFECTS OF GEOMETRIC PARAMETERS ON  
PERFORMANCE OF SOLAR CHIMNEY POWER PLANTS

A THESIS SUBMITTED TO THE GRADUATE SCHOOL OF NATURAL AND  
APPLIED SCIENCES OF CANKAYA UNIVERSITY



BY

OSAMA SABBAR NSAIF NSAIF

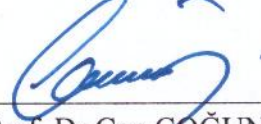
IN PARTIAL FULFILLMENT OF THE REQUIREMENTS FOR  
THE DEGREE OF MASTER OF SCIENCE IN  
MECHANICAL ENGINEERING

SEPTEMBER, 2019


Approval of the Thesis: **Numerical Study of The Effects Of Geometric Parameters  
On Performance Of Solar Chimney Power Plants**

Submitted by: Osama Sabbar NSAIF NSAIF

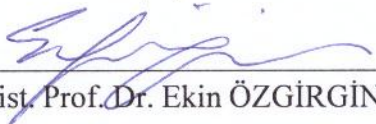
Approval of the Graduate School of Natural and Applied Sciences, Çankaya University.

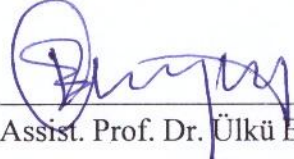
  
Prof. Dr. Can ÇOĞUN  
Director

I certify that this thesis satisfies all the requirements as a thesis for the degree of Master of Science.

  
Prof. Dr. Haşmet TÜRKOĞLU  
Head of Department

This is to certify that we have read this thesis and that in our opinion it is fully adequate, in scope and quality, as a thesis for the degree of Master of Science.

  
Assist. Prof. Dr. Ekin ÖZGİRĞİN YAPICI  
Supervisor

  
Assist. Prof. Dr. Ülkü Ece AYLI İNCE  
Co-Supervisor

**Examination Date: 09 / 09 / 2019**

**Examining Committee Members:**


Prof. Dr. Haşmet TÜRKOĞLU Çankaya Univ.

Prof. Dr. Selin ARADAĞ ÇELEBİOĞLU TOBB Univ.

Assist. Prof. Dr. Nureddin DİNLER Gazi Univ.


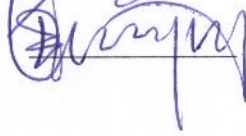
Assist. Prof. Dr. Ekin ÖZGİRĞİN YAPICI Çankaya Univ.

Assist. Prof. Dr. Ülkü Ece AYLI İNCE Çankaya Univ.







## STATEMENT OF NON-PLAGIARISM PAGE

I hereby declare that all information in this document has been obtained and presented in accordance with academic rules and ethical conduct. I also declare that, as required by these rules and conduct, I have fully cited and referenced all material and results that are not original to this work.

Name, Last name: Osama Sabbar NSAIF NSAIF

Signature : 

Date : 09 / 09 / 2019

## **ABSTRACT**

### **NUMERICAL STUDY OF THE EFFECTS OF GEOMETRIC PARAMETERS ON PERFORMANCE OF SOLAR CHIMNEY POWER PLANTS**

Osama Sabbar NSAIF NSAIF

M.Sc., Department of Mechanical Engineering

Supervisor: Assist. Prof. Dr. Ekin Özgirgin Yapıcı

Co-Supervisor: Assist. Prof. Dr. Ülkü Ece Ayli İnce

SEPTEMBER 2019, 84 Pages

The aim of the study is to get the best and the most efficient design of Solar Chimney Power Plant (SCPP) considering different chimney and collector parameters. SCPP is one of the most promising applications of solar energy because of the high reliability of the system in addition to the low cost of long-term energy production and low maintenance needs. Because of the reasons above, it has been a focus for researchers to increase efficiency of such systems. Solar chimney power plant is a thermal system containing three basic components; the solar collector, the solar chimney and the wind turbine.

SCPP has basic working principles which are the effect of greenhouse, chimney drag and conversion to kinetic energy. The air below the semi-transparent collector (glass) is heated up by the solar radiation which is coming from the top of the collector surface.

The heated air moves by buoyancy force to the center of the collector where the turbine is located. The heated air leads to a flow through the turbine and drives the turbine which rotates a generator and electric energy is obtained from that rotation. In this study, a 2-D computational fluid dynamics (CFD) analysis for the entire system of solar chimney power plant is done by using commercial program ANSYS 18.2.

After verifying the CFD results of the numerical model with the results of the experimental work and obtaining almost identical results, the main parameters like the height of tower, the diameter of the tower, the tower configuration, the diameter of the collector, the height of collector and the inclination angle of the collector which can effect on performance of SCPP has been changed and the influence of varying these parameters on the effectiveness and performance of the solar chimney system is studied. It is found through this study that all of the chimney and the collector parameters which are mentioned above have a direct impact on the effectiveness and performance of SCPP. Depending on the numerical results, it is found that the height and the diameter of the tower is considered as the most effective parameters which can affect largely on the value of the output power of SCPP and the height and diameter of chimney equal to 3.5 m and 25 cm are the best values considering the performance of the chimney. Also results shows that the diverging chimney configuration is the best tower geometry that can be utilized and it can improve and increase the performance of SCPP largely. The numerical findings shows that the increase of solar collector diameter leads to increasing the output power and the best value for the diameter of the collector is 400 cm (the maximum value). Furthermore, it is concluded that the height and inclination angle of the solar collector has an important effect on the output power and the best design for solar collector parameters is 6 cm height of the solar collector with 0 degree for the inclination angle of the solar collector.

**Keywords:** Solar Energy, computational fluid dynamics, CFD, Solar Chimney Power Plant, Numerical Simulation, SCPP.

## ÖZ

### GEOMETRİK PARAMETRELERİN GÜNEŞ BACASI GÜÇ SANTRALİNİN PERFORMANSINA ETKİSİNİN NUMERİK OLARAK İNCELENMESİ

Osama Sabbar NSAIF NSAIF

Yüksek Lisans, Makine Mühendisliği Anabilim Dalı

Tez Yöneticisi: Dr. Öğr. Üyesi. Ekin Özgirgin Yapıcı

Eş-Yönetici: Dr. Öğr. Üyesi Ülkü Ece Aylı İnce

EYLÜL 2019, 84 Sayfa

Bu çalışmanın öncelikli amacı, farklı baca ve kolektör parametreleri kullanarak güneş bacası güç santrali için en uygun ve en iyi tasarımı elde edebilmektir. Güneş bacası güç santrali güneş enerji uygulamaları arasında oldukça gelecek vadeden bir uygulamadır. Bunun sebebi, sistemin güvenilir, ucuz, uzun dönemli enerji üretebilen ve düşük onarım maliyetli olmasıdır. Bu sebeplerden ötürü, araştırmacılar güneş bacası sistemlerinin verimini artıracak çalışmalar yapmaktadırlar. Güneş bacası santralleri güneş kolektörü, baca ve rüzgar tribününden oluşmaktadır.

Güneş bacası santrallerinin çalışma prensibi oldukça basittir. Çoğunlukla camdan yapılmış kolektörün altında bulunan hava, güneşten gelen radyasyonla ısınan soğurucu tarafından ısıtılır ve yoğunluğu azalan hava kaldırma kuvveti etkisi ile yukarı bacaya doğru ilerler. Baca boyunca ilerlerken tam merkezde bulunan türbini çevirir ve

jeneratöre baęlı olan bu tribün sayesinde elektrik üretilir. Bu alıřmada güneř bacası santralinin hesaplamalı akıřkanlar dinamięi (HAD) analizleri, ANSYS 18.2 ticari yazılımını kullanarak yapılmıřtır.

Hazırlanan nümerik modelin deneysel sonuçlarla doęrulanmasından sonra, baca yükseklięi ve apı, kolektör yükseklięi, apı ve eęim aısı ve farklı baca geometrileri gibi parametreler deęiřtirilerek, bu parametrelerin güneř bacası santralinin performansı üzerinde yaptıęı etkiler arařtırılmıřtır.

Yukarıdaki paragrafta bahsi geen tüm parametrelerin güneř bacası santralinin güç ve verimi üzerinde doęrudan etkileri olduęu doęrulanmıřtır. Nümerik sonuçlar incelendięinde görölmektedir ki, en büyük etkiyi yapan parametreler bacanın boyu ve apıdır ve yapılan simölasyonlarda en iyi performans 3.5 m baca boyu ve 25 cm baca apında elde edilmiřtir. Ayrıca sonuçlar en verimli baca geometrisinin ıraksayan baca olduęu ve bunun bacanın gücünü oldukça fazla oranda artırdıęını göstermektedir. Nümerik bulgularla doęrulanmaktadır ki, solar kolektör apının artması elde edilen gücü artırmaktadır ve yapılan simölasyonlarda en iyi performans 400 cm olan en büyük apta elde edilmiřtir. Kolektör parametreleri göz önünde bulundurulduęunda en iyi konfigürasyon 6 cm kolektör yükseklięi ve 0 derece kolektör eęim aısı ile elde edilmiřtir.

**Anahtar Kelimeler:** Güneř Enerjisi, Hesaplamalı Akıřkanlar Dinamięi (HAD), Güneř Bacası Güç Santralı, Nümerik simölasyon.



## DEDICATION

Dedication to those who revolted against the tyrants, to those who said no to the oppressor,

To those who lost their lives for freedom, to every revolutionary around the world.



## ACKNOWLEDGEMENTS

First of all, I want to say thanks Allah for giving me strength and patience.

In fact, this thesis would not have been completed without the efforts of my supervisor Dr. Ekin ÖZGIRGIN YAPACI. I would like to express my great thanks and my most sincere gratitude to her guidance, support, encouragement and for helping me throughout the writing of my thesis.

I would like to express my special thanks to my Co-Supervisor: Dr. Instructor Ülkü Ece AYLI İNCE for advice and assistance throughout this thesis.

I would like to express my special appreciation and gratefulness to my father, my mother and my family for their immense support and encouragement to me during my study.

I would like to thank to all my friends especially (Maisarah, Eyad, Mahmood, Othman, Ahmed, Mahmood and Saad).

Special thanks to my friend Büşra Gülmemiş for encouraging and supporting me all the time.

## TABLE OF CONTENT

<b>ABSTRACT</b> .....	iv
<b>ÖZ</b> .....	vi
<b>LIST OF TABELS</b> .....	xii
<b>LIST OF FIGURES</b> .....	xiii
<b>LIST OF SYMBOLS</b> .....	xvi
<b>1- INTRODUCTION</b> .....	1
1.1 Motivation and Aim of the Thesis Study.....	1
1.2 Fundamentals.....	2
1.2.1. Renewable energy.....	2
1.2.2. Solar Energy.....	3
1.3 The Solar Chimney Power Plants (SCPP) .....	4
1.3.1 Historical review of solar chimney power plants.....	4
1.3.2 Working Principle of SCPP.....	7
1.3.3 Components of SCPP.....	8
1.3.3.1 The Chimney.....	8
1.3.3.2 The Collector.....	8
1.3.3.3 The Turbine.....	9
1.3.4 World Wide Solar Chimney Power Plants.....	10
1.4 Literature Review.....	12
<b>2- MATHEMATICAL MODELLING OF SCPP</b> .....	16
2.1 Introduction.....	16
2.2 Solar Chimney Performance Equations.....	16
2.3 Navier-Stokes Equations.....	19
2.4 Turbulence Model.....	20
2.4.1 Standard k- $\epsilon$ Turbulence Model.....	21
2.4.2 k- $\omega$ Turbulence Model.....	22
2.4.3 SST k- $\omega$ Turbulence Model.....	23

<b>3- NUMERICAL ANALYSIS OF SCPP .....</b>	<b>25</b>
3.1 CFD Model.....	25
3.1.1 Geometry of SCPP.....	25
3.1.2 Mesh generation.....	26
3.1.3 Simulation of SCPP.....	27
3.1.4 The Boundary conditions for SCPP.....	27
3.2 Mesh Independency study.....	28
3.3 The Turbulence Model Study.....	30
3.4 Validation of Numerical Results .....	31
3.5 Performance Study for SCPP.....	33
3.5.1. SCPP Chimney Parameters.....	33
3.5.1.1 Effect of Chimney Height.....	33
3.5.1.2 Effect of Chimney Diameter.....	34
3.5.2 Different Tower Geometries.....	34
3.5.3. Collector Parameters.....	36
3.5.3.1 Collector Diameter & Height.....	36
3.5.3.2 Inclination Angle of Collector.....	37
<b>4- RESULTS AND DISCUSSION.....</b>	<b>39</b>
4.1 Introduction.....	39
4.2 Effects of Solar Chimney Height on SCPP Performance.....	39
4.3 Effects of Solar Chimney Diameter on SCPP Performance.....	45
4.4 Effects of Solar Chimney Geometry on SCPP Performance.....	51
4.5 Effects of Collector Diameter on SCPP Performance.....	57
4.6 Effects of Collector Height on SCPP Performance.....	63
4.7 Effects of Inclination angle of collector on SCPP Performance.....	69
<b>5- CONCLUSIONS AND FUTURE WORK .....</b>	<b>76</b>
5.1 Conclusions .....	76
5.2 Recommendations for Future works.....	78
<b>LIST OF REFERENCES.....</b>	<b>80</b>

## LIST OF TABLES

<b>Table 1.1:</b> World Wide Solar Chimney Power Plants .....	11
<b>Table 3.1:</b> The boundary conditions which are considered for the under study SCPP.....	28
<b>Table 3.2:</b> Different chimney heights for cases 1-4 of Study 1.....	33
<b>Table 3.3:</b> Different chimney diameters for the cases 5-8 of Study 2.....	34
<b>Table 3.4:</b> Different geometries for the cases a-b-c-d of Study 3 .....	36
<b>Table 3.5:</b> Different collector diameters for the cases 9-13 of Study 4.....	37
<b>Table 3.6:</b> Different collector heights for the cases 14-17 of Study 5.....	37
<b>Table 3.7:</b> Different angle of collector for the cases 18-21 of Study 6.....	38

## LIST OF FIGURES

<b>Figure 1.1:</b> (a) Leonardo da Vinci's a smoke jack with its chimney. (b) Solar machine scheme presented by Architect Isidoro Cabanayes.....	4
<b>Figure 1.2:</b> (a) Prof Dubos's proposed solar power plant in the southern Sahara. (b) Principle of Professor Dubos's solar chimney. ....	5
<b>Figure 1.3:</b> The solar tower proposed by Prof Nazare.....	6
<b>Figure 1.4:</b> The prototype of Manzanares Power plant.....	6
<b>Figure 1.5:</b> A schematic of the solar chimney power plant.....	7
<b>Figure 1.6:</b> The tower structure of SCPP.....	8
<b>Figure 1.7:</b> The collector structure of the Manzanares SCPP.....	9
<b>Figure 1.8:</b> (a) A Single Turbine Solar Chimney Power Plant. (b) Multiple Turbines Solar Chimney Power Plant.....	10
<b>Figure 3.1:</b> SCPP model design .....	25
<b>Figure 3.2:</b> The meshing structure and the implementing result of the designed SCPP.....	26
<b>Figure 3.3:</b> The boundary conditions which are considered for the studied SCPP... ..	28
<b>Figure 3.4:</b> Illustration of the dimensions of the designed SCPP.....	29
<b>Figure 3.5:</b> The results of mesh independency study based on the studied system....	30
<b>Figure 3.6:</b> The result of turbulence model study based on the designed SCPP.....	31
<b>Figure 3.7:</b> The comparison of the experimental and numerical outcomes based on the designed SCPP temperature.....	32
<b>Figure 3.8:</b> The comparison of the experimental and numerical outcomes based on the designed SCPP velocity.....	32
<b>Figure 3.9:</b> Some of the different geometries of the chimney configurations.....	35
<b>Figure 3.10:</b> Schematic diagram of inclination angle of collector.....	38
<b>Figure 4.1:</b> The simulation results for the air temperature distribution among various tower heights for cases 1- 4 of study 1.....	40

<b>Figure 4.2:</b> The influence of SCPP's tower height on temperature profile for cases 1-4 of study 1.....	41
<b>Figure 4.3:</b> The simulation results for the flow velocity distribution among various tower heights for cases 1- 4 of Study 1.....	42
<b>Figure 4.4:</b> The influence of SCPP's tower height on the air velocity profile for cases 1- 4 of Study 1.....	43
<b>Figure 4.5:</b> The simulation results for the static pressure distribution among various tower heights for cases 1- 4 of Study 1.....	44
<b>Figure 4.6:</b> variation of power with respect to SCPP's tower height.....	45
<b>Figure 4.7:</b> The simulation results for the air temperature distribution among various tower diameters for cases 5 - 8 of Study 2.....	46
<b>Figure 4.8:</b> The effect of SCPP's tower diameter on its temperature profile for cases 5-8 of Study 2.....	47
<b>Figure 4.9:</b> The simulation results for the flow velocity distribution among various tower diameters for cases 5-8 of Study 2.....	48
<b>Figure 4.10:</b> The effect of SCPP's tower diameter on its velocity profile for cases 5-8 of Study 2.....	49
<b>Figure 4.11:</b> The simulation results for static pressure distribution among various tower diameters for cases 5-8 of Study 2.....	50
<b>Figure 4.12:</b> variation of power with respect to SCPP's tower diameter .....	51
<b>Figure 4.13:</b> The simulation results based on the different configuration of the studied SCPP chimney on the flow temperature for cases a-b-c-d of Study 3.....	52
<b>Figure 4.14:</b> The influence of different SCPP's tower configurations on its temperature profile for cases a-b-c-d of Study 3.....	53
<b>Figure 4.15:</b> The simulation results based on the different configuration of the studied SCPP chimney on the flow velocity for cases a-b-c-d of Study 3.....	54
<b>Figure 4.16:</b> The influence of different chimney configurations on its velocity profile for cases a-b-c-d of Study 3.....	55
<b>Figure 4.17:</b> The simulation results based on the different configuration of the studied SCPP chimney on the static pressure for cases a-b-c-d of Study 3.....	56
<b>Figure 4.18:</b> variation of power with respect to SCPP's chimney configurations.....	57
<b>Figure 4.19:</b> The simulation results for the air temperature distribution among various diameters of the SCPP collector for cases 9-13 of Study 4.....	58

<b>Figure 4.20:</b> The influence of SCPP’s collector diameter on its temperature profile for cases 9-13 of Study 4.....	59
<b>Figure 4.21:</b> The simulation results for the flow velocity distribution among various collector diameters of the SCPP for cases 9-13 of Study 4.....	60
<b>Figure 4.22:</b> The influence of SCPP’s collector diameter on its velocity profile for cases 9-13 of Study 4.....	61
<b>Figure 4.23:</b> The simulation results for the static pressure distribution among various collector diameters of the SCPP for cases 9-13 of Study 4.....	62
<b>Figure 4.24:</b> variation of power with respect to SCPP’s collector diameter.....	63
<b>Figure 4.25:</b> The simulation results for the air temperature distribution among various collector heights of the SCPP for cases 14-17 of Study 5. ....	64
<b>Figure 4.26:</b> The influence of SCPP’s collector height on its temperature profile for cases 14-17 of Study 5.....	65
<b>Figure 4.27:</b> The simulation results for air velocity distribution among various collector heights of the SCPP for cases 14-17 of Study 5.....	66
<b>Figure 4.28:</b> The influence of SCPP’s collector height on the air velocity profile for cases 14-17 of Study 5.....	67
<b>Figure 4.29:</b> The simulation results for the static pressure distribution among various collector height for cases 14-17 of Study 5.....	68
<b>Figure 4.30:</b> variation of power with respect to SCPP’s collector height .....	69
<b>Figure 4.31:</b> The simulation results for the air temperature distribution among various collector inclination angles of the SCPP for cases 18-21 of Study 6.....	70
<b>Figure 4.32:</b> The influence of SCPP’s collector inclination angle on its temperature profile for cases 18-21 of Study 6.....	71
<b>Figure 4.33:</b> The simulation results for the flow velocity distribution among various collector inclination angles of the SCPP’s or cases 18-21 of Study 6.....	72
<b>Figure 4.34:</b> The influence of SCPP’s collector inclination angle on its velocity profile for cases 18-21 of Study 6.....	73
<b>Figure 4.35:</b> The simulation results for the static pressure distribution among various collector inclination angles of SCPP’s for cases 18-21 of Study 6.....	74
<b>Figure 4.36:</b> variation of power with respect to inclination angle of the SCPP collector.....	75



## LIST OF SYMBOLS

$\Delta p$	Pressure difference between chimney base and the surrounding (Pa)
$\Delta p_t$	Pressure difference at turbine (Pa)
$\Delta p_f$	Friction loss in the chimney (pa)
$\Delta p_{in}$	Entrance loss (pa)
$\Delta p_{out}$	Exit kinetic energy loss (pa)
$\Delta T$	The temperature difference (K)
$A_{ch}$	Cross-sectional area of chimney ( $m^2$ ) coefficient ( $w/m^2.k$ )
$A_{coll}$	Collector surface area ( $m^2$ )
$c_p$	Specific heat capacity of air (kJ/kg. k)
$D_{ch}$	Chimney diameter (m)
$D_c$	Diameter of collector (m)
$f$	The wall friction factor
$G$	Solar radiation ( $W /m^2$ )
$g$	Gravitational acceleration ( $m/s^2$ )
$H_{ch}$	Height of chimney (m)
$H_c$	Height of collector (m)
$H_{Max}$	Maximum chimney height (m)
$H$	Chimney height (m)
$\dot{m}$	Mass flow rate of air (kg/s)
$P_i$	Pressure inlet
$P_o$	Pressure outlet
$P_{out}$	Power generated by the turbine (W)
$P_{Max}$	Maximum power (W)
$q$	Heat transferred to air stream ( $W/m^2$ )
$R_{coll}$	Collector radius (m)
$T_o$	Ambient temperature (K)

$U$	Overall heat transfer
$V$	Velocity (m/s)
$V_{ch}$	velocity inside the chimney (m/s)
$V_{turb.i}$	velocity at turbine inlet (m/s)
$V_{ch,o}$	velocity at chimney exit (m/s)
$v_{ch}$	The air velocity at chimney inlet (m/s)
$V_{ch,max}$	The maximum velocity inside the chimney
$\dot{Q}$	Heat gain in the collector (W)
$H_{ch}$	Height of chimney
$H_c$	Height of collector
$D_c$	Diameter of collector
$D_{ch}$	Diameter of chimney

### Greek Letters

$\beta$	Expansion rate
$\eta$	Total efficiency
$\eta_{tg}$	Efficiency of turbine generator
$\eta_{coll}$	Solar collector efficiency
$\eta_{Max}$	Maximum efficiency
$\gamma_{\infty}$	Lapse rate of temperature (K/m)
$\epsilon_{out}$	Exit pressure loss coefficient
$\epsilon_{in}$	Entrance pressure loss coefficient
$\rho$	Density (kg/m <sup>3</sup> )
$\rho_o$	Ambient density (kg/m <sup>3</sup> )
$\rho_{ch}$	The density of air at chimney inlet (kg/m <sup>3</sup> )
$\rho_{out}$	Density of air at outlet of the chimney (kg/m <sup>3</sup> )

## Subscripts

ch	chimney
c	collector
o	ambient
ch,o	outlet of the chimney
ch,i	inlet of the chimney
turb,i	turbine inlet



# CHAPTER 1

## INTRODUCTION

### 1.1 Motivation and Aim of the Thesis Study

In recent decades, demand for renewable energy has increased due to rising fuel prices, climate change and governments' willingness to rely heavily on renewable energies. Hence, the desire is towards making most of the renewable energy sources more widely used and improve their efficiency so that they can be relied to meet the market demand for energy. One of the renewable energy sources is the solar energy, due to low cost and low harmful emissions. Hence it considered as one of the most promising alternatives to fossil fuels. For the last few years, the cost of solar energy has decreased.

The main goal of the thesis is to study influence of several parameters of chimney like; height of chimney, diameter of chimney and different chimney configurations and also collector parameters such as diameter of collector, height of collector and the inclination angle of collector. The study also covers the impact of SCPP parameters on performance of SCPP and with the light of above, to determine a best design of SCPP. The investigations include:

- Developing a numerical method using a commercial CFD software for analyzing the solar chimney power plant.
- Verify the numerical method and comparing results obtained from the numerical model with an experimental work from the literature [1].
- Changing solar chimney parameters like chimney height, chimney diameter, chimney geometry, collector height, the inclination angle of collector and collector diameter and simulate all cases with different parameters.

- Examining the effects of these parameters and studying the behavior of the main air characteristics in the system
- Estimating the values of power for all cases depending on data from 3D numerical model.

## **1.2 Fundamentals**

### **1.2.1. Renewable energy**

Use of fossil fuels causes to emissions of some harmful gases including carbon dioxide ( $\text{CO}_2$ ),  $\text{NO}_x$ , etc.... Fuel combustion is a chemical process for reaction of particular poly carbon with air and producing thermal energy in addition to some other gasses considered as “emissions”. Many sources lead to increased carbon dioxide emissions, but the most damaging is fossil fuel burning. This increase in emissions naturally leads to significant damage to the environment and it represents the main cause of climate change. It is known that climate change affects people's lives, environmental life, agriculture, causing high temperatures in parts of the world, heavy rainfall in certain areas, drought in other areas, and leads to melting the ice which in fact causes rise in water levels in some areas [2]. Because of the significant damage previously listed, the need to rely massively on renewable energy consequently appears.

Renewable energy is sustainable and non-depletable energy which is obtained from sources like; water, sun, wind, tidal movement and geothermal. Renewable energy is characterized by its presence in a wide and permanent manner and it is clean and environmentally friendly and helps to alleviate the harm of gaseous or thermal emissions, avoid dangerous acid rain and do not impact negatively on the environment. In contrast to non-renewable sources, renewable energy does not contribute to climate change. Besides its many ecological and economic advantages, climate change has called on governments to adopt a renewable energy support strategy to reduce dependence on traditional energy sources as well as their desire to reduce carbon dioxide emissions and reduce global warming. Currently, the most sustainable energy is produced by hydroelectric power plants, and renewable energies that rely on wind and solar are extensively utilized in many countries around the world.

### **1.2.2. The Solar Energy**

The largest source of energy such as heat and light on the earth is the sun. The heat generated by the sun can be directly used in some thermal applications such as heating, cooling or drying etc. By the use of photovoltaics, solar energy could be transformed into electrical power by solar cell panels. Solar energy is considered as the greatest significant sources of sustainable energies, it is the most clean and environmental friendly energy type with no harmful environmental impact when used. Solar applications are many and wide, some of which use solar energy directly and some indirectly benefit from solar power. Basically there are primarily two kinds of the solar power systems. These are active and passive systems, which can transform solar radiation into electrical energy, or thermal power, but they are different in the way of energy conversion.

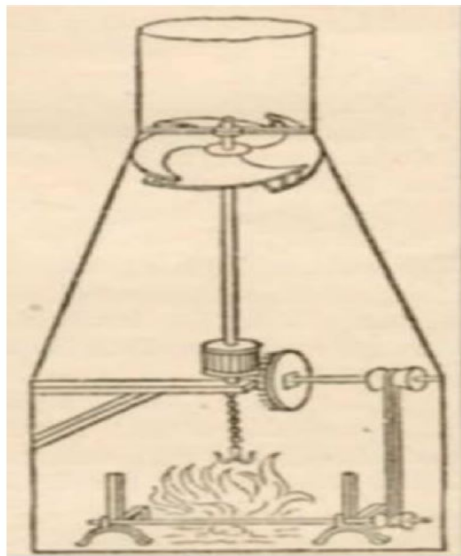
The systems of active solar power use heat transfer fluids (HTF) to take the thermal energy and absorb it. A solar collector which is a part of an active energy system can be placed on top of buildings to warm up the HTF. Then heated HTF moves in a system of tubes to warm the buildings. Active solar energy systems use additional devices such as a water pump and because of these devices active solar energy system requires extra power, besides the solar radiation to increase the systems performance. A photovoltaic solar panel (PV) array that is installed with a tracking system which the tracking system of PV panels move with the sun's movement in the sky during the day is also considered as an example of active solar system.

Passive solar systems refer to use the solar energy without depending on external devices such as pumps, fans, or electrical controls to run the system. The Passive power systems could be utilized for air conditioning applications and producing electricity in indirect way. The principle work of passive solar energy systems is absorbing solar energy by a collector facing sun and that the energy is stored in absorber like a masonry wall, floor, or water container. After that the energy stored in absorber is used to heat or cool the building or for other things like industrial processes. There are a lot of examples of passive solar systems and one of these applications is the solar chimney power plant.

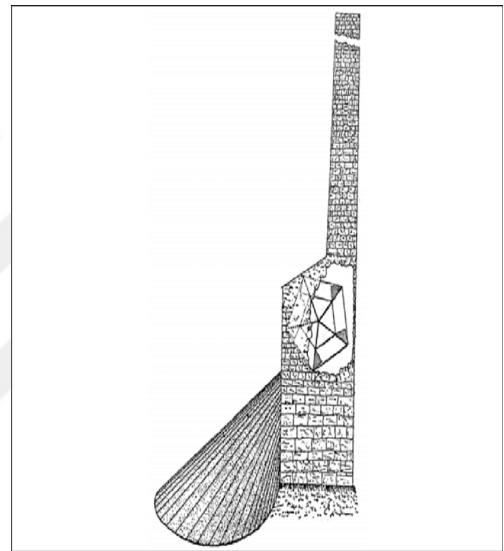
### 1.3 The Solar Chimney Power Plants (SCPP)

#### 1.3.1 Historical review of solar chimney power plants

The Italian brilliant engineer Leonardo da Vinci (April 1452-May 1519) made the first sketches of SCPP called a smoke jack as displayed in Fig 1.1 a. Leonardo da Vinci's windmills principle work is getting benefit from movement of hot air rising in a chimney to turning the windmill by making the roasting spit rotate which is already linked to windmill [2].



(a)

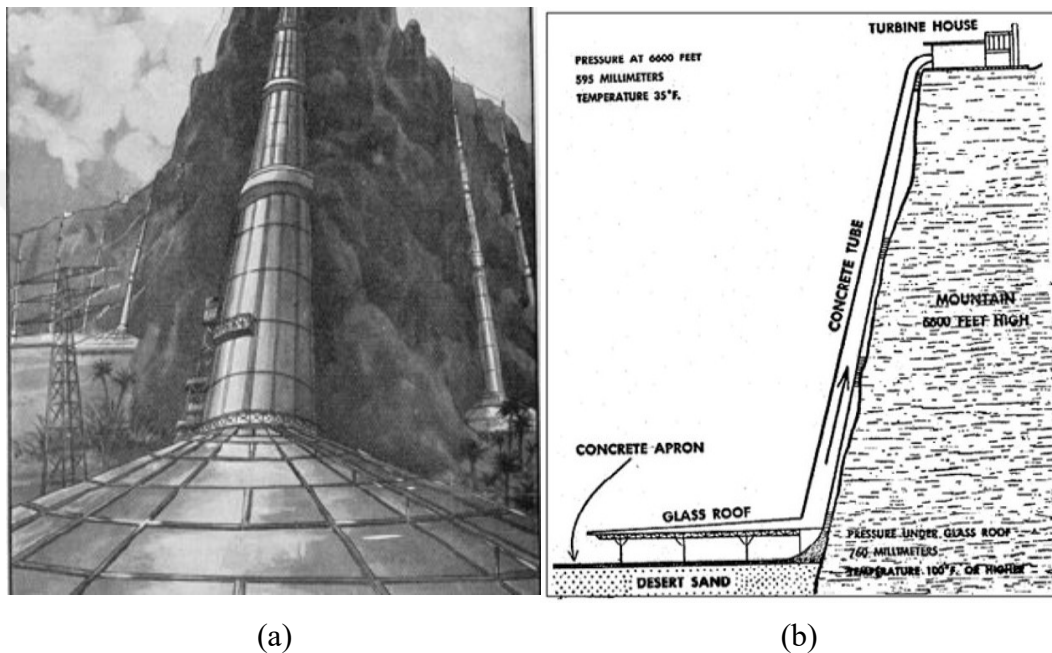


(b)

**Figure 1.1:** (a) Leonardo da Vinci's a smoke jack with its chimney [3]. (b) Solar machine scheme presented by Architect Isidoro Cabanayes [3].

In 1903, Spanish architect Isidoro Cabanyes presented the first solar chimney power plant for producing electricity. His proposition (solar engine project) described how to produce electrical power from the solar tower that contains a heater linked to a tower in the building and the fan rotated by hot air and this lead the wind propeller to produce electricity as shown Fig 1.1 b [4].

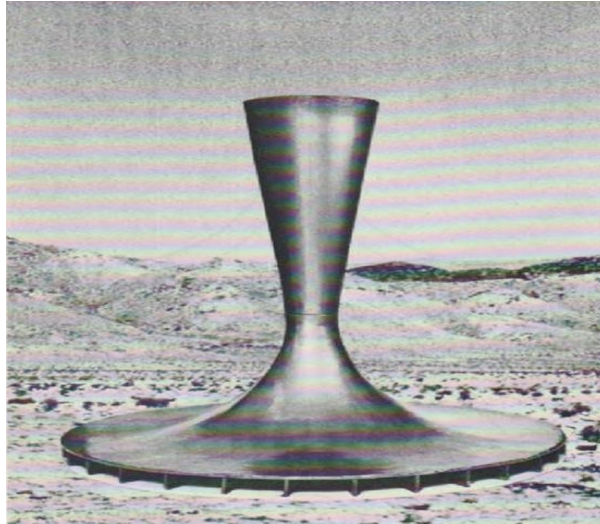
In the year of 1926, engineer Bernard Dubos presented to the French Academy of Sciences a SCPP's structure in the North of Africa with a solar tower placed on the inclines of the high height mountain as presented in Figure 1.2 a. [5]. Dubos stated that the maximum velocity of air could be increased up to 50 m/s in the tower and that tremendous quantity of power can be obtained by using wind turbines as shown in Figure 1.2 b. The Academy of Sciences advised to follow up the Dubos's idea, particularly in the region in the North of Africa which has not enough fuel and power as Engineer Bernard already discovered [6].



**Figure 1.2:** (a) Prof Dubos's proposed solar power plant in the southern Sahara [3].  
 (b) Principle of Professor Dubos's solar chimney [3].

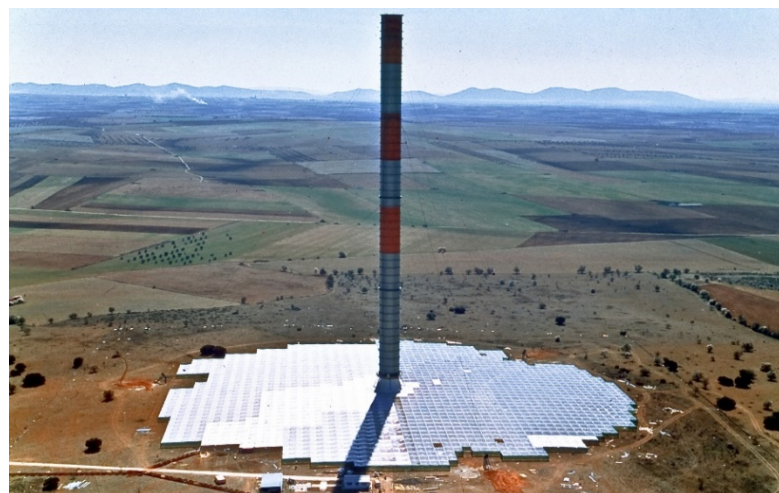
After several years, the solar chimney has developed significantly which the French scientist Nazare got a French patent for his SCPP design in 1964. The design presented a long chimney with a height of 300 m with configuration almost like a diffuser as displayed in Fig 1.3 [7]. After Nazare went to Algeria, he noted small sand tornadoes called dust devils in the southern Saharan desert. He designed an apparatus called an "aerothermal power station. It can pull warm air from the desert into the tower and accelerate it through a 300 m tall tower and produce some energy through turbines.





**Figure 1.3:** the solar tower proposed by Prof Nazare [3].

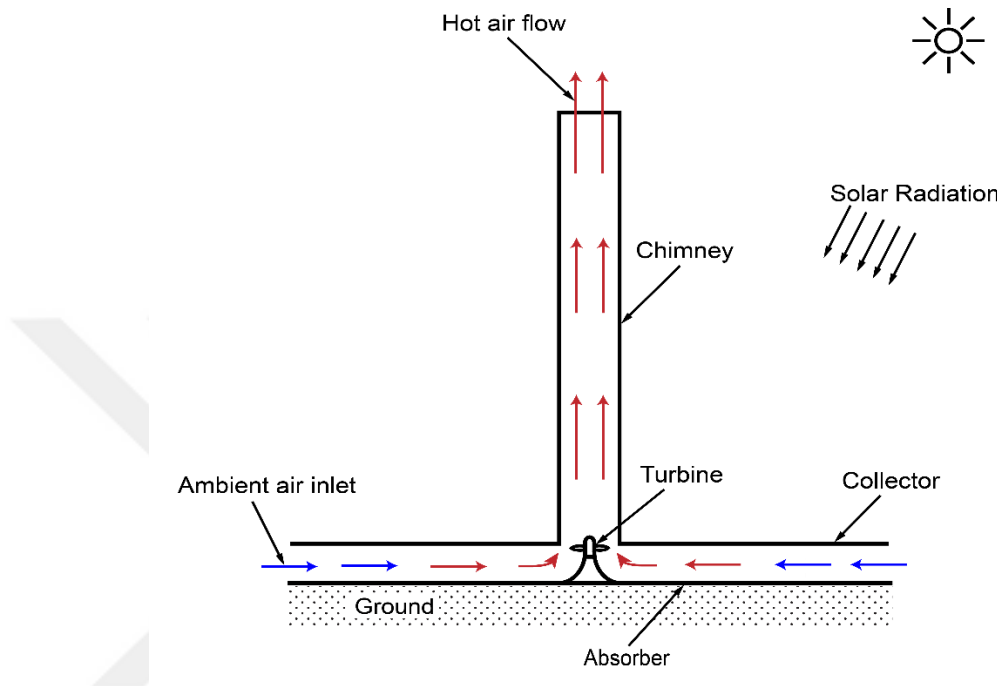
In 1982, The Ministry of Research and Technology in Germany supported the structure of the first prototype of SCPP. Prof. Dr. Ing. Jorg Schlaigh and his partners designed and built the construction of SCPP in Manzanares, which is located 150 km south of Madrid. Manzanares prototype was designed with 46000 m<sup>2</sup> collector area made of glass, height of tower about 195 m and diameter of the tower about 10 m as presented in Figure 1.4. In the middle of the tower at the base, there was a turbine installed and the maximum power output of Manzanares power plant was 50 kW [4].



**Figure1.4:** the prototype of Manzanares Power plant [8].

### 1.3.2 Working Principle of SSCP

Solar chimney power plant takes advantage of solar radiation and generates electrical energy with the help of a turbine, based on the effect of greenhouse and tower drag flow.



**Figure 1.5:** A schematic of the solar chimney power plant

Total solar radiation (both direct and diffuse) passes through the roof of the collector and are absorbed and transmitted. The transmitted radiation hits the absorber under the roof of collector and some of it is absorbed by ground and other part is re-released to the air. Through the effects of natural convection, the heated absorber surface heats the air, and air temperature inside the greenhouse rises. The high-temperature and lower density air raises to the tower due to the buoyancy effect. Because of the temperature difference between the ambient air entering to the chimney and air at the chimney exit, a pressure difference is created. As shown in Figure 1.5 a wind turbine is located at the base of the chimney and by the kinetic energy of the moving air, turbine blades rotate and produce power.

### 1.3.3 Components of SCPP

#### 1.3.3.1 The Chimney

The chimney (tower) is considered as the main element of SCPP and it is placed at the center region of SCPP and it is considered also as an engine produce the thermal power for SCPP. The temperature change between cold air at the up and hot air on the bottom generates a buoyancy driven flow in the chimney and creates a pressure difference. There are many factors that contribute in design of the tower such as decreased friction losses and increased pressure difference in the tower. The pressure difference is directly proportional to the height of the chimney. Therefore, increasing the chimney height is an important factor for improving the efficiency of the chimney and the total efficiency of the system. Many materials are suggested in the construction of a tower like steel sheet tubes supported by cables as displayed in Fig 1.6 and a reinforced concrete[9, 10].



**Figure 1.6:** The tower structure of SCPP [11].

#### 1.3.3.2 The Collector

The solar air collector (greenhouse) is considered as the heat exchanger of SCPP where the total radiation is absorbed by the floor and re-released to the air below the roof of collector and transformed it into thermal energy in forms of hot air. By help of the greenhouse effect, thermal energy is then transformed to kinetic energy. The solar collector is constructed from transparent material like plastic or glass has elevated

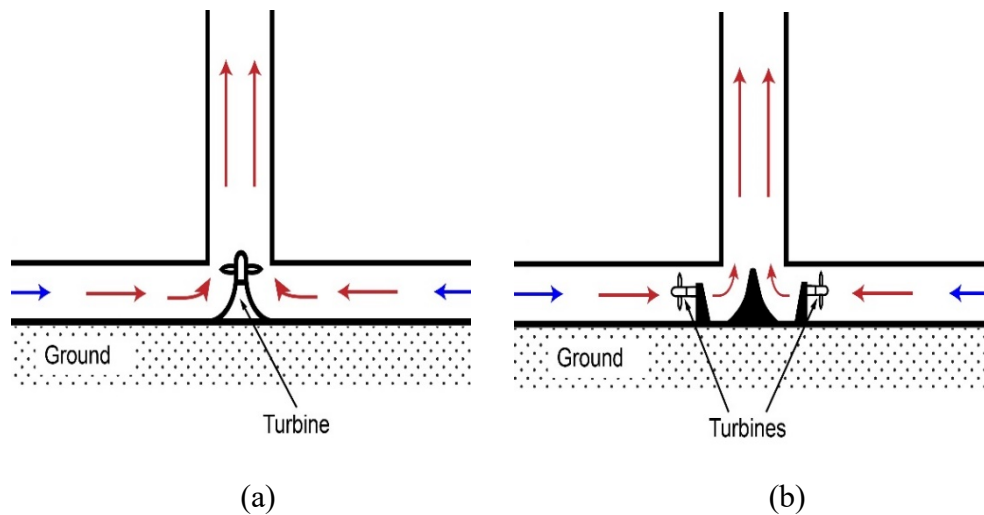
transparency to normal solar irradiation also has minimum transparency to the infrared irradiation released from the absorber; therefore, choosing a good material for collector with good thermal and optical properties is important to reduce energy losses and increase the efficiency of SCPP. Also, collector roof should be placed over the absorber by using some types of support structure. The aim of placing the collector roof above the ground is to allow air intake around the perimeter from the ambient. Fig 1.7 shows the solar collector structural design of Manzanares power plant. The ground acts like a heat storage where the ground keeps some of the solar irradiation and re-emits it over the night or in cloudy days. Therefore, to enhance the solar chimney power plant performance during the night and during the cloudy days, it is essential to select an absorber material with good properties and a good insulator ground [12].



**Figure 1.7:** The collector structure of the Manzanares SCPP [8].

### **1.3.3.3 The Turbine**

The most important part in solar chimney power plant is the turbine which generates power for the plant. As hydroelectric plants the turbine operates as pressure-staged generators and it transforms the kinetic energy of the heated air into mechanical power and that leads to produce electricity.



**Figure 1.8:** (a) A Single Turbine Solar Chimney Power Plant. (b) Multiple Turbines Solar Chimney Power Plant.

Turbine is located at the bottom center of the tower, for purpose of maintenance and to make the generating equipment linked easily. Some of SCPPs use a vertical axes single turbine placed inside the tower at center of base and the other plants use multiple horizontal turbines as presented in Fig 1.8. Turbines used in SCPP are basically wind turbines and they are relatively subjected to steady flow when compared to other wind power plants.

#### 1.3.4 World Wide Solar Chimney Power Plants

In last two decades, researchers and companies have become increasingly interested in the solar chimney because of its many advantages. As a result, many numerical and experimental studies for SCPPs are done all over the world. All these studies and prototype sought to estimate the efficiency of the SCPPs in different environmental conditions and variable dimensions in a try to reach the highest performance and efficiency for SCPP. Most of the simulation studies were based on analyzing the results and comparing them with the model found in Manzanares prototype. These studies provide a complete picture of SCPPs and clearly show the factors affecting on SCPP performance. These studies provide the groundwork for researchers to work on developing an optimal design of SCPP and building a highly efficient commercial solar

chimney power plants. Examples of these studies for different locations and the detail of the structural dimensions and power values are presented in Table 1.1.

**Table 1.1:** World Wide Solar Chimney Power Plants.

SCPP	Power (kw)	Collector diameter (m)	Chimney height (m)	Collector material	Chimney diameter (m)	Radiation
Manzanares, Spain [9, 10]	36–41 kW	240	194	plastic membrane /glass	10.16	850–1040 W/m <sup>2</sup>
Yinchuan, China, [13]	110–190 kW	500	200	glass	10	600 W/m <sup>2</sup>
Mediterranean Region [14]	2.8–6.2MW	1250	550	single glass collector roof	82	1200–1600 kWh/m <sup>2</sup> per year
Arabian Gulf Region [15]	8 MW	1000	500	double glass	100	185 W/m <sup>2</sup>
Adrar, Algeria [16]	140–200 kW	500	200	Glass, plastic etc	10	800 W/m <sup>2</sup>
Qinghai-Tibet Plateau in China [17]	100 MW	5650	1000	-	80	800 W/m <sup>2</sup>
Kerman, Iran [18]	4.035 kW	40 m × 40 m square	60	double glazing glasses	3	
5 cities in Iran [19]	1–2 MW	1000	350	glass or plastic film		6665–7436 MJ/m <sup>2</sup> /year
7 cities in Iran [20]	175–265 MWh/year	244	194.6	transparent glass	5.08	4650–7481 MJ/m <sup>2</sup> /year

## 1.4 Literature Review

Ayadi et al. [21] presented a numerical and an experimental model to see the influence of the height of chimney on the air flow properties inside the SCPP. The experimental model of the solar chimney power plant was constructed at the University of Sfax in Tunisia. The experimental model is built with a tower height of 3 m, a tower diameter of 0.16 m, diameter of collector 2.750 m and height of collector 0.05 m. The numerical findings were compared with experimental results, and the computational results have been validated and used for simulating the flow inside SCPP. For solving the governing equations, a commercial software "Ansys Fluent 17.0" is used. CFD results which have been obtained from numerical simulations show that the tower height can affect greatly on the airflow characteristics of the SCPP.

Zhou et al. [22] presented a theoretical model of Solar Chimney Power Plant. A theoretical analysis for the chimney height of SCPP was done to get the best performance from the optimal design of tower height. The theoretical model was verified with data of Manzanares solar chimney prototype. Results showed that using lapse rate of atmospheric temperature with standard value for the analysis, the highest power value was 102.2 KW at the ideal height of 615 m which is less than the highest tower height with value of power output reach to 92.3 kW. Also in this theoretical study a sensitivity analysis for the effect of the collector roof radius and different atmospheric temperatures lapse rates on maximum height of tower was done. The results showed the maximum height can be affected by atmospheric temperature lapse rate which increasing of the atmospheric temperature lapse rate leads to increase the value of the maximum height of chimney progressively and the maximum power for ideal height can be obtained by using a larger collector diameter.

Kasaeian et al. [23] carried out an analytical and an experimental study at University of Tehran to make a geometrical optimizing for a SCPP prototype. A mathematical model that describes the flow inside SCPP was presented and the effectiveness evaluation of SCPP was studied with different geometric parameters. 2D numerical analysis have been done to study the influences of geometric parameters on the performance of SCPP. The numerical results were confirmed by comparing it with the experimental results from SCPP prototype which has been built with 2 m high tower

and 3 m collector diameter. The outcomes showed that the height of collector inlet equal to 6 cm, the height of tower equal to 3 m, and the diameter of tower equal to 10 cm were the ideal parameters for SCPP prototype. Also this analysis indicated that the geometrical parameters of SCPP are the most significant variables which can affect the performance of SCPP and can lead the velocity magnitude to be increased from 4% to 25% for different cases.

Maia et al. [24] analyzed the flow of air inside the SCPP through a numerical and analytical study of SCPP. An accurate turbulent flow theoretical analysis was done and the equations that describe the turbulent flow inside the SCPP were modeled and studied numerically by solving the equations of mass, energy, momentum, and the turbulent flow. The numerical outcomes were confirmed by comparing the numerical outcomes with the experimental results which got from the experimental prototype. It was observed through the analysis that the most important physical parameters in SCPP are the height and radius of the tower. An increase in the value of mass flow rate and reduction in the temperature of airflow occurred when both the tower height and radius was increased.

Hu et al. [25] numerically studied many types of chimney geometries based on the influence of increasing the upper radius of tower on the driving potential of the SCPP. In this study, cylindrical chimney, divergent outlet chimney (DOSC), divergent inlet chimney (DISC) and divergent chimney (DSC) are examined and their aerodynamic characteristics and their ability to generate power were revealed. The simulation results showed that the DSC has a better effectiveness for the power production than the cylindrical SC which it is almost higher by 13.5 times than the cylindrical tower and increasing in power with the DISC in range from 2 to 10 times while the DOSC increasing at maximum to about 5 times. They found that performance of the system depends on the tower configuration parameters which have significant influences on the expansion loss in the divergent tower. The power output range reach to 52 kW during long period (7 hours) was obtained by variable tower exit and the power output for the SCPP was enhanced by 60% as a result of changing the chimney geometry.

Bouabidi et al. [26] presented a numerical model to study the effect of the chimney configurations on SCPP performance and to simulate the airflow inside SCPP. For the numerical analysis of the SCPP, four types of tower geometries; standard, divergent,



convergent and opposing tower are studied. To validate numerical results, an experimental model was developed and many measurements were done. By comparing the numerical results with data from the experimental work, it turned out that there was good approval. The airflow properties of the SCPP like the air temperature distribution, the pressure change and the velocity magnitude were studied through this analysis. The results indicated that the chimney geometry has a significant influence on the changing of the velocity behavior which occurs due to the pressure distribution resulted from the variation of chimney geometry. The SCPP performance is enhanced with divergent and opposing tower by the increasing of velocity and maximum velocity appears at divergent geometry.

Toghraie et al. [27] carried out a 3D CFD simulation to examine the impacts of configuration parameters on the airflow characteristics and the SCPP performance. The numerical model was simulated by solving Navier-Stokes equations and the  $k - \epsilon$  turbulence model for the CFD model of SCPP. The effect of changing heat flux, height of collector roof, diameter of the collector, height of the tower and radius of the tower on the airflow characteristics and performance were examined. The outcomes indicated that the SCPP efficiency and output power can be changed positively with changing the height of the tower and diameter of the collector but change negatively with height of the collector and the chimney radius which have optimum ranges for the maximum values for the effectiveness of SCPP and output power of the power plant.

Li et al. [28] evaluated the performance of a SCPP through a theoretical model and the results has been validated by the data of the Manzanares SCPP in Spain. The theoretical model studies the effects of airflow and thermal losses and the rate of temperature changes at the tower. Depending on the solar radiation there is a highest power range for the solar chimney for specific solar irradiation values due to the effect of the installation of the turbines, flow and heat losses inside SCPP. After a certain diameter of collector roof, power of the SCPP increases slowly and this leads to be a restriction for the maximum diameter of collector while no such restriction for height of tower, in light of the modern technology of construction.

Hassan et al. [29] have done a 3D computational fluid dynamics analysis of SCPP to demonstrate the impacts of slope angle of collector and diverging angle of the chimney

on effectiveness of Manzanares SCPP in Spain. The analysis was done by using DO and RNG k-  $\epsilon$  models and the numerical outcomes were verified by comparing it with the results which were obtained from Manzanares prototype in Spain. The numerical simulations were done by varying inclination angle of collector as 4°, 6°, 8° and 10° sequentially and diverging angle of the chimney in the range of 1°- 3° whereas all other SCPP parameters were constant. The numerical results showed that gradual increasing in the air velocity occurred by increasing inclination angle of collector but it dropped after higher than 6° and this affected negatively on the overall performance of SCPP. Also results showed that using a chimney diverging angle equal to 1° made a significant increase in velocity from 9.1 m/s to 11.6 m/s which leads to increase the value of power by 108%. So, they found that, as compared to increasing height of tower and radius of collector roof, by using diverging tower, high power and high performance of SCPP can be obtained.

## CHAPTER 2

### MATHEMATICAL MODELLING OF SCPP

#### 2.1 Introduction

To have a better view about the operation process of SCPP and to find the solutions to improve the performance of SCPP, an analytical analysis should be conducted. In this chapter the solar chimneys' performance equations are presented. Moreover, The Navier-Stokes Equations that govern the air flow inside the Solar Chimney Power Plant is given and turbulence models that is used are described in this chapter.

#### 2.2 Solar Chimney Performance Equations

Based on the following equations, the performance and efficiency of the solar chimney is calculated [30, 31]. By considering  $A_{coll}$  and  $G$  as the area of the roof of collector and solar irradiation, respectively, the efficiency of collector can be written as follows [32]:

$$\eta_{coll} = \frac{\dot{Q}}{A_{coll} G} \quad (1)$$

In Eq.1  $\dot{Q}$ , which is useful heat utilized by the SCPP and is defined as,

$$\dot{Q} = \dot{m} C_p \Delta T \quad (2)$$

In Eq. 2,  $\dot{m}$  is the mass flow rate of air,  $c_p$  is the specific heat capacity of air and  $\Delta T$  is the temperature difference between ambient and inlet of the tower. Mass flow rate in Eq. 2 can be obtained as,

$$\dot{m} = \rho_{ch} v_{ch} A_{ch} \quad (3)$$

In Eq. 3,  $\rho_{ch}$ ,  $v_{ch}$  and  $A_{ch}$  are defined as the air density at tower inlet, the velocity of air at tower inlet and cross-sectional area of chimney. By considering Eq. 2 and 3, the Eq. 1 can be rewritten as follows,

$$\eta_{coll} = \frac{\rho_{ch} v_{ch} A_{ch} C_p \Delta T}{A_{coll} G} \quad (4)$$

In order to find the pressure change between tower base and the ambient;  $\Delta p$  Eq. 5 is used [31].

$$\Delta p = \Delta p_t + \Delta p_f + \Delta p_{in} + \Delta p_{out} = 0.00353 g H \cdot \left( \frac{\pi G \eta_{coll}}{c_p \ln} R_{coll}^2 - \frac{g}{2 c_p} H + \frac{1}{2} \gamma_{\infty} H \right) \quad (5)$$

Where,  $g, H, R_{coll}$  and  $\gamma_{\infty}$  are gravitational acceleration, chimney height, collector radius and the lapse rate of atmospheric temperature [31], respectively.  $\Delta p_t, \Delta p_f, \Delta p_{in}$  and  $\Delta p_{out}$  are pressure differences at turbine, pressure drop due to friction loss in the tower, inlet loss and the loss in the outlet kinetic energy, respectively. Eq. 5 can be rewritten as follows,

$$\Delta p = \Delta p_t + \Delta p_f + \Delta p_{in} + \Delta p_{out} \quad (6)$$

According to Eq. 6 the  $\Delta p_t$  can be obtained as;

$$\Delta p_t = \Delta p - \Delta p_f - \Delta p_{in} - \Delta p_{out} \quad (7)$$

In Eq. 7, friction loss in the chimney is,

$$\Delta p_f = f \frac{H}{D} \frac{1}{2} \rho V_{ch}^2 \quad (8)$$

The parameters  $f, D$  and  $\rho$  in Eq. 8 are the wall friction factor, chimney diameter and density, respectively. The velocity inside the chimney,  $V_{ch}$ , is,

$$V_{ch} = \sqrt{\frac{2 g H \Delta T}{T_0}} \quad (9)$$

where,  $T_0$  is ambient temperature. Entrance loss,  $\Delta p_{in}$  is calculated as can be seen in Eq. 10,

$$\Delta p_{in} = \varepsilon_{in} \frac{1}{2} \rho V_{turb,i}^2 \quad (10)$$

where,  $\epsilon_{in}$  is entrance pressure loss coefficient. Furthermore, the velocity at turbine inlet,  $V_{turb,i}$  is calculated as;

$$V_{turb,i} = \sqrt{\frac{2 g H \Delta T}{3 T_o}} \quad (11)$$

By considering  $\rho_{out}$  as density of air at outlet of the chimney, and  $\epsilon_{out}$  as exit pressure loss coefficient,  $\Delta p_{out}$  can be calculated as;

$$\Delta p_{out} = \epsilon_{out} \frac{1}{2} \rho_{out} V_{ch,o}^2 \quad (12)$$

In Eq. 12,  $V_{ch,o}$  is, [33]

$$V_{ch,o} = V_{ch} \left( \frac{A_{ch}}{A_{ch,o}} \right) \quad (13)$$

By combining Eq. 7, 8, 10, 12,  $\Delta p$  in Eq.6 can be rewritten as follows,

$$\Delta p = 0.00353 g H \cdot \left( \frac{\pi G \eta_{coll}}{c_p \dot{m}} R_{coll}^2 - \frac{g}{2 c_p} H + \frac{1}{2} \gamma_{\infty} H \right) \quad (14)$$

Power which is generated by turbine,  $P_{out}$ , can be calculated as, [34]

$$P_{out} = \eta_{tg} \Delta p_t \cdot V_{ch,max} \cdot A_{ch} \quad (15)$$

Where  $\eta_{tg}$  is the efficiency of turbine generator. Inside the tower,  $V_{ch,max}$  the maximum velocity can be achieved as follows,

$$V_{ch,max} = \sqrt{\frac{2 g H_{ch} \Delta T}{T_o}} \quad (16)$$

Moreover, for SCPP, the total efficiency can be obtained as [31],

$$\eta = \frac{P_{out}}{\pi R_{coll}^2 G} \quad (17)$$

By considering  $U$  as overall heat transfer coefficient and  $\eta_{coll}$  as solar collector efficiency, the maximum height of the chimney can be calculated as follows [31]:

$$H_{Max} = \frac{c_p \dot{m}}{U \pi D} \cdot \ln \left( \frac{\pi^2 U D G \eta_{coll} R_{coll}^2}{c_p \dot{m}^2 (g - \gamma_{\infty} c_p)} + 1 \right) \quad (18)$$

### 2.3 Navier-Stokes Equations

Navier-Stokes equations are the equations of continuity, momentum and conservation of energy for a Newtonian fluid. The Navier-Stokes equations are used to solve compressible and incompressible flow which can be inviscid or viscous flow. General N-S equations can be seen below:

Navier–Stokes continuity equation in general form:

$$\frac{\partial \rho}{\partial t} + \nabla \cdot (\rho \mathbf{u}) = 0 \quad (19)$$

Navier-Stokes momentum equation (convective form) in general form:

$$\rho \left( \frac{\partial \mathbf{u}}{\partial t} + \mathbf{u} \cdot \nabla \mathbf{u} \right) = -\nabla \bar{p} + \mu \nabla^2 \mathbf{u} + \frac{1}{3} \mu \nabla (\nabla \cdot \mathbf{u}) + \rho \mathbf{g} \quad (20)$$

For the specific problem of solar chimney, 2-D consideration is presented in the following part.

By considering  $\rho$ ,  $u$  and  $v$  as air density, velocity in axis direction and velocity in radial direction, respectively. [35], 2-D, steady state continuity equation can be written as:

$$\frac{\partial(\rho u)}{\partial z} + \frac{1}{r} \frac{\partial(r \rho v)}{\partial r} = 0 \quad (21)$$

and 2-D, steady state momentum equations:

$$\frac{\partial(\rho u u)}{\partial z} + \frac{1}{r} \frac{\partial(r \rho u v)}{\partial r} = \frac{\partial p}{\partial z} + (\rho - \rho_0)g + 2 \frac{\partial}{\partial z} \left[ (\mu + \mu_t) \frac{\partial u}{\partial z} \right] + \frac{1}{r} \frac{\partial}{\partial r} \left[ (\mu + \mu_t) r \left( \frac{\partial u}{\partial z} + \frac{\partial v}{\partial r} \right) \right] \quad (22)$$

$$\frac{\partial(\rho u v)}{\partial z} + \frac{1}{r} \frac{\partial(r \rho v v)}{\partial r} = -\frac{\partial p}{\partial r} + \frac{\partial}{\partial z} \left[ (\mu + \mu_t) \left( \frac{\partial v}{\partial z} + \frac{\partial u}{\partial r} \right) \right] + 2 \frac{1}{r} \frac{\partial}{\partial r} \left[ (\mu + \mu_t) r \frac{\partial v}{\partial r} \right] - \frac{2(\mu + \mu_t)v}{r^2} \quad (23)$$

where,  $p$ ,  $\mu$  and  $g$  are pressure, kinematic viscosity coefficient and gravitational acceleration. Moreover, the  $\mu_t$  is defined as chimney top's kinematic viscosity coefficient.

2-D steady state energy equation is obtained as follows:

$$\frac{\partial uT}{\partial z} + \frac{1}{r} \frac{\partial(rvT)}{\partial r} = -\frac{1}{\rho} + \frac{\partial}{\partial z} \left[ \left( \frac{\mu}{Pr} + \frac{\mu_t}{\sigma_t} \right) \frac{\partial T}{\partial z} \right] + \frac{1}{\rho r} \frac{\partial}{\partial r} \left[ \left( \frac{\mu}{Pr} + \frac{\mu_t}{\sigma_t} \right) r \frac{\partial T}{\partial z} \right] \quad (24)$$

Where  $\sigma_T$  is the turbulent Prandtl number for T which is considered as  $\sigma_T = 0.9$  [35].

The buoyancy in the solar chimney is modeled based on Boussinesq Approximation. By considering  $\beta$  as expansion rate, the body force term of Eq. 22 is,

$$g(\rho - \rho_0) = \rho_0 \beta g(T - T_0) \quad (25)$$

#### 2.4 Turbulence Model

The Rayleigh number is the measure for the strength of buoyancy-driven flow resulted from the natural airflow. Rayleigh number less than  $10^7$  refers to laminar flow, with transition region in the range of  $10^7 < Ra < 10^{11}$ .

Which Rayleigh number can be calculated as:

$$Ra = Gr \cdot Pr = \frac{g\beta\Delta T}{\nu^2} L^3 \cdot Pr \quad (26)$$

The Rayleigh number for the studied solar chimney model is  $8 \times 10^8$  which indicates the flow is turbulent. Turbulent flow is defined by fluctuating velocity fields. These fluctuations mix transferred amounts like momentum and energy, and also cause changes in the transported amounts. There is not any exact turbulence model which is universally used for all kinds of turbulence fluid problems. To select the most suitable model for the intended application, firstly, it is required to understand the abilities and restrictions of several different choices.

Some of the Turbulence models are, Spalart-Allmaras, Standard k- $\epsilon$  Model, RNG k- $\epsilon$  Model, Realizable k- $\epsilon$  Model, Standard k- $\omega$  Model, Shear-Stress Transport (SST) k- $\omega$  Model and Reynolds Stress Model (RSM). In the following part, the Standard k- $\epsilon$  and Shear-Stress Transport (SST) k- $\omega$  turbulence models, which are the most commonly used turbulence models are described.

### 2.4.1 Standard k-ε Turbulence Model

The k-ε model was developed in the early 1970s. As the strengths and weaknesses of the standard k-ε turbulence model have become known, many improvements were made to enhance effectiveness of this model. The k-ε turbulence model concentrates on the mechanisms which has an impact on the turbulent kinetic energy, k [36]. By considering K and k as the mean kinetic energy and turbulent kinetic energy, the immediate kinetic energy of a turbulent flow, k(t) is obtained as follows [37]:

$$K = \frac{1}{2} (U^2 + V^2 + W^2) \quad (27)$$

$$k = \frac{1}{2} (\overline{u'^2} + \overline{v'^2} + \overline{w'^2}) \quad (28)$$

$$k(t) = K + k \quad (29)$$

By considering ε as the dissipation rate of k. If k and ε are known, the turbulent viscosity model can be calculated as:

$$v_t \propto \vartheta \ell \propto k^{1/2} \frac{k^{3/2}}{\varepsilon} = \frac{k^2}{\varepsilon} \quad (30)$$

In Eq. 30,  $v_t$ ,  $\vartheta$  and  $\ell$  are kinematic turbulent viscosity, velocity scale and a length scale.

The turbulent kinetic energy k and its dissipation rate ε are found from the following transport equations:

$$\frac{\partial}{\partial t} (\rho k) + \frac{\partial}{\partial x_i} (\rho k u_i) = \frac{\partial}{\partial x_j} \left[ \left( \mu + \frac{\mu_t}{\sigma_k} \right) \frac{\partial k}{\partial x_j} \right] + k + b - \rho \varepsilon - Y_M + S_K \quad (31)$$

$$\begin{aligned} \frac{\partial}{\partial t} (\rho \varepsilon) + \frac{\partial}{\partial x_i} (\rho \varepsilon u_i) = & \frac{\partial}{\partial x_j} \left[ \left( \mu + \frac{\mu_t}{\sigma_\varepsilon} \right) \frac{\partial \varepsilon}{\partial x_j} \right] + 1 \varepsilon \frac{\varepsilon}{k} (k + C_{3\varepsilon} b) - \\ & (C_{2\varepsilon} \rho \frac{\varepsilon^2}{k}) + S_\varepsilon \end{aligned} \quad (32)$$



The steady state k-ε equations that describe problem in SCPP can be calculated as follows [35],

$$\frac{\partial(uk)}{\partial z} + \frac{1}{r} \frac{\partial(rv_k)}{\partial r} = \frac{1}{\rho} \frac{\partial}{\partial z} \left[ \left( \mu + \frac{\mu_t}{\sigma_k} \right) \frac{\partial k}{\partial z} \right] + \frac{1}{\rho r} \frac{\partial}{\partial r} \left[ \left( \mu + \frac{\mu_t}{\sigma_k} \right) r \frac{\partial k}{\partial r} \right] + G_k - \varepsilon \quad (33)$$

$$\frac{\partial(u\varepsilon)}{\partial z} + \frac{1}{r} \frac{\partial(rv\varepsilon)}{\partial r} = \frac{1}{\rho} \frac{\partial}{\partial z} \left[ \left( \mu + \frac{\mu_t}{\sigma_\varepsilon} \right) \frac{\partial \varepsilon}{\partial z} \right] + \frac{1}{\rho r} \frac{\partial}{\partial r} \left[ \left( \mu + \frac{\mu_t}{\sigma_\varepsilon} \right) r \frac{\partial \varepsilon}{\partial r} \right] + \frac{\varepsilon}{k} (C_{1k} - C_{2\varepsilon}) \quad (34)$$

Where

$G_k$  represents the generation of turbulence kinetic energy due to the mean velocity gradients defined as:

$$G_k = -\mu_t \left( 2 \left( \left( \frac{\partial u}{\partial z} \right)^2 + \left( \frac{\partial v}{\partial r} \right)^2 + \left( \frac{v}{r} \right)^2 \right) + \left( \frac{\partial u}{\partial r} + \frac{\partial v}{\partial z} \right)^2 \right) \quad (35)$$

Where  $\sigma_k$  and  $\sigma_\varepsilon$  is the turbulent Prandtl numbers for k and ε respectively,  $c_1$  and  $c_2$  are two constants for the turbulent model

The constants,  $C_1 = 1.44$ ,  $C_2 = 1.92$ ,  $\sigma_k = 1.0$ ,  $\sigma_\varepsilon = 1.3$  and  $C_\mu = 0.09$

And  $\mu_t = \frac{C_\mu \rho k^2}{\varepsilon}$ .

The main advantages of the standard k-ε turbulence model are; it is comparatively easy to carry out, leads to steady computation that converge comparatively readily, reasonable expectation for various flows.

Some of the main disadvantages of the standard k-ε turbulence model are [38]:

- Weak expectation for:
  - Rotating, swirling and strong separation flows,
  - Axisymmetric jets
  - Fully developed flows in non-circular ducts.
- Work only for fully developed turbulent flows.

#### 2.4.2 k-ω Turbulence Model

One of the most used turbulence models is the k-ω turbulence model. The proposed model developed to use as the solution of transport equations for the turbulent kinetic energy k and the turbulence frequency ω. One of the main point about k-ω is that, the

numerical behavior of it, is similar to the k- $\epsilon$  models. The k- $\omega$  model is based on the two-equation model which is given by the following [39]:

$$\frac{\partial(\rho k)}{\partial t} + \frac{\partial}{\partial x_j}(\rho u_j k) = P - \beta * \rho k \omega + \frac{\partial}{\partial x_j} \left[ \left( \mu + \sigma_k \frac{\rho k}{\omega} \right) \frac{\partial k}{\partial x_j} \right] \quad (36)$$

$$\frac{\partial(\rho \omega)}{\partial t} + \frac{\partial}{\partial x_j}(\rho u_j \omega) = \frac{\gamma \omega}{k} P - \beta \rho \omega^2 + \frac{\partial}{\partial x_j} \left[ \left( \mu + \sigma_\omega \frac{\rho k}{\omega} \right) \frac{\partial \omega}{\partial x_j} \right] + \frac{\rho \sigma_d}{\omega} \frac{\partial k}{\partial x_j} \frac{\partial \omega}{\partial x_j} \quad (37)$$

The numerical behavior of k- $\omega$  model is similar to that of the k- $\epsilon$  models.

### 2.4.3 SST k- $\omega$ Turbulence Model

The shear stress transport (SST) k- $\omega$  model is one of the most commonly used turbulence models. SST k- $\omega$  model is presented by Menter (1994) by modifying the standard k- $\omega$  model and a transformed k- $\epsilon$  model. The SST k- $\omega$  model is a two-equation eddy-viscosity turbulence model that is widely used in CFD analysis to model the compressible and incompressible turbulent flows. For the last 20 years, this model has been altered to be more accurate and reflects certain flow conditions. The first and second transported variables are turbulent kinetic energy, k and the specific dissipation,  $\omega$  [40].

The transport turbulent kinetic energy (k) equation for k- $\omega$  model is presented as follows [41]:

$$\frac{\partial(\rho k)}{\partial t} + \frac{\partial}{\partial x_i}(\rho U_i k) = \frac{\partial}{\partial x_i} \left[ \left( \mu + \frac{\mu_t}{\sigma_k} \right) \text{grad}(k) \right] + P_k - \beta * \rho k \omega \quad (38)$$

Where:

$$P_k = \left( 2\mu_t \frac{\partial U_i}{\partial x_j} \cdot \frac{\partial U_i}{\partial x_j} - \frac{2}{3} \rho k \frac{\partial U_i}{\partial x_j} \delta_{ij} \right) \quad (39)$$

$\sigma_k$  and  $\beta^*$  are constants.

The transport turbulent frequency  $\omega$  equation for the k- $\omega$  model is presented as follows:

$$\frac{\partial p \omega}{\partial t} + \frac{\partial}{\partial x_i} (\rho U_i \omega) = \frac{\partial}{\partial x_i} \left[ \left( \mu + \frac{\mu_t}{\sigma_{\omega,1}} \right) \text{grad}(\omega) \right] + \gamma_2 \left( 2\rho \frac{\partial U_i}{\partial x_j} \cdot \frac{\partial U_i}{\partial x_j} - \frac{2}{3} \rho \omega \frac{\partial U_i}{\partial x_j} \delta_{ij} \right) - \beta_2 \rho \omega^2 + 2 \frac{\rho}{\sigma_{\omega,2}} \frac{\partial k}{\partial x_k} \frac{\partial \omega}{\partial x_k} \quad (40)$$

where:

$$\beta^* = 0.09, \beta_2 = 0.083, \sigma_k = 1, \sigma_{\omega,1} = 2, \sigma_{\omega,2} = 1.17, \gamma_2 = 0.44$$

The main advantages of the SST k- $\omega$  model can be regarded as [36]:

- Compared to k- $\epsilon$  and the standard k- $\omega$ , SST k- $\omega$  can expect separation and reattachment in a better way.
- The SST k- $\omega$  model has the capability to handle the sensitivity to freestream turbulence levels and others flaws in the base model.
- It does not need further adjustment to use it for the viscous region.
- The SST provides a stand for more additions like the Scale-Adaptive Simulation (SAS) and laminar-turbulence transition.

## CHAPTER 3

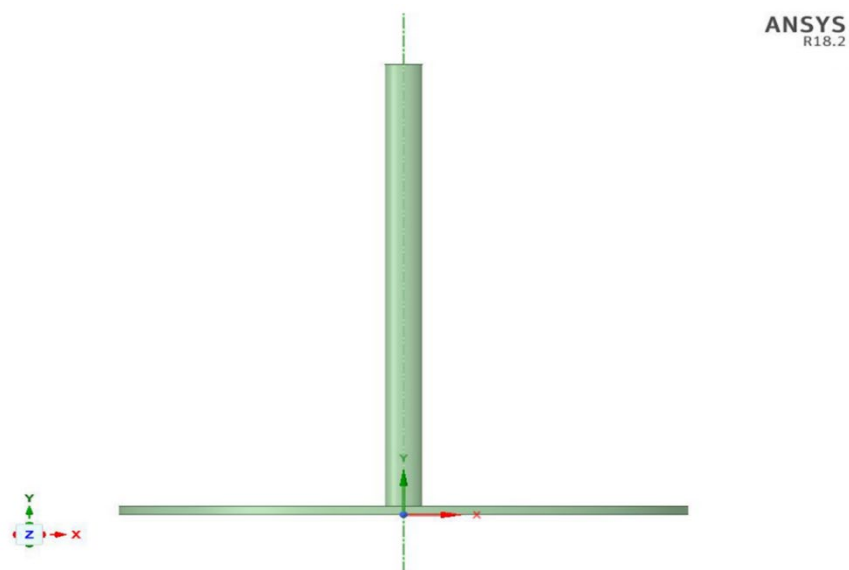
### NUMERICAL ANALYSIS OF SCPP

#### 3.1 CFD Method

In this part, the computational fluid dynamics method is described which is build to evaluate the efficiency and performance of SCPP based on the different chimney and collector characteristics, like height, diameter, geometry and angle.

##### 3.1.1 Geometry of SCPP

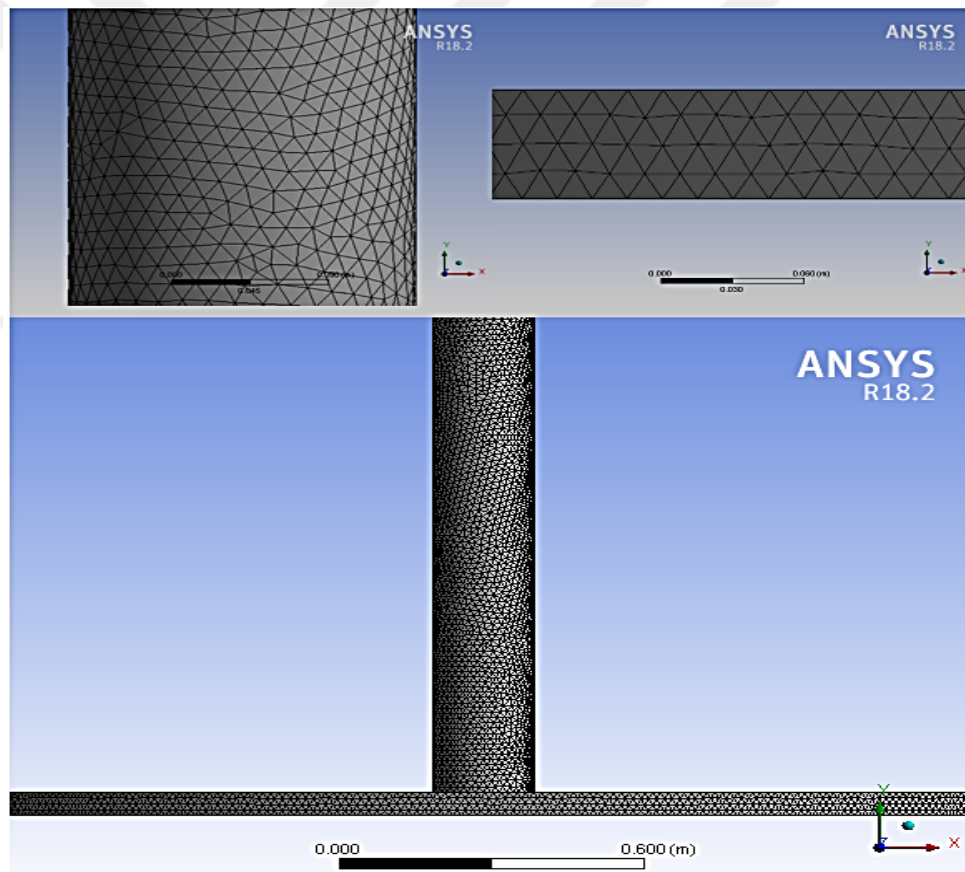
To analyze the efficiency and performance of SCPP, at the first step, a 2D geometry model of SCPP is build by the commercial CFD software; ANSYS 18.2 by using 2D Modeling Software (Space Claim Direct Modeler) [42]. The SCPP numerical model consists of four main parts as ground, collector, chimney and fluid zone and all these components are drawn as 2D geometries. Figure 3.1 presents the proposed designed model.



**Figure 3.1:** SCPP model design

### 3.1.2 Mesh generation

The process of meshing of the designed solar chimney power plant have been done automatically by using ANSYS Meshing in ANSYS Workbench. The tetrahedral mesh shape is chosen as the structure of the meshing for the proposed system. Since the geometry of the studied system is simple, the tetrahedral shape covers the area of system more accurate than hexahedral elements. Meshing area consists of 1000651 elements and 202338 nodes. Moreover, the geometric shape is divided into 5 parts, which are; pressure inlet (at inlet of collector), pressure outlet (at the exit of chimney), chimney wall, wall- collector (glass) and wall-absorber (aluminum). After the mesh independency study, one million mesh has been selected. Figure 3.2 illustrates the defined meshing structure.



**Figure 3.2:** The meshing structure and the implementing result of the designed SCPP.

### 3.1.3 Simulation of SCPP

The CFD simulation is done by ANSYS Fluent solver 18.2. The main assumptions and considerations about the simulation can be regarded as:

- Steady state condition for the entire analysis.
- Air is assumed ideal gas and incompressible.
- The pressure based solver is considered as the main solver.
- The chimney is perfectly insulated (adiabatic boundary conditions).
- Flow is considered as viscous flow.
- For Pressure-velocity coupling scheme, SIMPLE algorithm is used.
- The Green- Gauss Cell- Based method is used to compute the gradients.
- The values of the highest residual is  $10^{-6}$

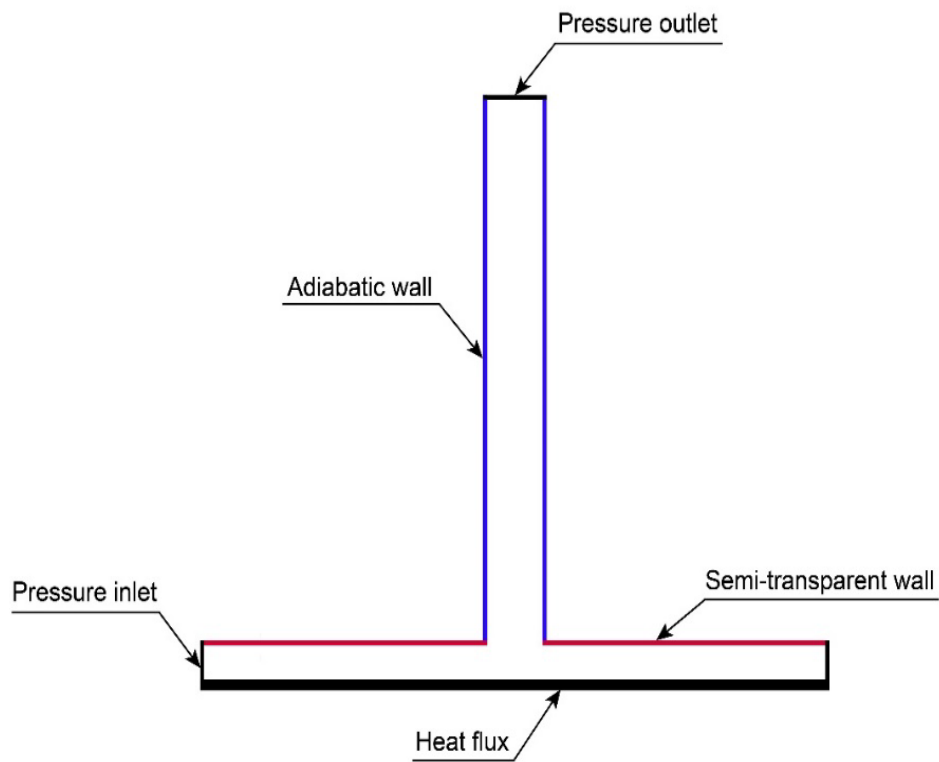
Moreover, the PRESTO and the STANDARD ALGORITHM schemes are used for pressure and pressure equation, respectively. Also in the simulation, the SECOND ORDER UPWIND scheme is used.

### 3.1.4 The Boundary conditions for SCPP

The boundary conditions which are considered for solving and simulating SCPP system are presented in the following. The BOUSSINESQ approximation is used to model the buoyancy flow. Moreover, the collector roof semi-transparent wall is utilized with solar irradiation of  $850 \text{ W/m}^2$  which is same with experimental study of Ghalamchi et. al. [1]. The absorber emissivity is 0.55 and the collector glass emissivity is 0.9. Furthermore, the chimney is perfectly insulated (with zero heat flux), the operation pressure is 101325 Pa therefore the pressure inside the solar chimney considered as gauge pressure and operation temperature is 302 K. Table 3.1 presents the boundary conditions which are considered for the system under study. The value of heat flux is founded by multiply the value of solar radiation  $850 \text{ W/m}^2$  by the value of the collector glass emissivity which is 0.9 and the heat flux value it be  $765 \text{ W/m}^2$ . Figure 3.3 depicts the proposed solar chimney power plant boundary conditions.

**Table 3.1:** The boundary conditions which are considered for the under study SCPP.

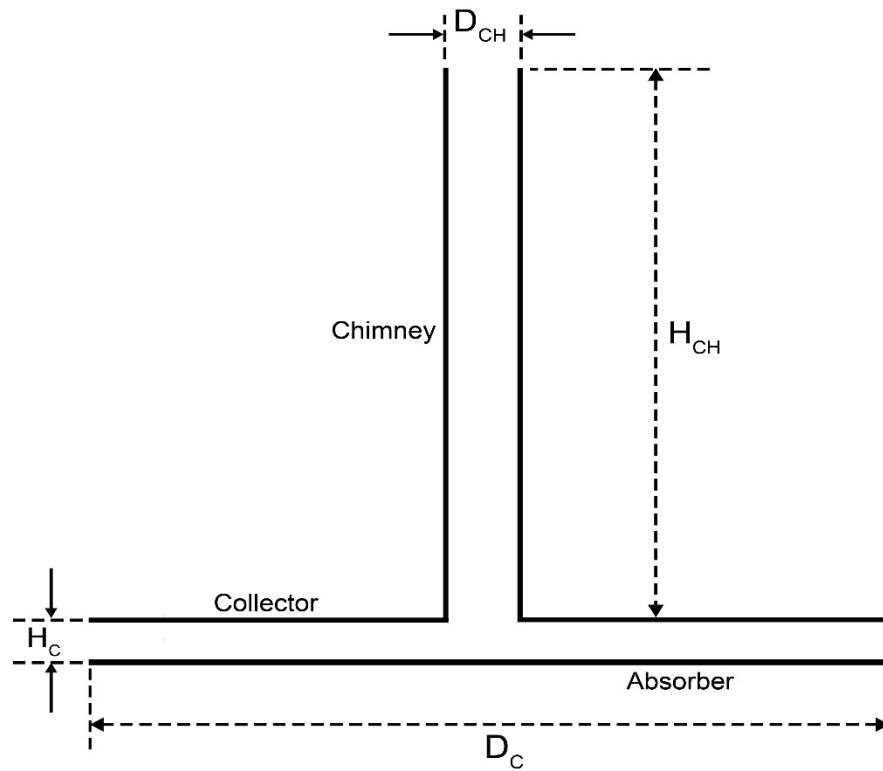
Boundary	Type	Parameters
Collector inlet	Pressure inlet	$P_i = 0 \text{ Pa}$ , $T=T_a$
Absorber	Heat flux Wall	$q=765 \text{ W/m}^2$
Chimney wall	Adiabatic wall	$q= 0 \text{ W/m}^2$
Collector	Wall and Convection	$T_a= 302 \text{ k}$ $h = 5 \text{ W/m}^2\text{K}$
Chimney outlet	Pressure outlet	$P_o = 0 \text{ Pa}$



**Figure 3.3:** The boundary conditions which are considered for the studied SCPP.

### 3.2 Mesh Independency Study

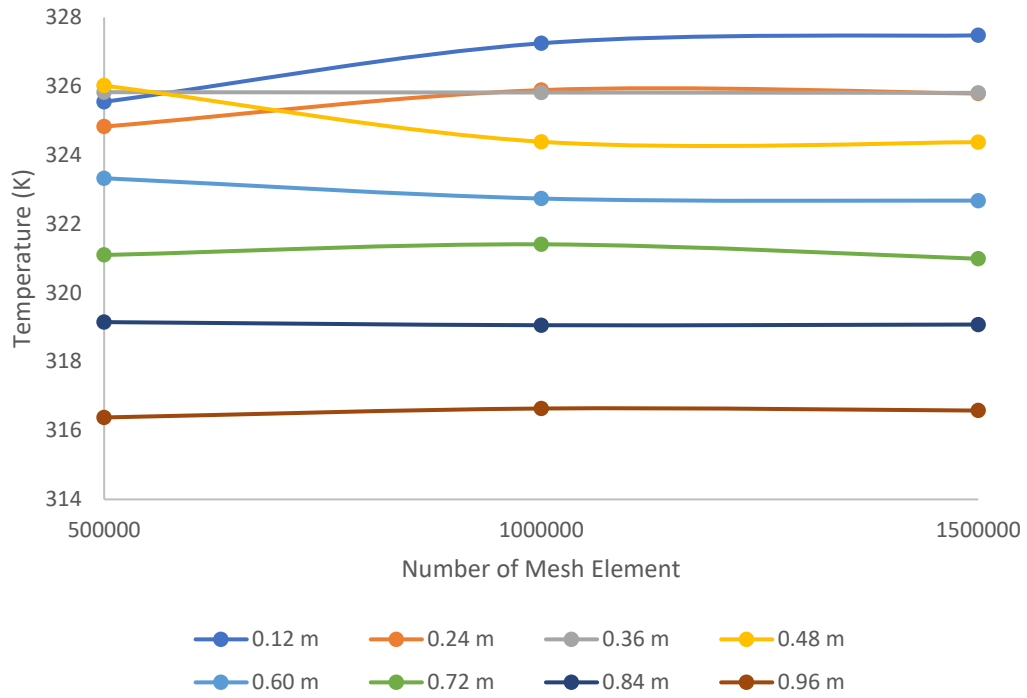
The dimension of the designed SCPP are presented in Figure 3.4. According to the Figure 3.5,  $H_{ch}$ ,  $D_{ch}$ ,  $H_c$  and  $D_c$  are defined as, height of chimney, diameter of chimney, height of collector and diameter of collector with values 300 cm, 20 cm, 6 cm and 300 cm, respectively.



**Figure 3.4:** Illustration of the dimensions of the designed SCPP.

For the mesh independency study, the considered dimensions of the SCPP are based on best case of the Ghalamchi et. al. [1]. The meshes which are implemented on the studied system are three different tetrahedral mesh structures with  $5 \times 10^5$ ,  $1 \times 10^6$  and  $1.5 \times 10^6$  elements. The mesh independency results are considered as a function of temperature distribution through the collector. Furthermore, due to the results, after  $10^6$  number of mesh elements, the Root Mean Square (RMS) errors decrease to % 1.27 for the maximum point. By considering the computational analysis time and cost, using one million mesh elements are appropriate for computing the solution. Figure 3.5. illustrates the results of mesh independency study based on the studied solar chimney power plant.

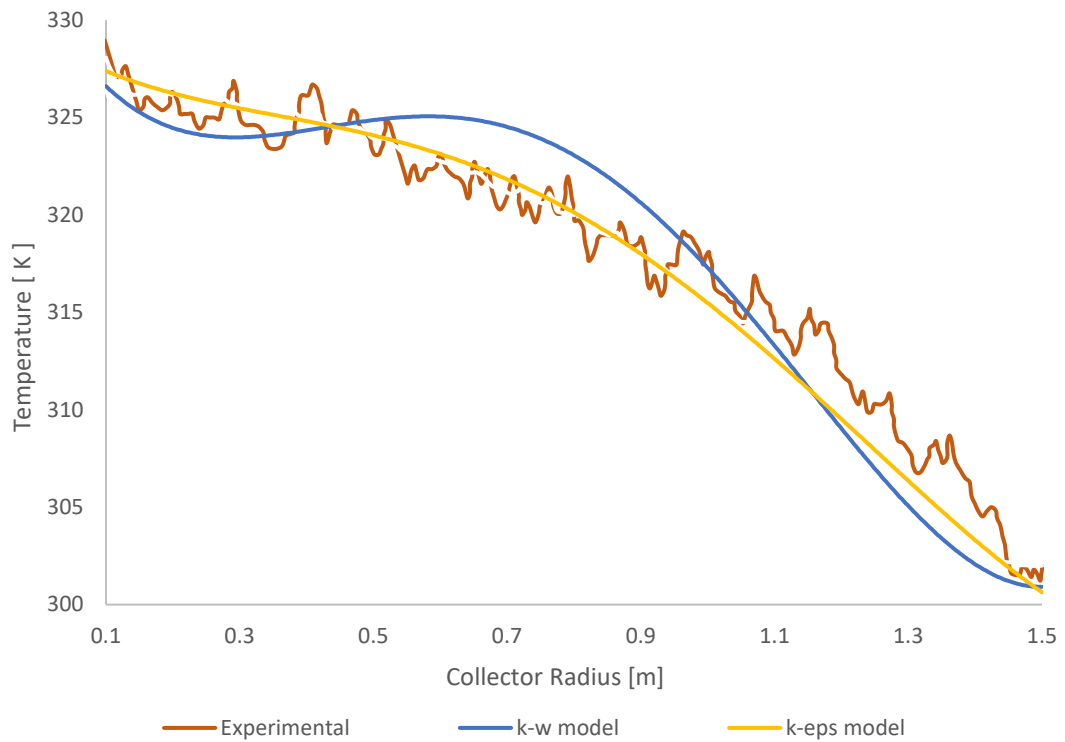




**Figure 3.5:** The results of mesh independency study based on the studied system.

### 3.3 The Turbulence Model Study

In order to decide on the turbulence model of the proposed SCPP, the  $k-\epsilon$  and  $k-\omega$  models which are represented in section 2.4.1 and 2.4.2 are examined. According to the numerical studies the  $k-\epsilon$  turbulence model performance is much better than  $k-\omega$ . The  $k-\omega$  model overestimates the temperature values. Figure 3.6 depicts the result of turbulence model study based on the dimensions which are given in section 3.2. Figure 3.6 is a proof of the better performance of the  $k-\epsilon$  in validating the experimental results compared to the  $k-\omega$  model.



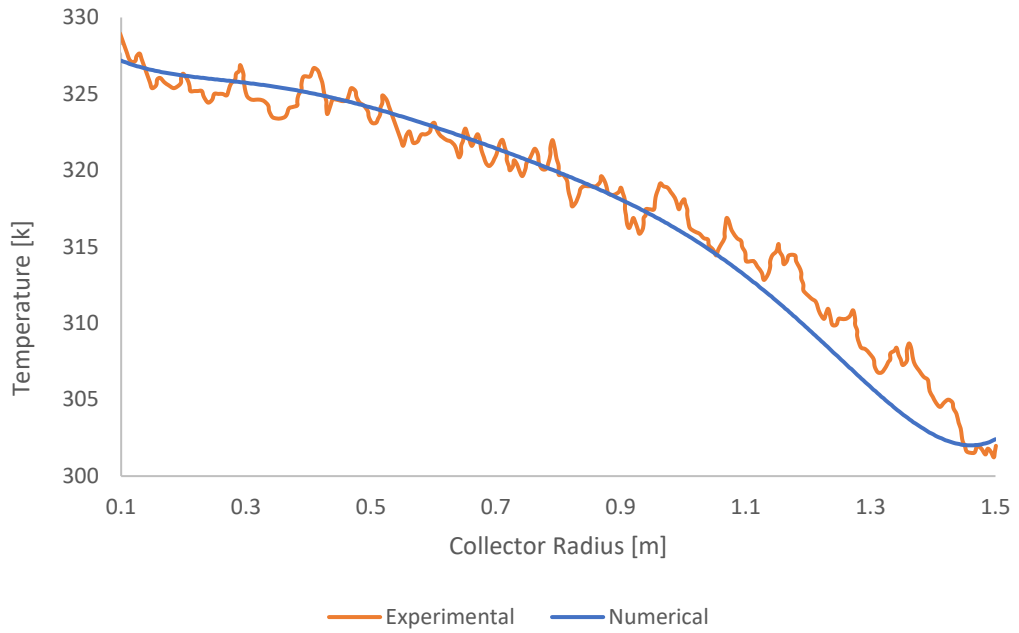
**Figure 3.6:** The result of turbulence model study based on the designed SCPP.

### 3.4 Validation of Numerical Results

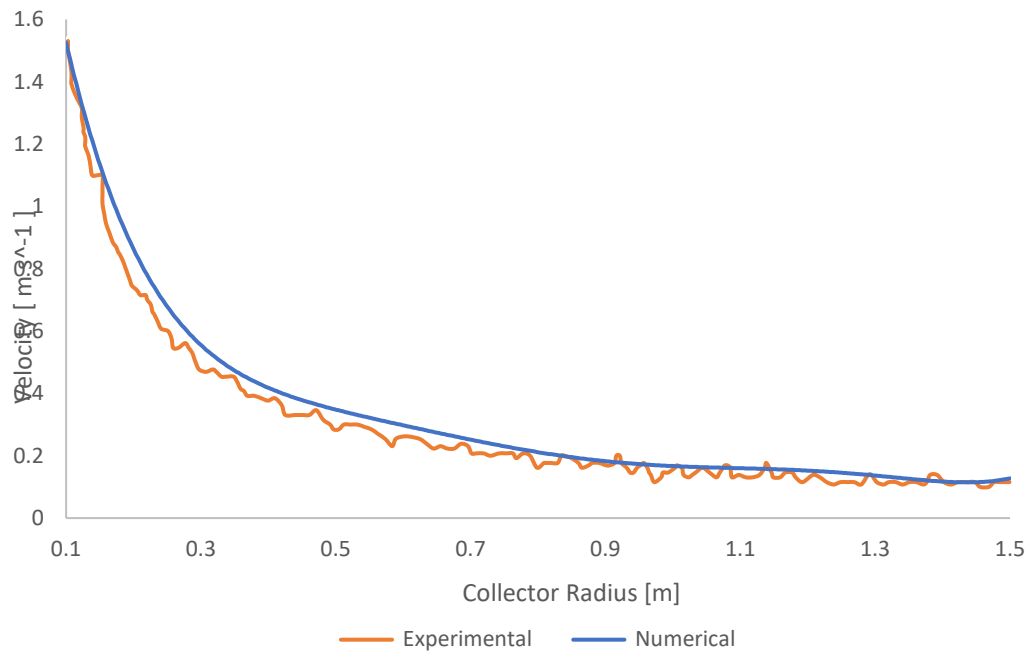
To validate the effectiveness of the aforementioned turbulence model, numerical results are used to compared with one of the cases of Ghalamchi et.al [1] which has similar dimensions as the studied system. The main parameters which are used to do the validation process can be regarded as:

- Using of one million mesh elements and k-  $\epsilon$  turbulence model,
- The temperature and velocity distribution through collector radius are found and compared with the experimental results,

Based on the obtained results of the numerical simulations, Maximum Relative Mean Errors (RMS) are less than 6.4% and 4.5% for temperature and velocity distributions respectively. Figure 3.7 and 3.8 presents the numerical model validation results.



**Figure 3.7:** The comparison of the experimental and numerical outcomes based on the designed SCPP temperature.



**Figure 3.8:** The comparison of the experimental and numerical outcomes based on the designed SCPP velocity.

As it is depicted in Figure 3.7 and Figure 3.8, the performance of the computed numerical model is validated since it is acceptable close to the experimental results.

### 3.5 Performance Study for SCPP

#### 3.5.1. SCPP Chimney Parameters

The main parameters of the chimney which have a direct impact on the effectiveness of the SCPPs can be considered as chimney height and diameter. In the following parts, these two parameters are analyzed regarding SCPP performance.

##### 3.5.1.1 Effect of Chimney Height

According to the researches which have done about the effect of SCPP's chimney height [21, 24], it has been revealed that, by increasing the height of the tower of SCPP, efficiency and power will increased too, but in the other hand when the height of tower is increased too much, the air pressure will decreased and the mass flow rate and velocity of air will be increased. Also, it will be costly and difficult to construct an extremely tall chimney.

In Table 3.2, the parameters  $H_{ch}$ ,  $D_{ch}$ ,  $R_c$  and  $H_c$  are defined as, height of chimney, fixed diameter of chimney, fixed radius of collector and fixed height of collector, respectively.

**Table 3.2:** Different chimney heights for cases 1-4 of Study 1.

Case	$H_{ch}$ (cm)	$D_{ch}$ (cm)	$R_c$ (cm)	$H_c$ (cm)
<b>1 (verification case)</b>	300	20	150	6
<b>2</b>	150	20	150	6
<b>3</b>	250	20	150	6
<b>4</b>	350	20	150	6

Tables 3.2 represents the different chimney heights regarding different scenarios which are considered to study performance of the SCPP under various chimney heights.

### 3.5.1.2 Effect of Chimney Diameter

According to the analysis which have been done by other researchers [23], [43], it is determined that increasing the radius of the chimney increases the mass flow rate values and decreases the air temperature. Moreover, the results demonstrated that the chimney tower diameter has a greater impact than the height of chimney.

**Table 3.3:** Different chimney diameters for the cases 5-8 of Study 2.

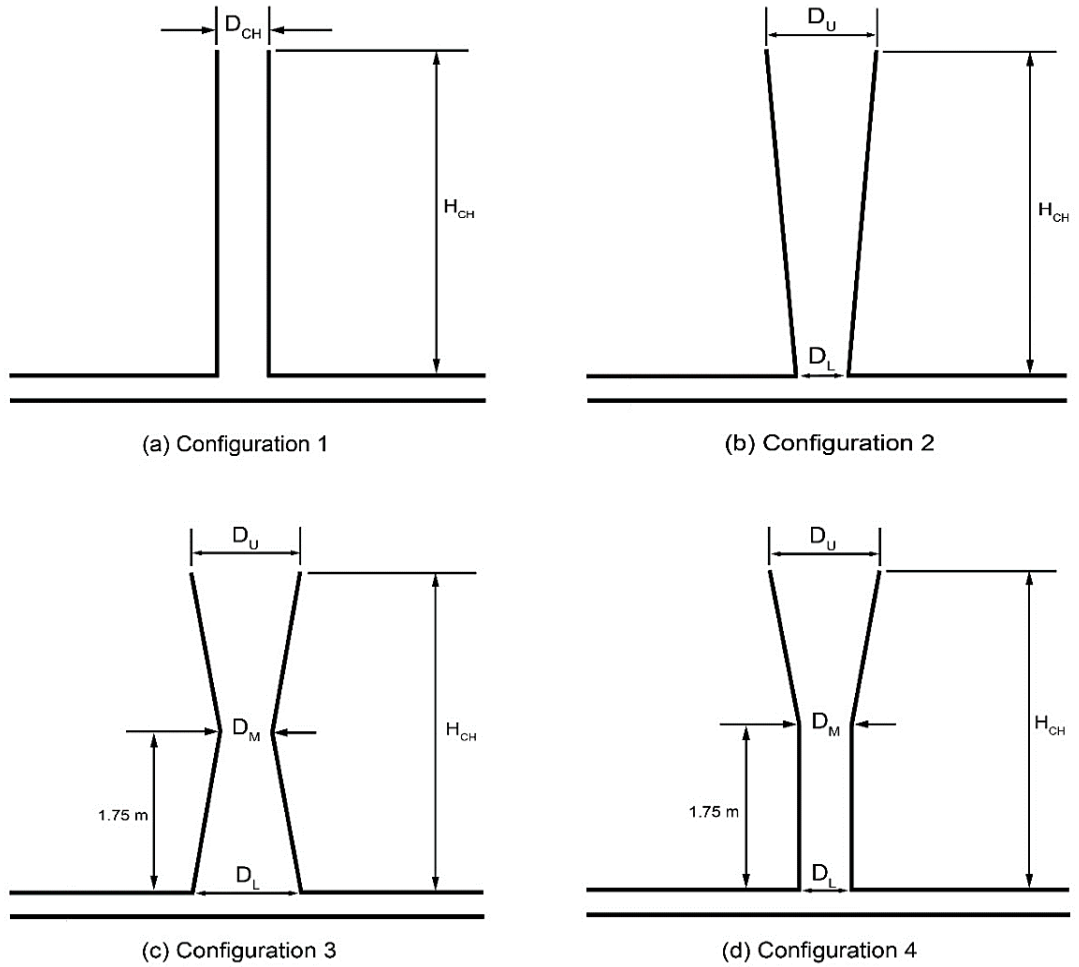
Case	D <sub>ch</sub> (cm)	H <sub>ch</sub> (cm)	R <sub>c</sub> (cm)	H <sub>c</sub> (cm)
5	20	350	150	6
6	15	350	150	6
7	25	350	150	6
8	35	350	150	6

Tables 3.3 represents the different cases with different chimney diameters which are considered to study the changes in performance of the studied SCPP under various diameter dimensions.

### 3.5.2 Different Tower Geometries

It has been observed that the effectiveness of the solar chimney power plant is influenced by geometrical parameters of SCPP [26],[44]. In the following part, effect of geometrical changes of the SCPP tower which have effect on the studied SCPP are presented. The change in tower geometry produces the differences in the air velocity values. The calculation of the maximum value of the air velocity within the SCPP can be obtained by choosing the efficient optimal geometry.

Figure 3.9 illustrate some of the different geometrical chimney configurations. Through this study, the effect of four chimney configurations on SSCP performance are studied. These configurations are standard chimney (case a), diverging chimney (case b), converging-diverging chimney (case c) and standard-diverging chimney (case d) as shown in Figure 3.9.



**Figure 3.9:** Some of the different geometries of the chimney configurations.

Tables 3.4 represents the different chimney configurations dimensions which are considered to find the changes in performance of the studied SCPP under various dimensions.

**Table 3.4:** Different geometries for the cases a-b-c-d- of Study 3.

Case	H <sub>ch</sub> (cm)	D <sub>ch</sub> (cm)	R <sub>c</sub> (cm)	H <sub>c</sub> (cm)	D <sub>U</sub> (cm)	D <sub>M</sub> (cm)	D <sub>L</sub> (cm)
a	350	25	150	6	-	-	-
b	350	25	150	6	35	-	25
c	350	25	150	6	35	25	35
d	350	25	150	6	35	25	25

### 3.5.3. Collector Parameters

Some of the parameters caused by the collector, which have effect on SCPP's to improve their performance can be regarded as, slope angle of the roof, the air velocity distribution, the temperature change of the air and the pressure difference. Regarding this fact, solar collector radius and the collector height can be considered as the important elements which directly impact the efficiency of the SCPP.

#### 3.5.3.1 Collector Diameter & Height

The bigger the radius of the collector, it means an increase in the power output [28, 45]. Due to the numerical results, the diameter dimensions have effect directly on the air characteristics.

Moreover, the collector height is one of the most important elements which have effects the performance of the SCPP [27, 46]. In fact, by increasing the height of the roof too much, the output power decreases.

**Table 3.5:** Different collector diameters for the cases 9-13 of study 4.

Case	R <sub>c</sub> (cm)	H <sub>c</sub> (cm)	H <sub>ch</sub> (cm)	D <sub>U</sub> (cm)	D <sub>L</sub> (cm)
9	100	6	350	35	25
10	125	6	350	35	25
11	150	6	350	35	25
12	175	6	350	35	25
13	200	6	350	35	25

Tables 3.5 represents the different collector diameter dimensions which are considered to find the changes in performance of the studied SCPP under different dimensions.

**Table 3.6:** Different collector heights for the cases 14-17 of Study 5.

Case	H <sub>c</sub> (cm)	R <sub>c</sub> (cm)	H <sub>ch</sub> (cm)	D <sub>U</sub> (cm)	D <sub>L</sub> (cm)
14	4	200	350	35	25
15	6	200	350	35	25
16	8	200	350	35	25
17	10	200	350	35	25

Tables 3.6 represents the different collector height dimensions which are considered to find the changes in performance of the studied SCPP under various dimensions.

### 3.5.3.2 Inclination Angle of Collector

The collector roof angles impact directly on air characteristics like temperature, velocity and pressure. After getting the best dimensions from previously conducted study explained in former parts, four different angles of the collector roof have been studied as written in Table 3.7. Through the literature studies it shown that the velocity of air increase at a negative slope angle for roof at the tower inlet where the wind

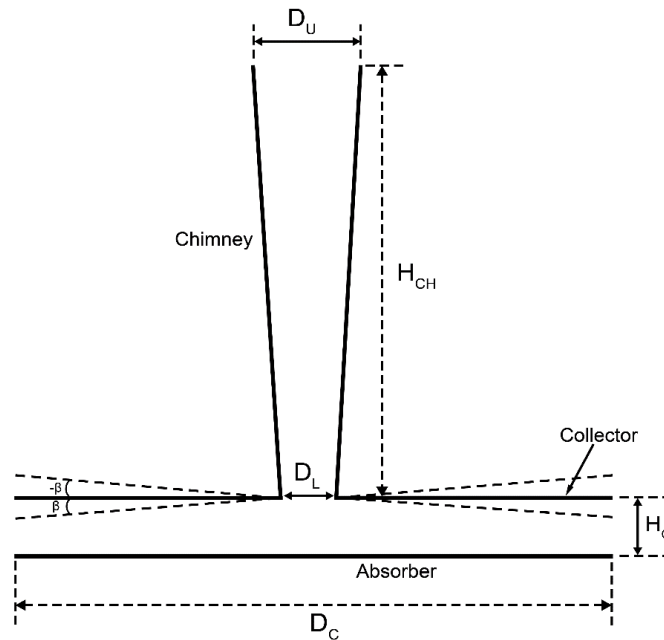


turbine is placed and the increase of the collector roof angle value can increase the pressure difference. Moreover, the slope angle of the roof affects directly on the static pressure inside the solar chimney [29, 47]. Fig 3.10 presents the Schematic diagram of inclination angle of collector.

**Table 3.7:** Different angle of collector roof for the cases 18- 21 of study 6.

Case	$\beta$ (inclination angle of collector)	$H_c$ (cm)	$R_c$ (cm)	$H_{ch}$ (cm)	$D_U$ (cm)	$D_L$ (cm)
18	0	6	200	350	35	25
19	0.5	6	200	350	35	25
20	-0.5	6	200	350	35	25
21	-1	6	200	350	35	25

Tables 3.7 represents the different angles the collector roof which are considered to find the changes in performance of the studied SCPP under various height dimensions.



**Figure 3.10:** Schematic diagram of inclination angle of collector.

## CHAPTER 4

### Results and Discussion

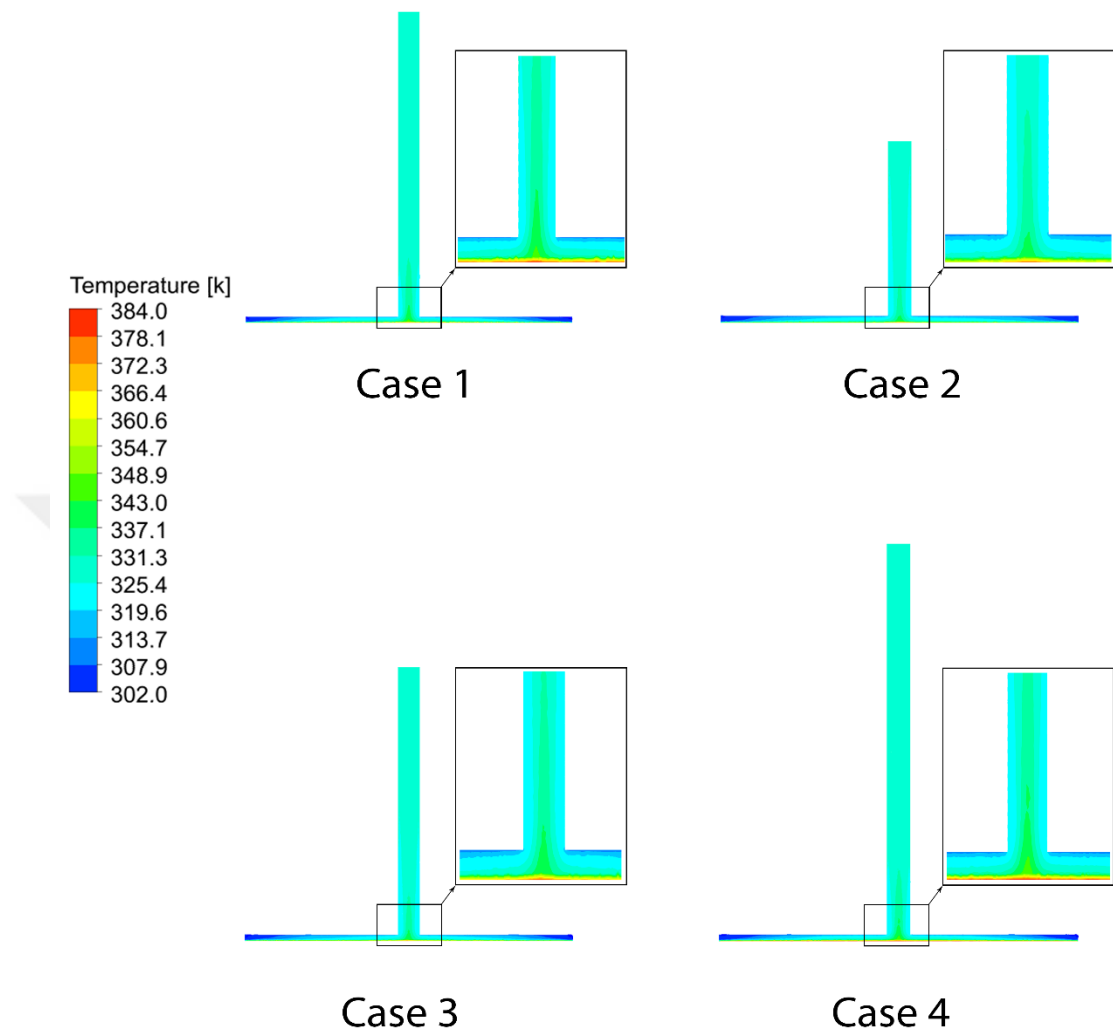
#### 4.1 Introduction

In Chapter 4, the findings which are obtained from the CFD simulations of SCPP are presented and discussed. Different chimney and collector parameters like tower height, tower diameter, tower configuration, collector diameter, collector height and inclination angle of the collector has been studied. To study the effect of changing each parameter, the output power and the air characteristics like temperature, velocity and pressure are examined. Power values are calculated by using SCPP performance equations in CH 2 especially equation 15.  $\Delta T$  is the temperature difference between ambient and inlet of the tower and  $V_{ch,max}$  is maximum velocity inside the chimney which are taken from numerical results and  $\Delta p_t$  is the pressure differences at turbine which is calculated by using equation 7. As mentioned before, k- $\epsilon$  turbulence model, one million number of mesh and 20000 number of iterations are used for whole simulations.

#### 4.2 Effects of Solar Chimney Height on SCPP Performance

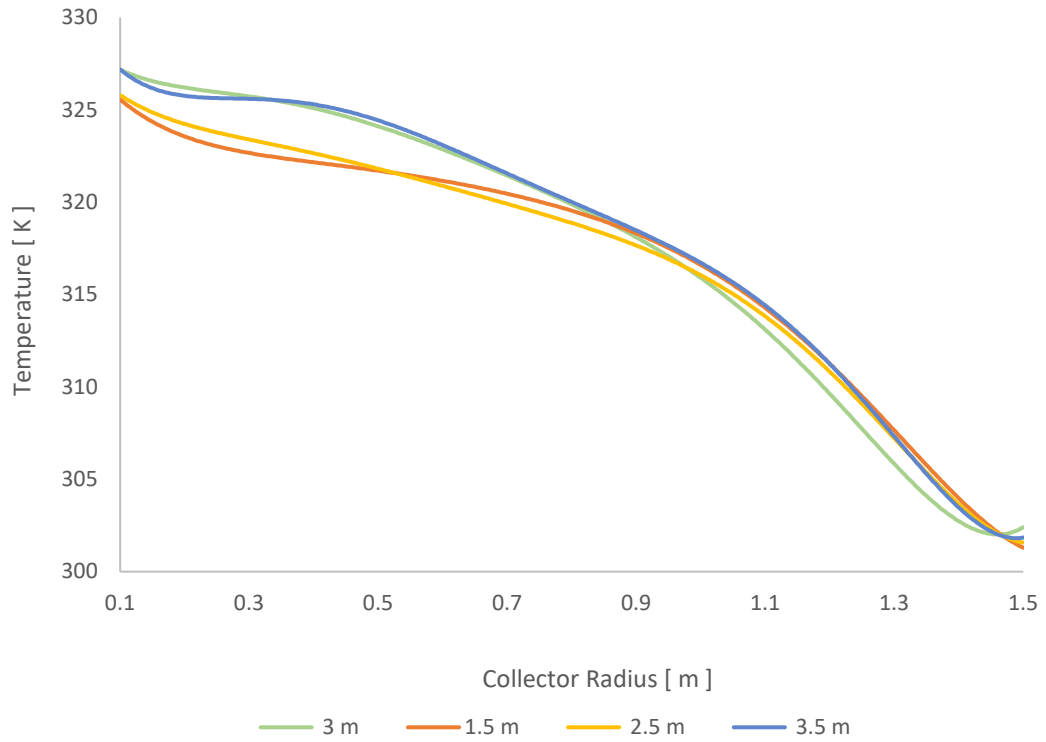
As it is mentioned in Chapter 3, one of the main elements which has direct impact on the SCPPs performance is the height of the tower. In the current study, the tower heights are considered between 150 cm to 350 cm as shown in Table 3.2.

Figure 4.1 shows the temperature field for different tower heights. According to these results, the change in tower height is accompanied by a slight change in the amount of temperature along the solar collector. For all cases, the area which has the highest temperature is the absorber wall since the absorber behaves as a heat storage which is exposed to solar irradiation.



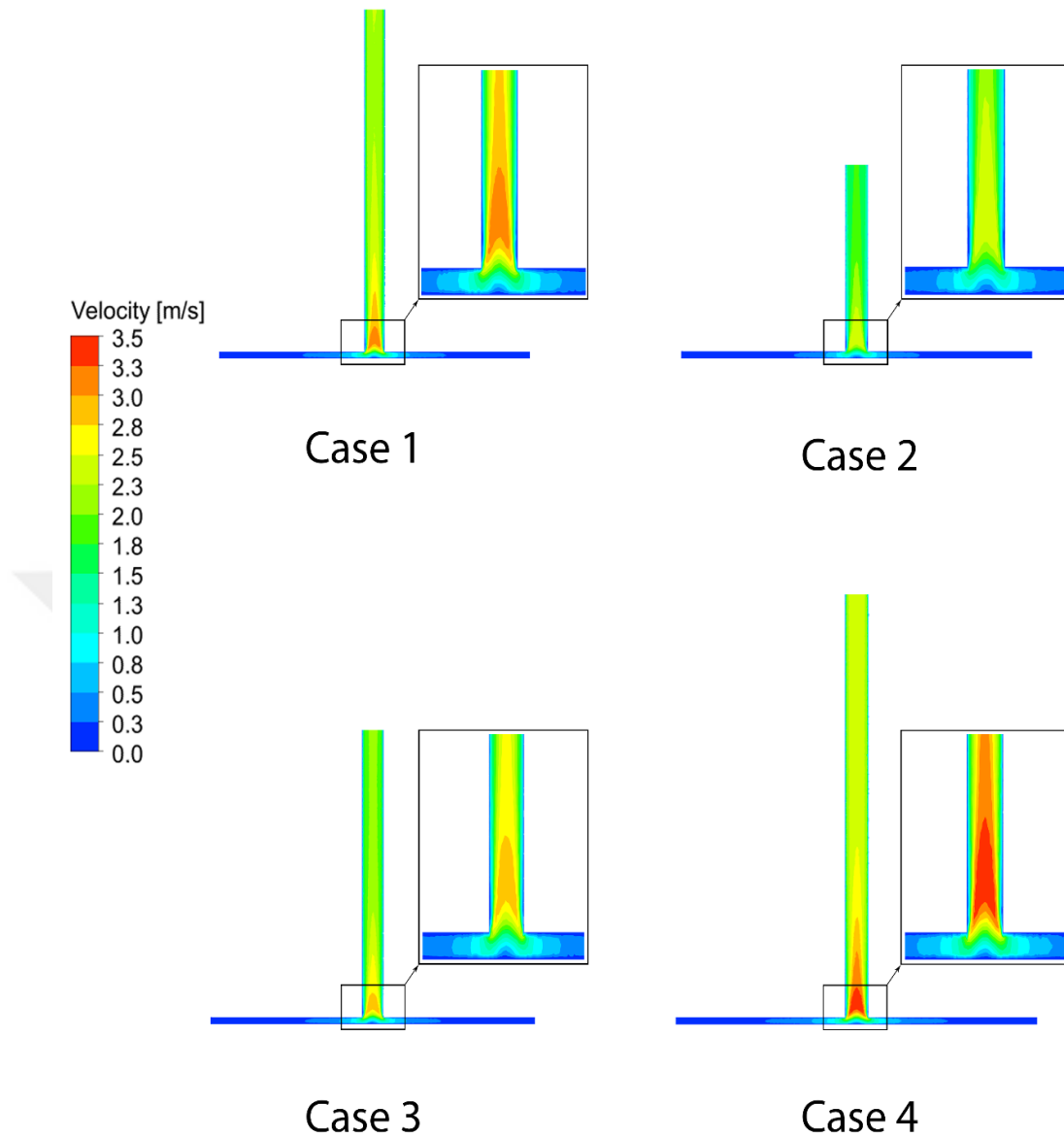
**Figure 4.1:** The simulation results for the air temperature distribution among various tower heights for cases 1-4 of study 1.

The impact of change SCPP's tower height on the air temperature profiles are represented in Figure 4.2. Figure 4.2 shows the distribution of temperature along the collector diameter for different cases of tower height, the temperature values increases with increasing tower height until reaching a specific height after which the change becomes less significant.



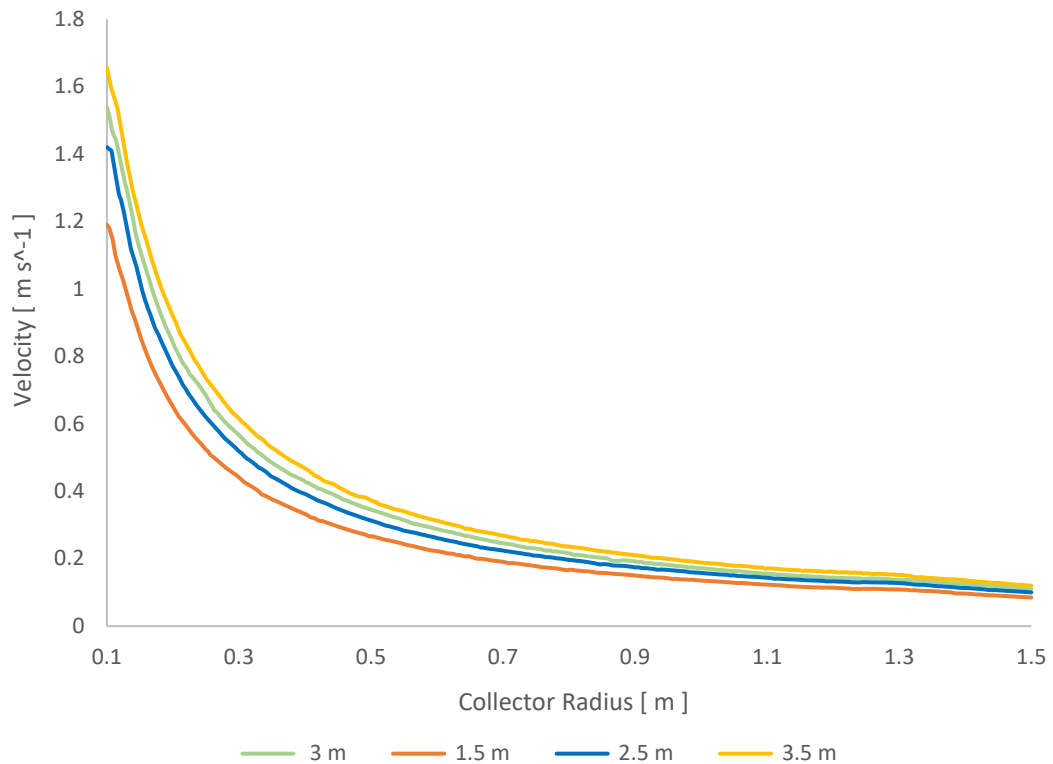
**Figure 4.2:** The influence of SCPP's tower height on temperature profile for cases 1-4 of study 1.

Figure 4.3 represents the distribution of air velocity for different dimensions as contours. It is evident that the value of velocity at the entrance of the collector is low and starts to increase along the collector till the collector exit which is located at the inlet of the tower. As presented in Figure 4.3 the maximum air velocity is located in the area at the inlet of tower and the intensity of this area and the value of air velocity increases by increasing the tower height.



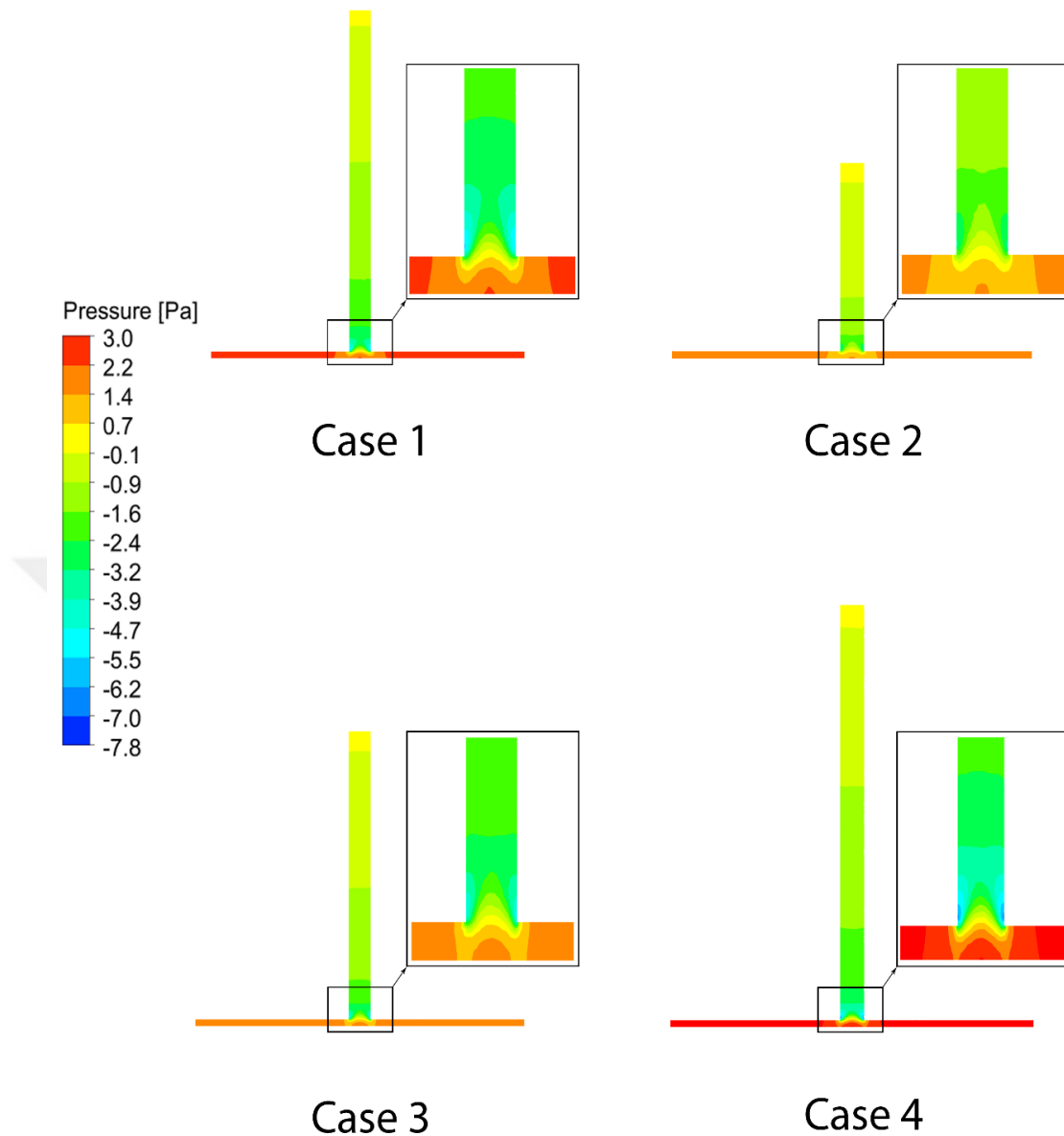
**Figure 4.3:** The simulation results for the flow velocity distribution among various tower heights for cases 1-4 of Study 1.

The distribution of air velocity inside SCPP for different cases of tower height is presented in Figure 4.4. Figure 4.4 confirms that increasing of tower height affects the values of air velocity until highest tower which is equal to 3.5 m and this increase of velocity values occurs due to increasing of the pressure difference between entrance of collector and the exit of the tower.



**Figure 4.4:** The influence of SCPP's tower height on the air velocity profile for cases 1-4 of Study 1.

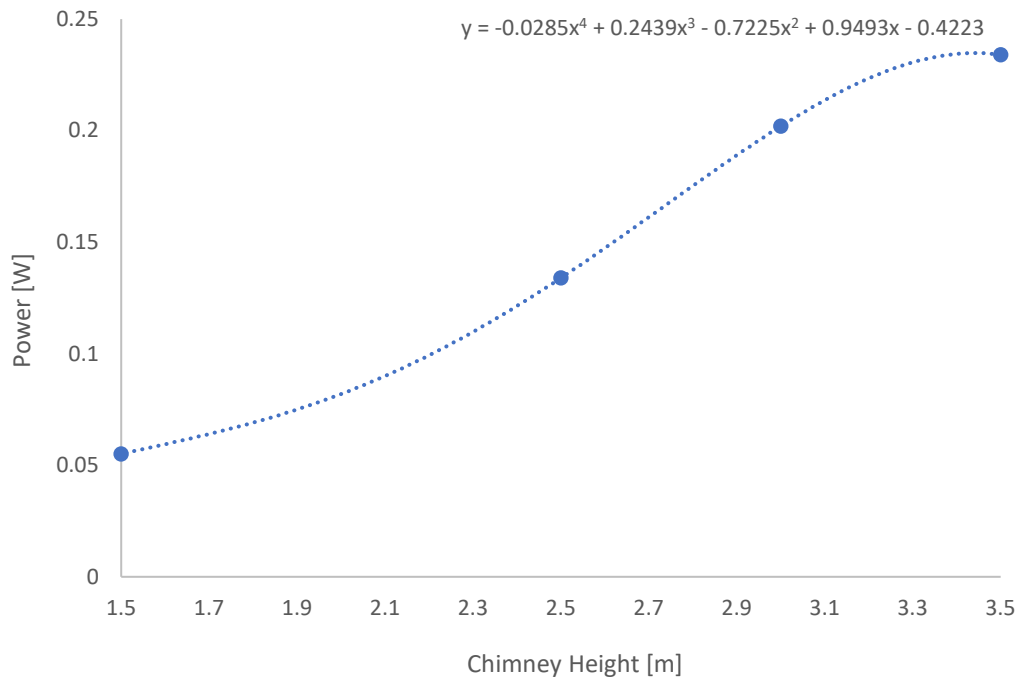
Figures 4.5 illustrates the impact of changing the height of the studied tower on the static pressure variation. The considered contours are 3m, 1.5m, 2.5m and 3.5m, which the results based on them are mentioned with case 1, case 2, case 3 and case 4 in Figure 4.5. Based on the results which are depicted in Figure 4.5, when the height of the studied SCPP is increased, the difference of air pressure will be increased. The value of static pressure is small at entrance of the tower inlet near tower wall and it starts to increase along the chimney until reaches the maximum value at tower exit. In addition, the pressure difference in the tower is in charge of the airflow along the tower. Therefore the increasing in the height of tower will lead to increasing the flow rate that inside the tower.



**Figure 4.5:** The simulation results for the static pressure distribution for different tower heights for cases 1-4 of Study 1.

According to the findings which are obtained from Figure 4.3, 4.4 and 4.5, when the height of the SCPP tower is increased, flow rate and velocity of air increases. Figure 4.6 illustrates the impact of the height of the tower on the output power of the studied SCPP. From Figure 4.6, it has been noticed that increasing the chimney height leads to a steep increase in output power, but after reaching a critical point of tower height as presented in Figure 4.6, the increase in power of SCPP is slight compared to before. According to Figure 4.6, the simulation findings corroborate that, when the height of the SCPP

tower increase, then the power of it will be increased too but a critical height should be considered for construction cost and feasibility of the chimney.



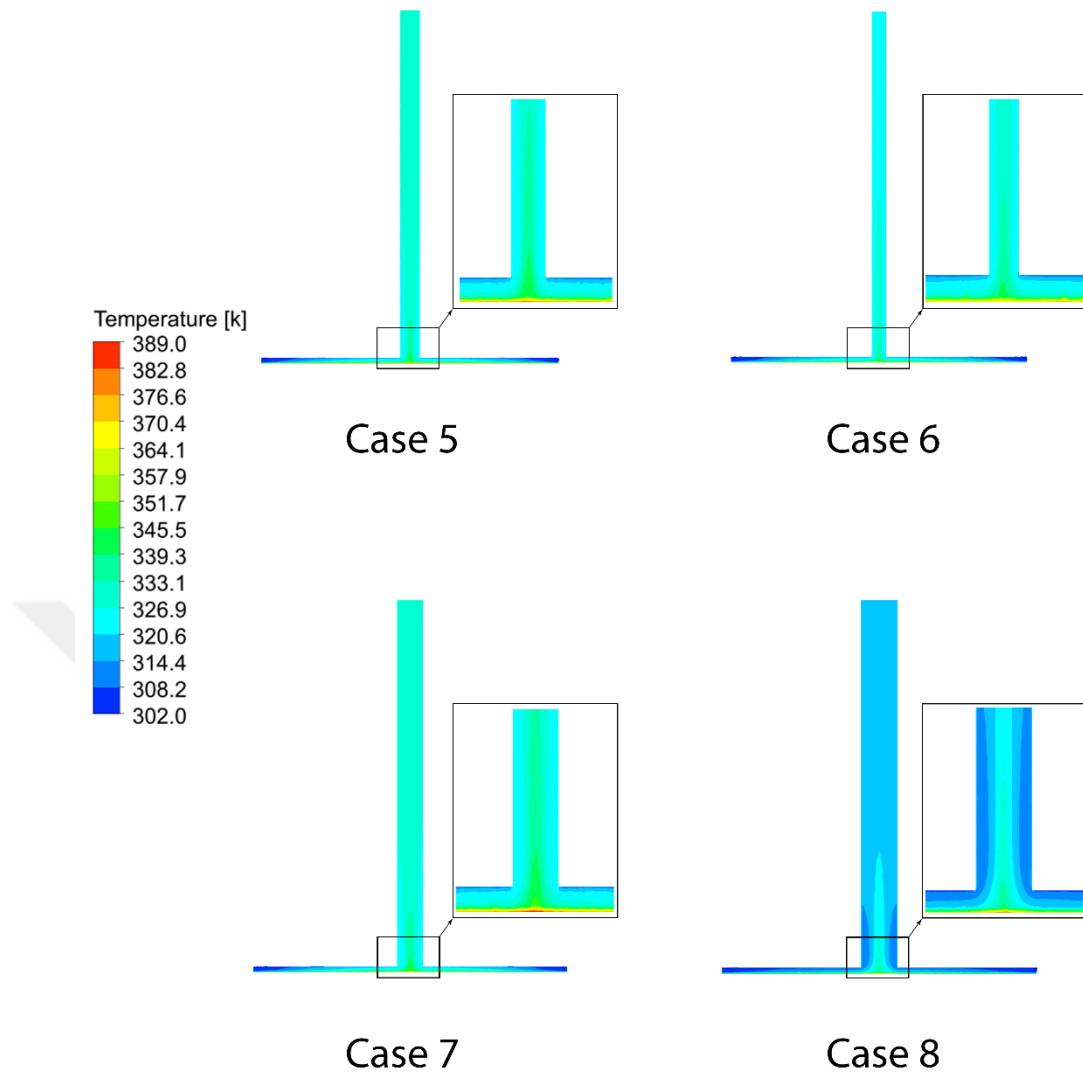
**Figure 4.6:** variation of power with respect to SCPP's tower height.

### 4.3 Effects of Solar Chimney Diameter on SCPP Performance

In the following, simulation results which are based on different diameter dimensions of solar chimney are presented. The diameter of the studied SCPP chimney are considered as, 20 cm (case 5), 15 cm (case 6), 25 cm (case 7) and 35 cm (case 8).

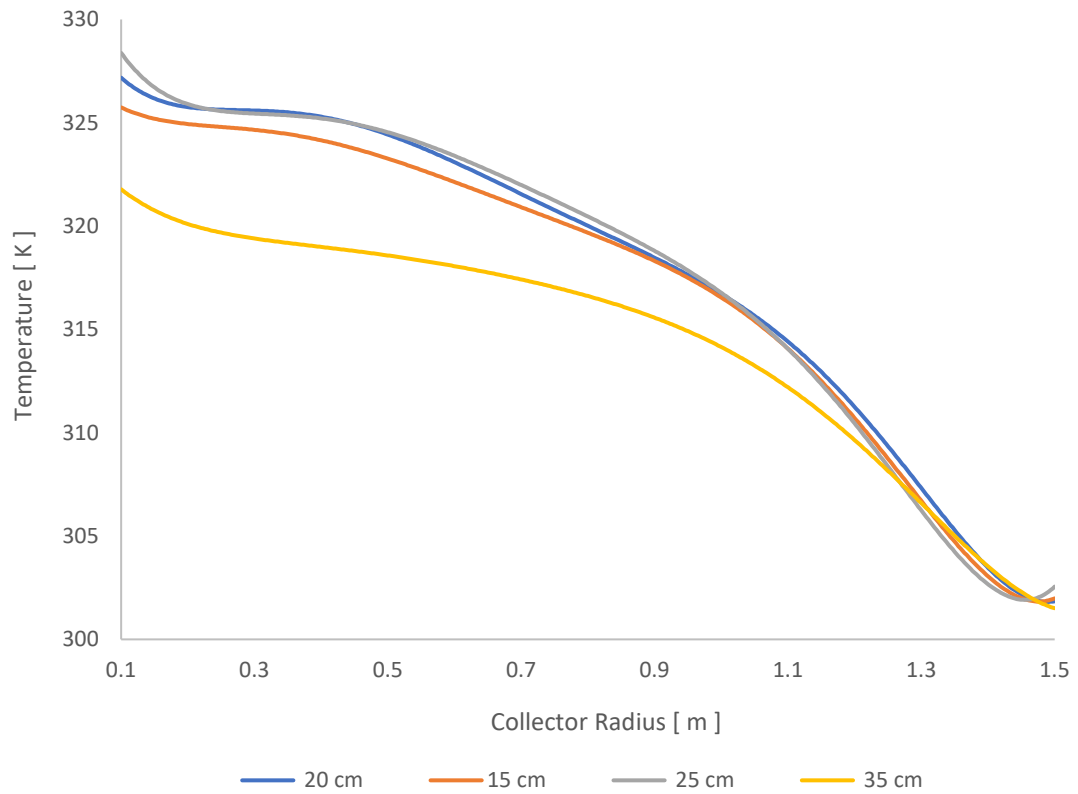
The influence of diameter change of the studied SCPP's tower on the temperature of air which is flowing inside the chimney is illustrated in Figure 4.7. As shown in Figure 4.7 the maximum value of temperature exists at the base (on the absorber especially at the inlet of the tower) and minimum temperature value on the collector roof. Also it is clear that the tower diameter has a big effect on temperature distribution especially at the entrance of the chimney.





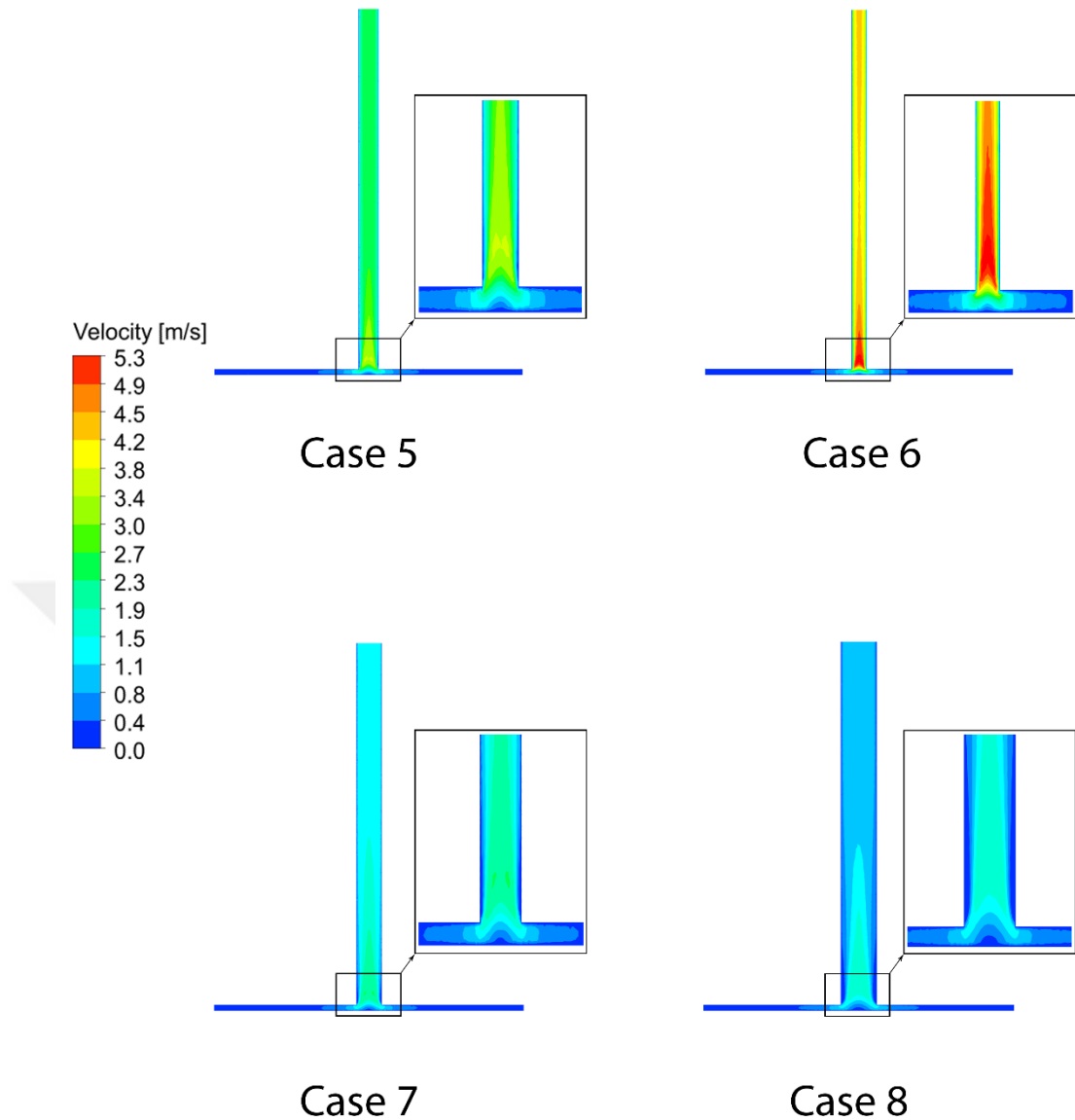
**Figure 4.7:** The simulation results for the air temperature distribution among various tower diameters for cases 5-8 of Study 2.

Figure 4.8 represents the influence of changing the tower diameter on the air temperature profile. From Figure 4.8 it has been noted that the air temperature inside SCPP increases with increasing tower diameter until reaching a best value (around 25 cm) and after that the temperature starts to drop due to the requirement of high thermal power to heat large volume of chimney tower caused by the large diameter.



**Figure 4.8:** The effect of SSCP's tower diameter on its temperature profile for cases 5-8 of Study 2.

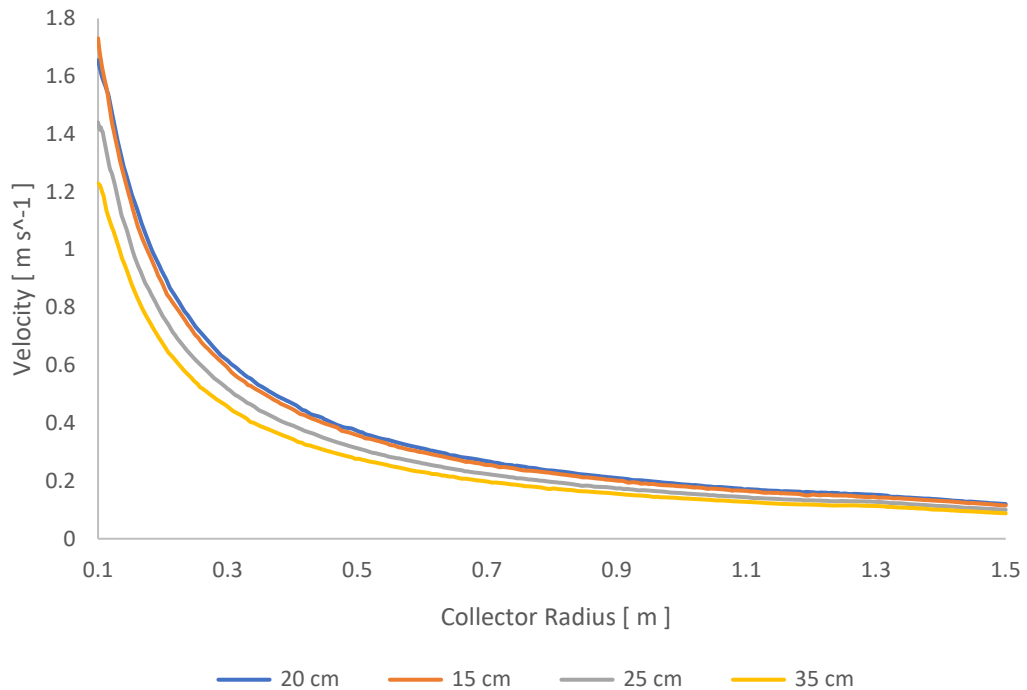
Figure 4.9 represents the influence of change in diameter of the studied SSCP's tower on the air velocity of the flow inside. The velocity contour shows that the highest value of air velocity exists at tower inlet where the maximum pressure difference occurs but it starts to decrease along the tower and the minimum air velocity value for SSCP appears at the entrance of the collector.



**Figure 4.9:** The simulation results for the flow velocity distribution among various tower diameters for cases 5-8 of Study 2.

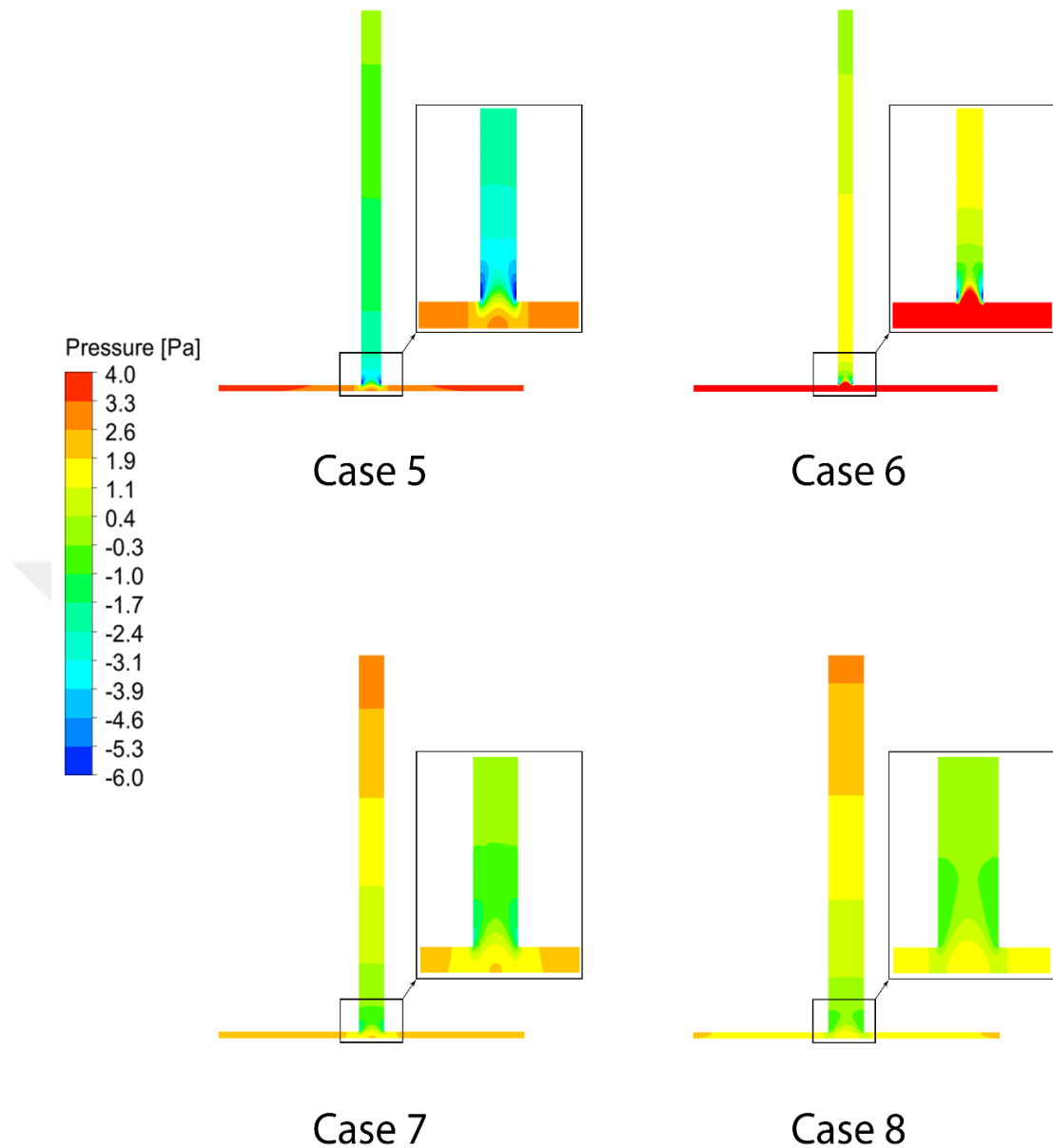
Figure 4.10 represent the influence of changing SCPP tower diameter on the air velocity. Due to Figure 4.10 it can be seen that, the air velocity increases in the direction of inlet to center of the chimney. Also it is clear that the air velocity decreases with increasing chimney diameter first, which the air velocity reaches to its maximum value at case 6 and its minimum value at case 8. This decreasing in air velocity values are caused by pressure change which decrease with changing of chimney diameter. As a conclusion, the results show that the diameter of tower has significant impacts on the

distribution of air velocity inside the tower and it can be considered as an important parameter to improve the effectiveness of SCPP.



**Figure 4.10:** The effect of SCPP’s tower diameter on its velocity profile for cases 5-8 of Study 2.

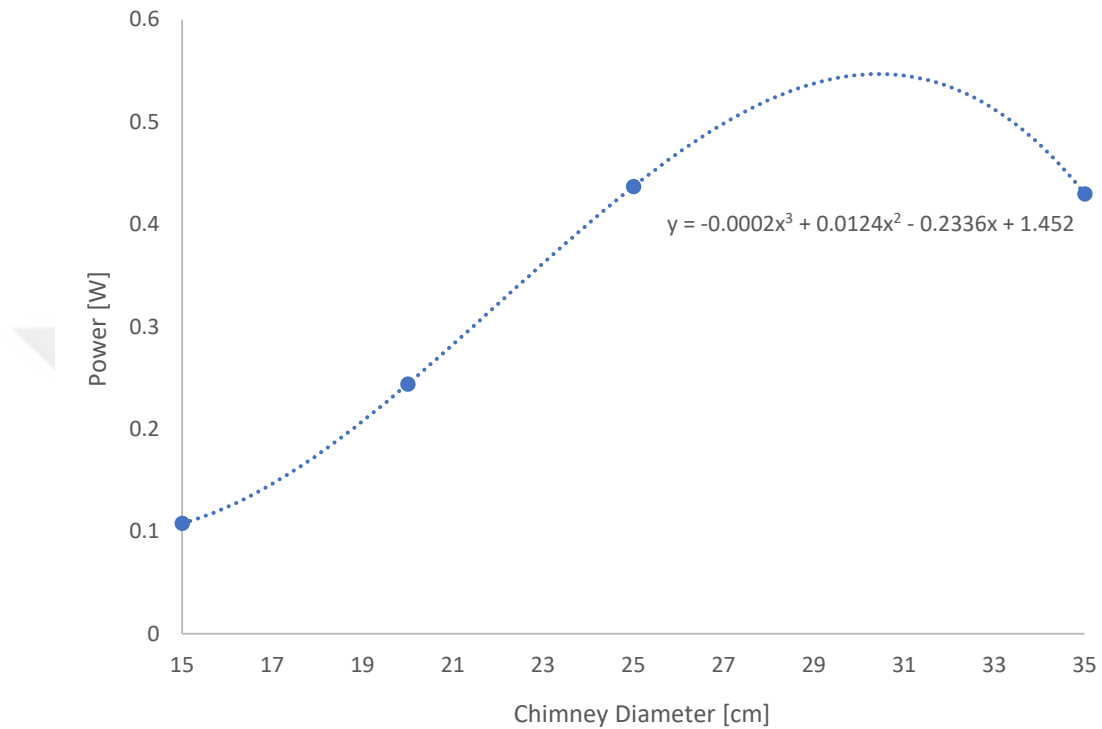
Figure 4.11 illustrates the effect of change of chimney diameter on the static pressure. According to the proposed results, increasing the diameter of the chimney produces the drop in the mass flow rate which cause the pressure decrease. From Figure 4.11 it is obvious that the pressure is maximum on the collector, it decreases until reaches the minimum value at the inlet of the tower and starts increasing until the outlet of the tower. From the results, the diameter of the tower has an important influence on the pressure difference that happen in area between the collector outlet and the tower inlet. Furthermore, it is clear that the pressure difference decreases relatively with increasing tower diameter and this leads to decrease of the velocity value.



**Figure 4.11:** The simulation results for static pressure distribution among various tower diameters for cases 5-8 of Study 2.

The variations in the tower diameter on the output power of SCPP is illustrated in Figure 4.12. From results it has been noted that increasing diameter of the tower leads to increase of the output power until reaching some specific value of tower diameter. After that best point, the value of the output power starts to decrease and from that point, it has an adverse impact on the power and efficiency. This decrease in the value of the output power is because the air temperature and the pressure difference decreases largely after that point. For this reason, the increasing in the diameter of the

chimney is determined by the power factor and this leads to choose a best diameter for the tower. Moreover, according the simulation results the best choice for the diameter of the tower is 25 cm.

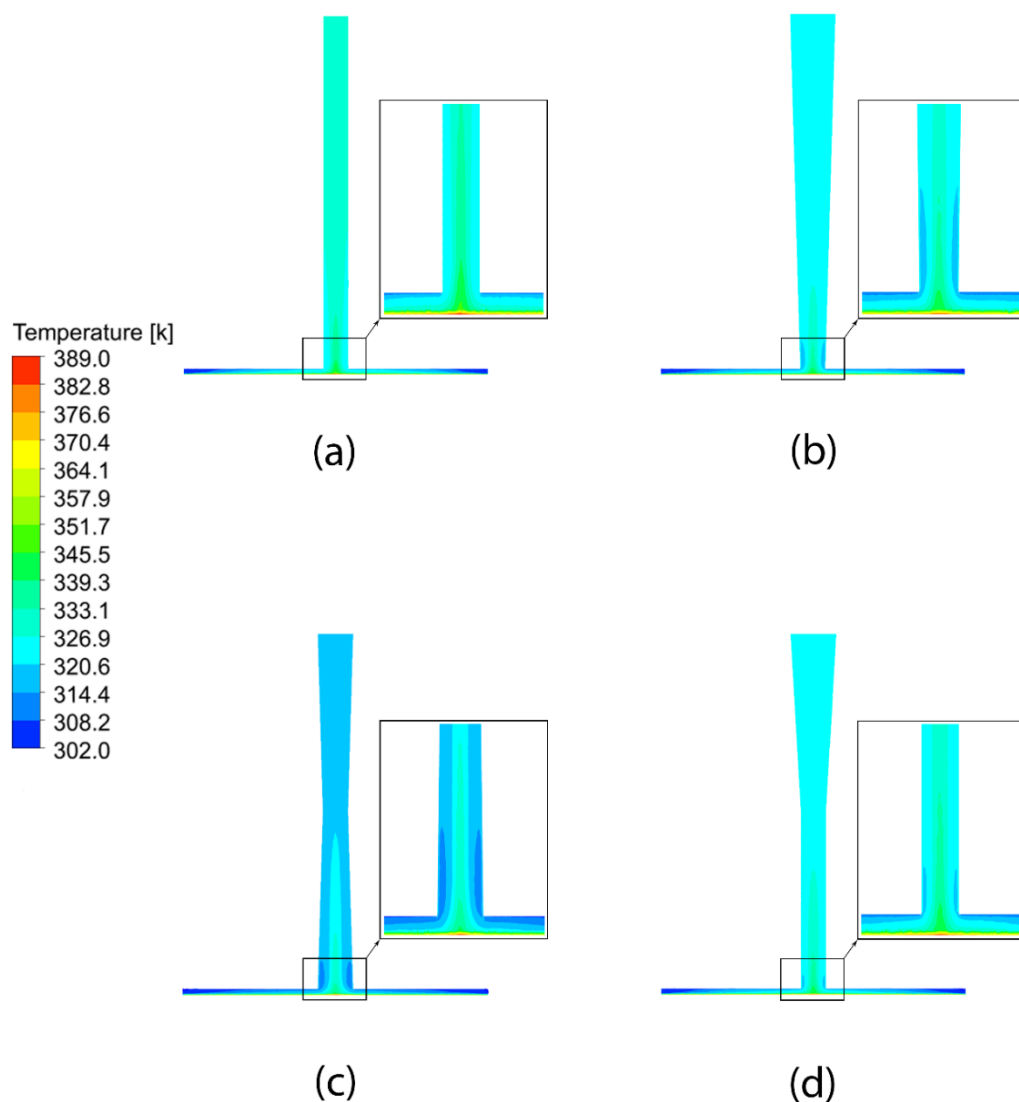


**Figure 4.12:** variation of power with respect to SCPP's tower diameter.

#### 4.4 Effects of solar chimney geometry on SCPP Performance

Based on the section 4.2 and 4.3, it has been noted that the performance of the studied SCPP is related to the geometrical parameters like the tower height and diameter. In the following part, four different structure of chimneys which are usually used for the SCPP are analyzed in terms of their performance on regarding air pressure, temperature and velocity. In the following the chimneys configurations considered are, standard chimney (case a), diverging chimney (case b), converging-diverging chimney (case c) and standard-diverging chimney (case d), which can be seen in Figure 3.10 and Table 3.4.

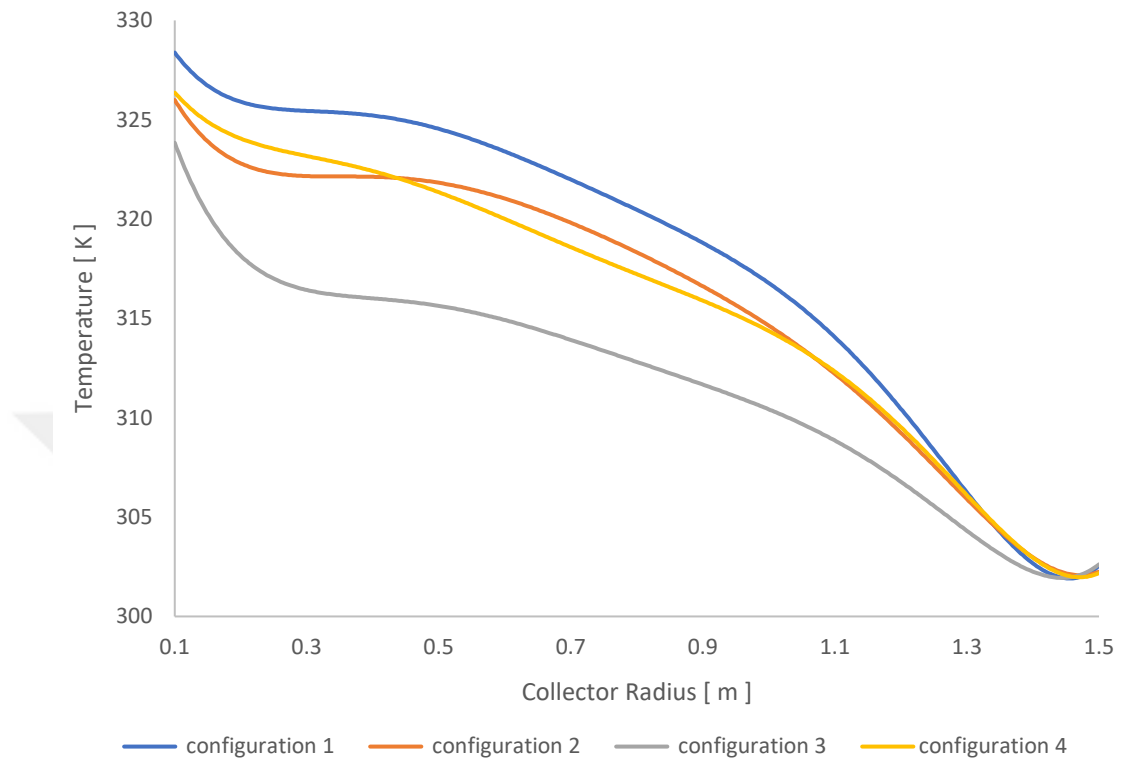
Figure 4.13 represents the changes in the temperature of the air inside SCPP based on different chimney configurations. From Figure 4.13, it has been noted that the first half of the tower has the biggest changes in temperature distributions especially at inlet of the tower. Due to Figure 4.13 the contours show how the air temperature is affected by changing the configurations of tower and it is obvious that at the converging-diverging tower the air temperature at the entrance of tower is affected badly and it changes slightly with diverging tower and standard-diverging tower.



**Figure 4.13:** The simulation results based on the different configuration of the studied SCPP chimney on the flow temperature for cases a-b-c-d of Study 3.

Figure 4.14 represents the distribution of air temperature inside SCPP for different configurations of the tower. It can be seen that, temperature distribution trends are same for all cases except the converging-diverging tower (case c) which has different

temperature distribution especially at the area at end of collector near to tower entrance. Also it noticed that, the standard tower (case a) has the highest air temperature throughout the collector diameter.

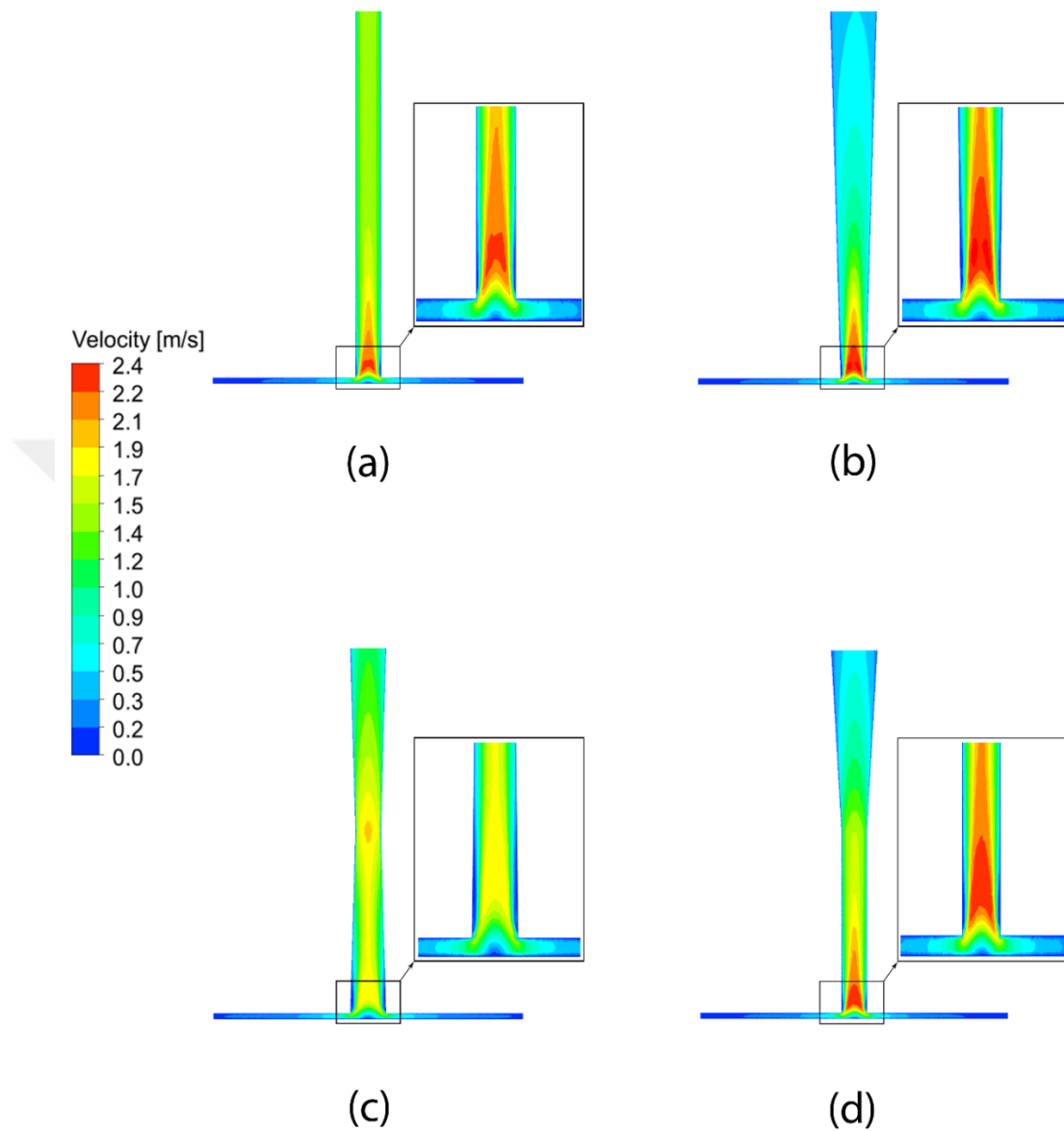


**Figure 4.14:** The influence of different SCPP's tower configurations on its temperature profile for cases a-b-c-d of Study 3.

Figure 4.15 illustrates the air velocity contours based on different tower configurations. It is clear that the biggest changes happen at the inlet of tower which effect largely on airflow velocity, therefore the design of this region is so important to increase the efficiency of SCPP. The contours indicate that the maximum air velocity appears at entrance region of the tower for all cases but the velocity gradient differs among the different configurations. For both the standard-diverging (case d) and diverging tower (case b), velocity is decreasing near the exit but for standard (case a) and the converging-diverging (case c) tower the velocity magnitude is almost same among the tower. Moreover, the area which has the maximum velocity near the tower inlet differs also from geometry to another and the maximum velocity region is at the diverging tower. Furthermore, the converging-diverging configuration (case c) has the



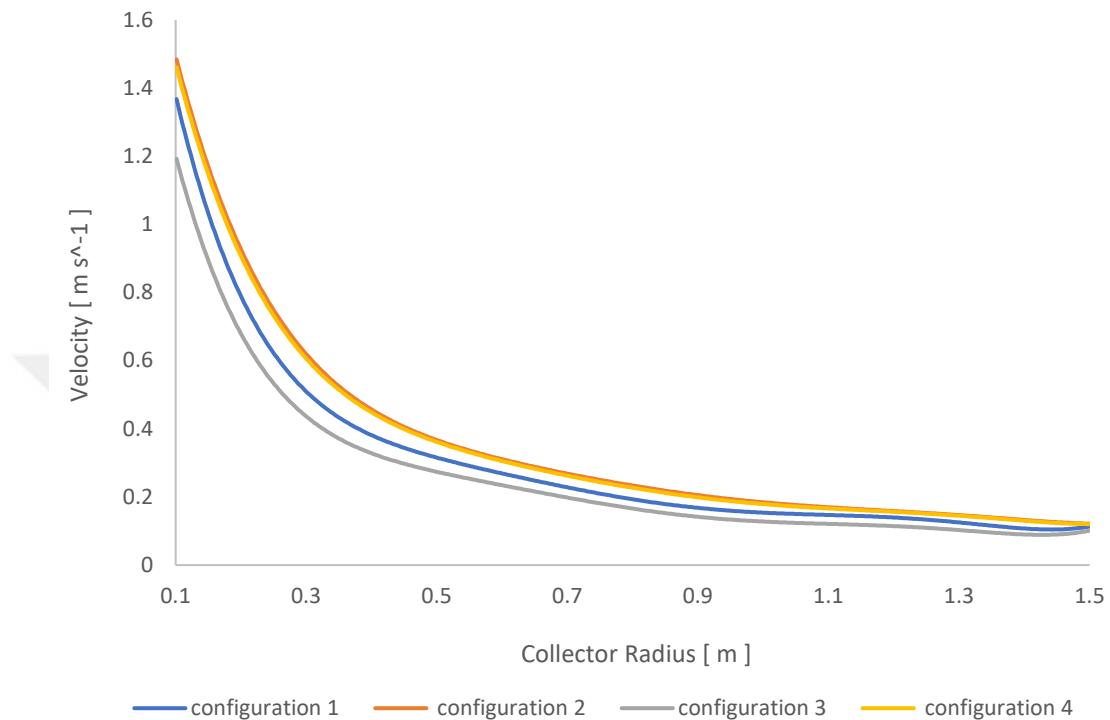
highest value of velocity at the middle of the tower because of area reduction and this is not advantageous for the turbine configuration.



**Figure 4.15:** The simulation results based on the different configuration of the studied SCPP chimney on the flow velocity for cases a-b-c-d of Study 3.

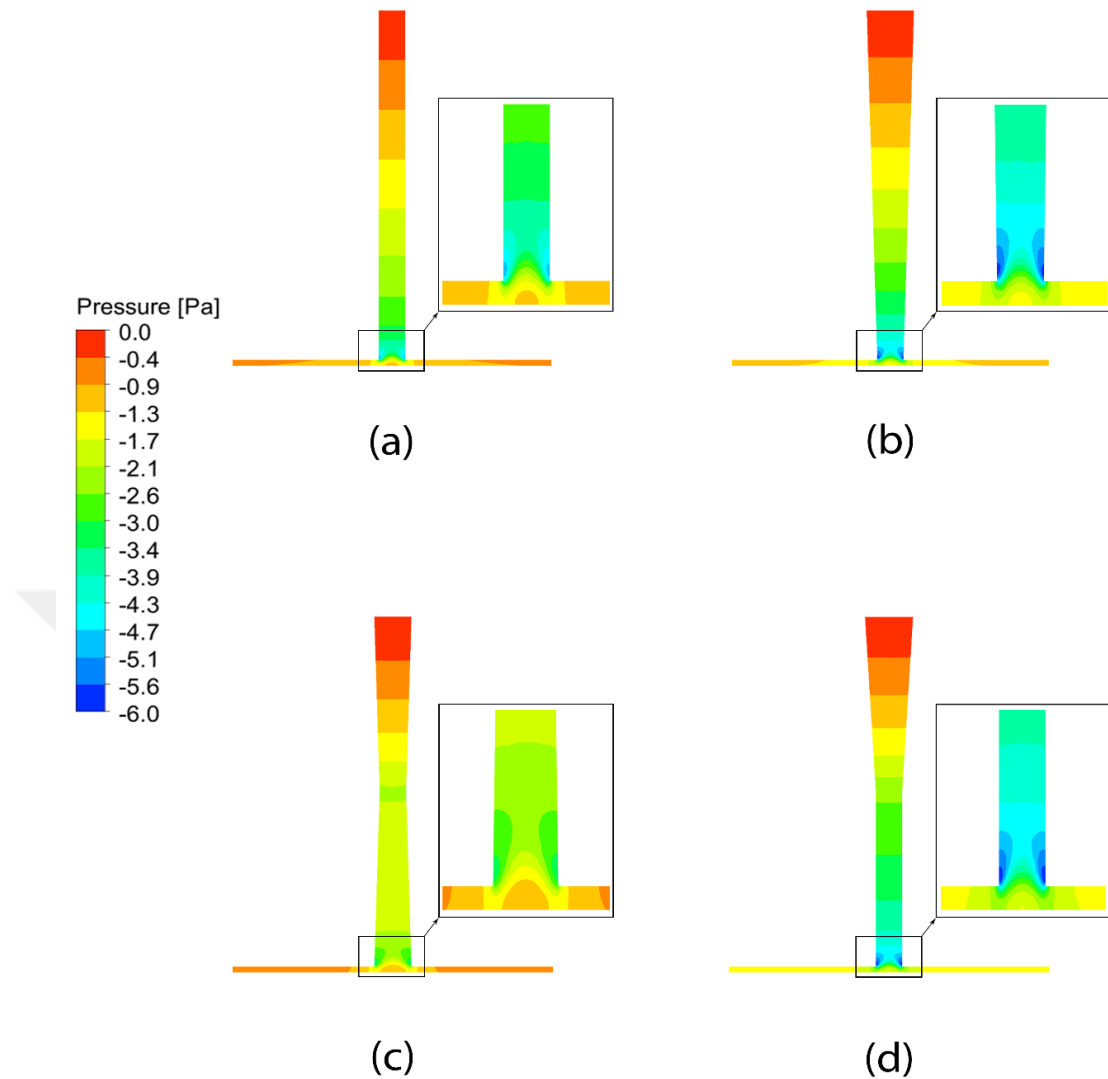
The distribution of air velocity inside SCPP for different tower configurations are displayed in Figure 4.16. Due to Figure 4.16 results shows that trend lines of air velocity are similar for all configurations but the highest value for each case differs from geometry to another. Moreover, the diverging tower (case b) has the maximum

velocity compared to other configurations and the converging-diverging tower (case c) has the lowest magnitude of air velocity. The outcomes indicate that changing the tower configuration has impacts on the air velocity thus effects largely on the effectiveness of the whole SCPP.



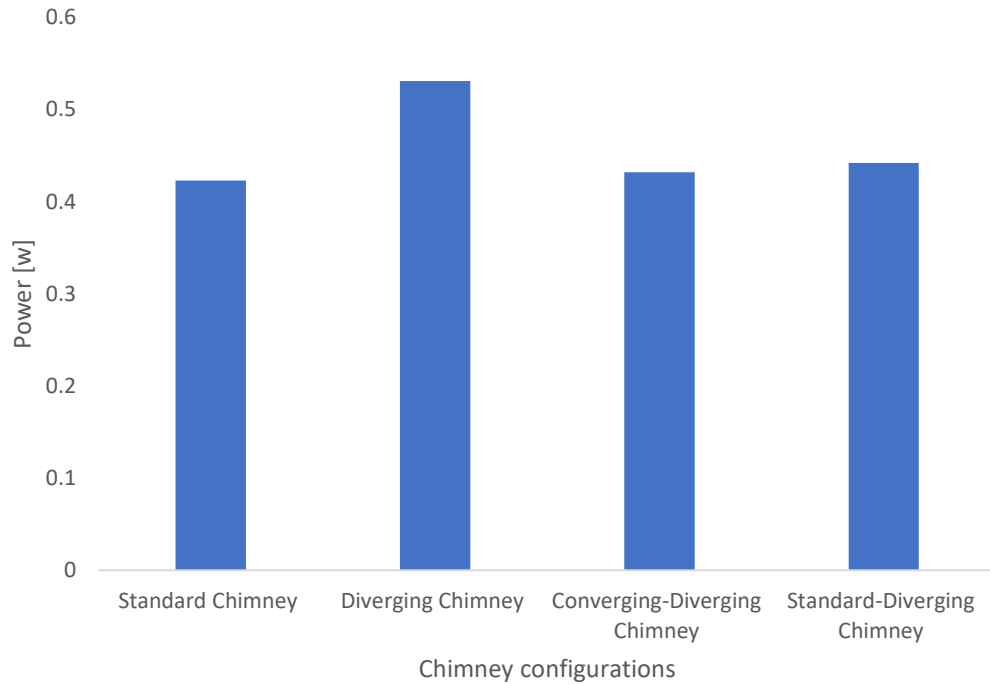
**Figure 4.16:** The influence of different chimney configurations on its velocity profile for cases a-b-c-d of Study 3.

The impact of varying the tower configuration on pressure distribution is illustrated in Figure 4.17. The contours indicate the presence of high and low pressure areas along both collector and tower but the distribution differs from configuration to another. For all considered geometries of different cases, the maximum pressure difference occurs at the inlet of the tower but among all configurations, maximum pressure difference happens in both the diverging tower (case b) and the standard-diverging tower (case d). The lowest pressure difference occurs in the converging-diverging tower (case c). The results confirm that the area at inlet of the tower is very important for the flow and it can have a significant effect on magnitude of the velocity due to the pressure imbalance which produces the air flow inside the SCPP. Based on the above, choosing an appropriate design and configuration is an important factor in increasing the pressure difference thus the air velocity which leads to improve the performance of SCPP.



**Figure 4.17:** The simulation results based on the different configuration of the studied SCPP chimney on the static pressure for cases a-b-c-d of Study 3.

The values of the output power of the SCPP for the different tower configurations are presented in Figure 4.18. The energy production which can be obtained from turbine is proportional to magnitude of the air velocity inside the SCPP. Therefore, the key to raise the value of the energy production is increasing the magnitude of the air velocity and thus the value of pressure difference. According to findings, it is obvious that the value of SCPP's output power is affected by the shape of the tower. Furthermore, it has been noted that the divergent tower (case b) is the best configuration which is chosen for the best design of the tower due to its highest output power and relatively simpler geometry compared to other configurations of cases c and d.



**Figure 4.18:** variation of power with respect to SCPP's chimney configurations.

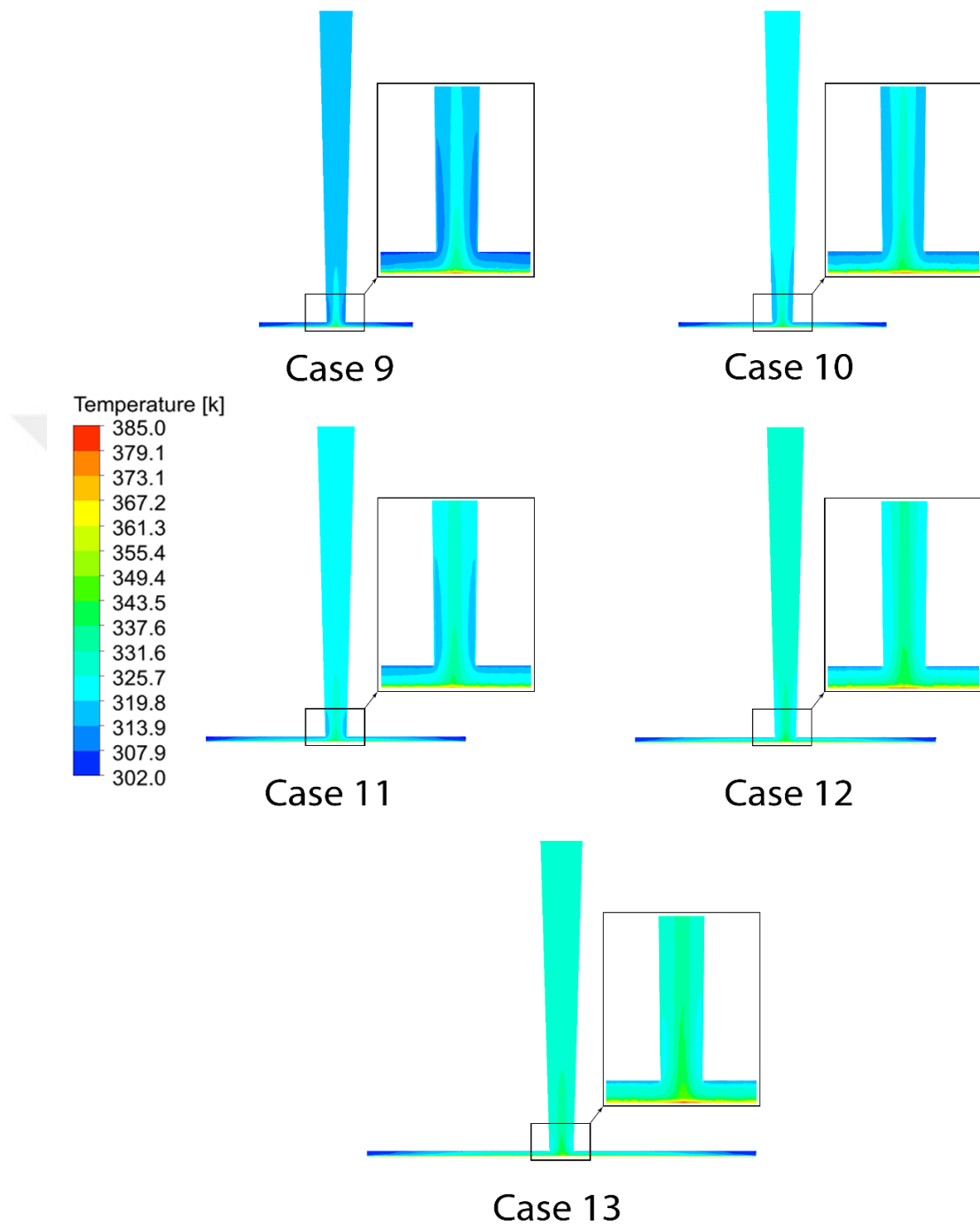
#### 4.5 Effects of Collector Diameter on SCPP Performance

In the following part, the impact of the magnitude of the diameter of the solar collector on the studied SCPP's performance are presented. According to Table 3.5 the considered diameters for assessing the performance of the SCPP are, 200, 250, 300, 350 and 400 cm, respectively.

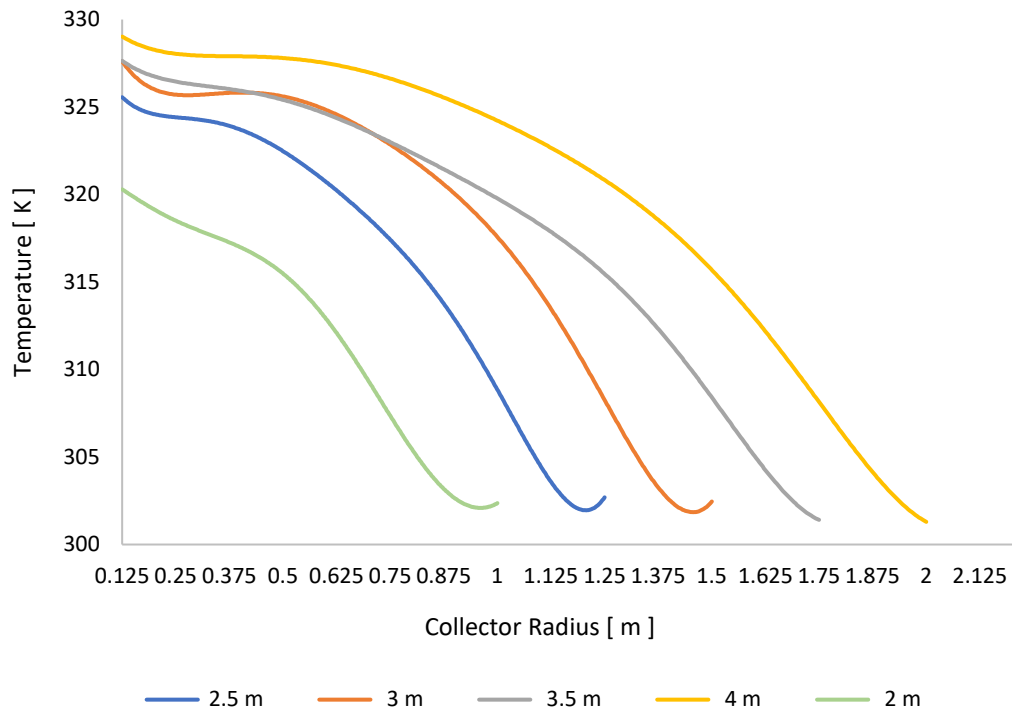
The distribution of air temperature for different collector diameters are presented in Figure 4.19. Due to the results, it is obvious that the maximum temperature exist at absorber and lowest temperature at the entrance of collector and the air temperature starts to increase until reaching to the maximum value at entrance of the tower. From Figure 4.19, It is noteworthy that the area located at entrance of the tower is affected by varying the diameter of the collector and the temperature gradient increases by increasing collector diameter.

The influence of change of SCPP collector diameter on the air temperature is presented in Figure 4.20. The results indicate that increasing collector diameter increases the temperature values. Moreover, the temperature distribution curve is similar for all

diameters, but its value differs and increases by increasing the collector diameter until reaches the maximum value at collector diameter equal to 4 m (case 13).

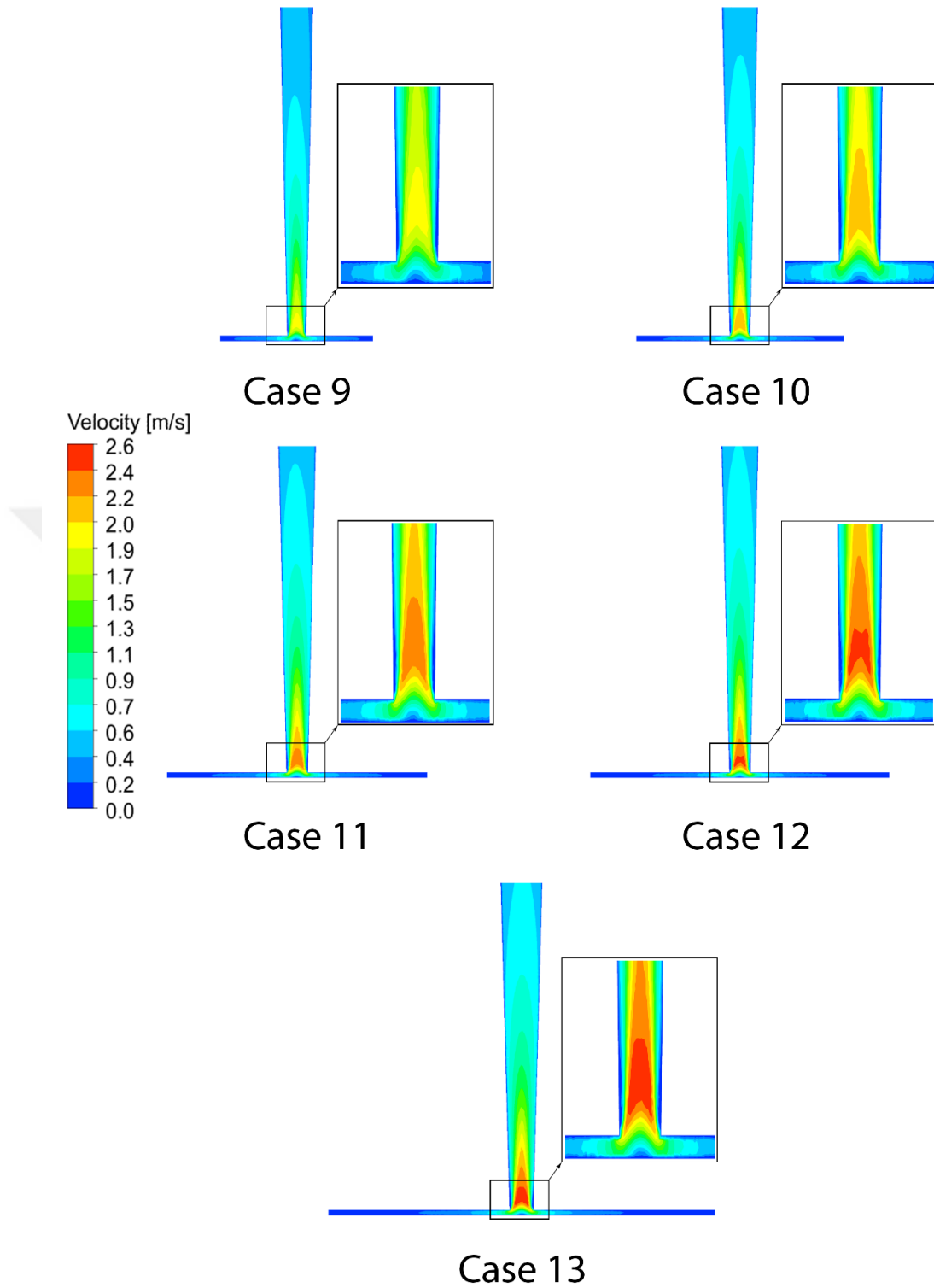


**Figure 4.19:** The simulation results for the air temperature distribution among various diameters of the SCPP collector for cases 9-13 of Study 4.



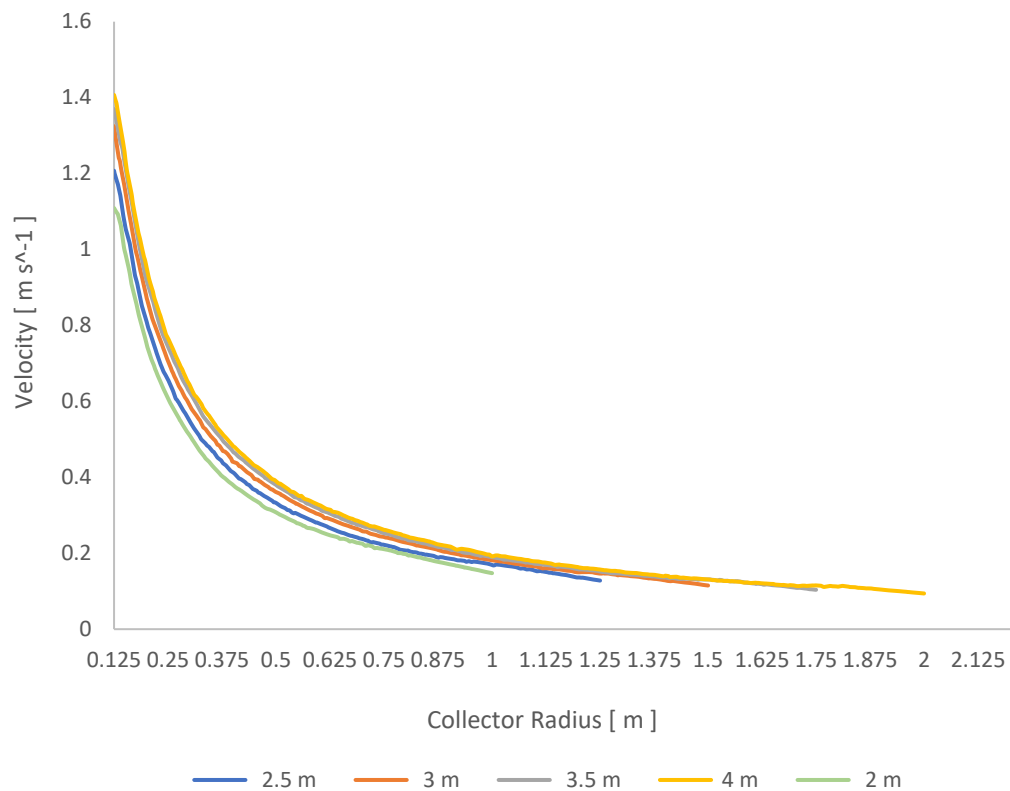
**Figure 4.20:** The influence of SCPP’s collector diameter on its temperature profile for cases 9-13 of Study 4.

The influence of change in diameter of the studied SCPP’s on the air velocity are presented in Figure 4.21. The contours shows similar velocity distribution for all cases but the magnitude of the air velocity differs from diameter to another. From Figure 4.21. It is clear that the area at entrance of the tower has the maximum velocity change by changing the value of diameter.



**Figure 4.21:** The simulation results for the flow velocity distribution among various collector diameters of the SCPP for cases 9-13 of Study 4.

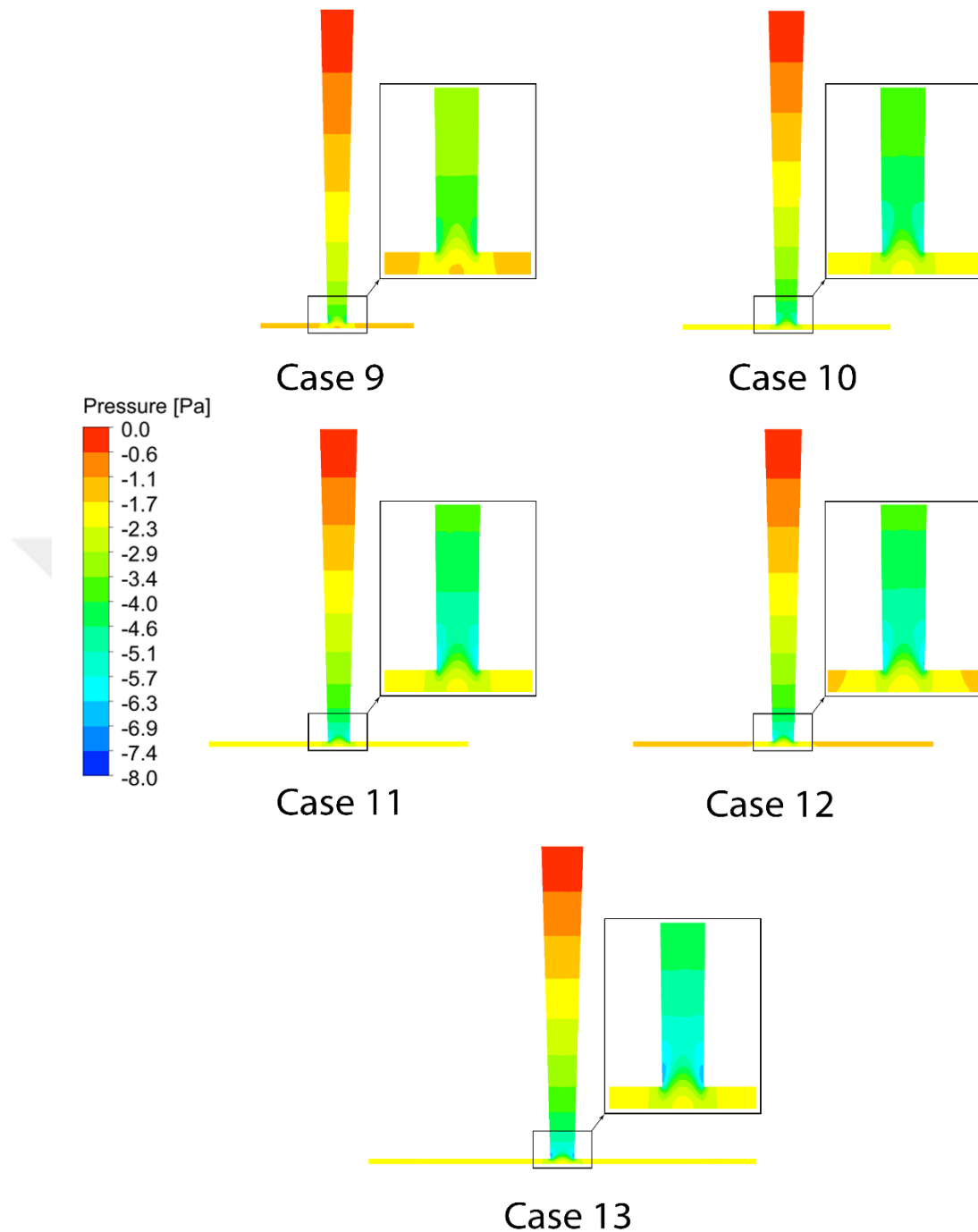
The influence of change of SCPP collector diameter on the air velocity is represented in Figure 4.22. The results shows that the velocity of air is affected largely by varying collector diameter. Moreover, the velocity profiles are the same for all considered cases but the maximum value for each curve differs with increasing of collector diameter and at collector diameter equal to 4m (case 13) it reaches to highest air velocity. Thus, the diameter of the collector is one of the most important parameters which affects directly on the performance of SCPP.



**Figure 4.22:** The influence of SCPP’s collector diameter on its velocity profile for cases 9-13 of Study 4.

The influence of change of SCPP collector’s diameter on the flow pressure is illustrated in Figure 4.23. Due to the outcomes, it is clear that the maximum value of pressure it at the exit of the tower and less value for the pressure occurs at entrance of the collector. For all considered cases, the area which has maximum pressure difference exist at end of the collector and the entrance of the tower. Furthermore, the value of pressure difference is increasing by increasing of collector diameter and this leads to increase of the values of velocity which effects positively on performance of the SCPP.

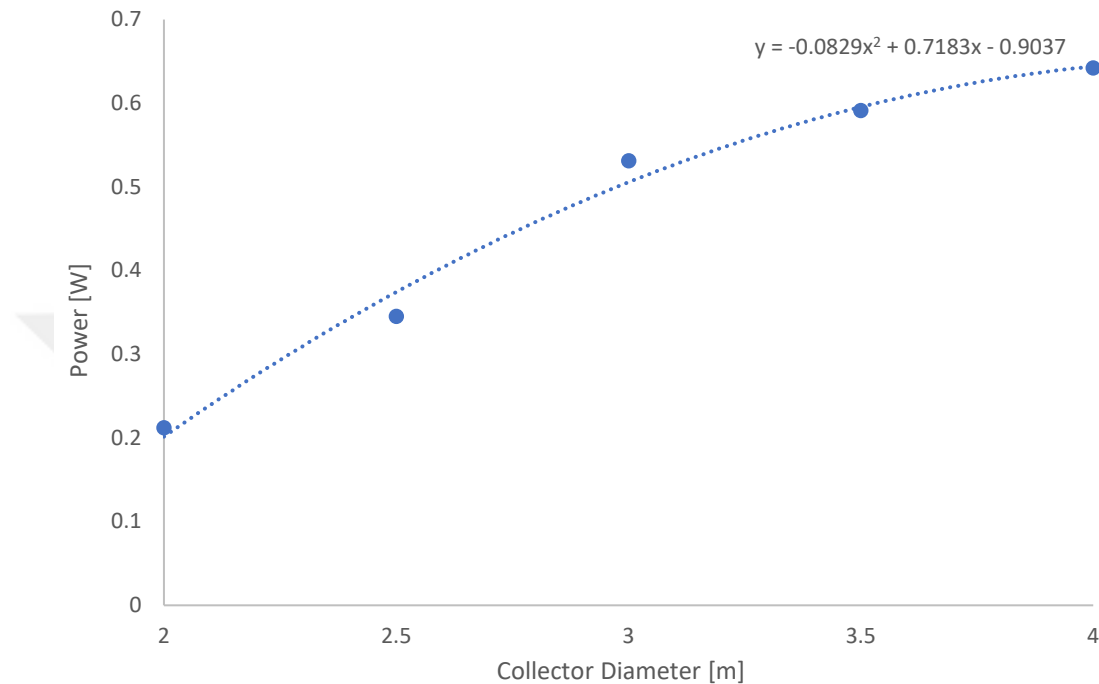




**Figure 4.23:** The simulation results for the static pressure distribution among various collector diameters of the SCPP for cases 9-13 of Study 4.

The impact of changing the solar collector diameter on the output power of SCPP is illustrated in Figure 4.24. Due to findings, it has been noted that there is an increase in the value of energy directly proportional to the increase in diameter of the solar collector. It is also noticeable that the value of the output power of SCPP approaches stability when the value of the diameter of the solar collector reaches 4m (case 13). Therefore, the SCCP collector with 400 cm diameter has better performance in terms

of pressure difference to increase the temperature and velocity of the air for producing power. From the above, it can be concluded that, increasing the diameter of the solar collector is of importance on the efficiency and effectiveness of the solar chimney system, and it can be considered as an important and influential factor in increasing the value of output power of SCPP.

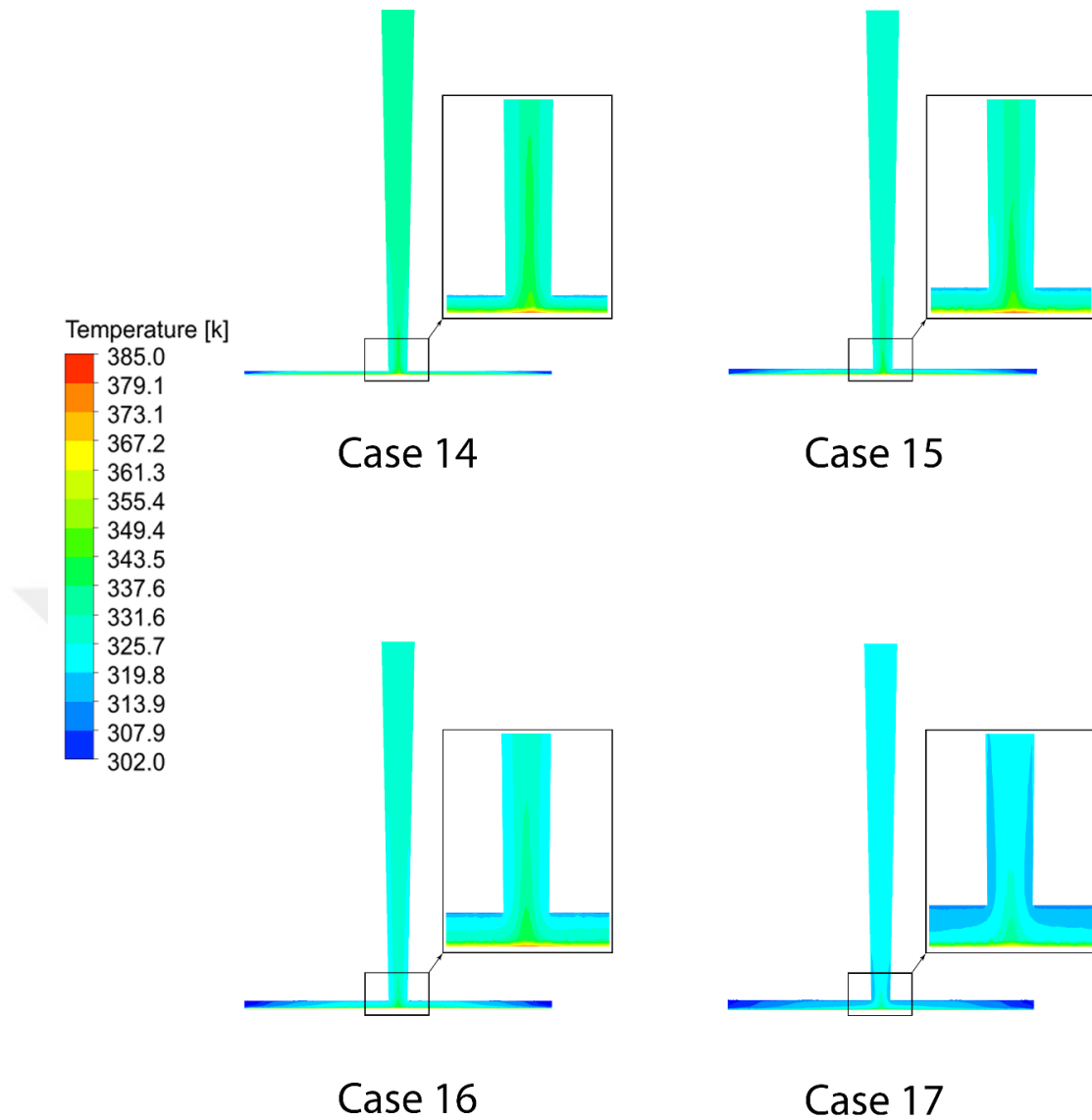


**Figure 4.24:** variation of power with respect to SCPP’s collector diameter.

#### 4.6 Effects of Collector height on SCPP Performance

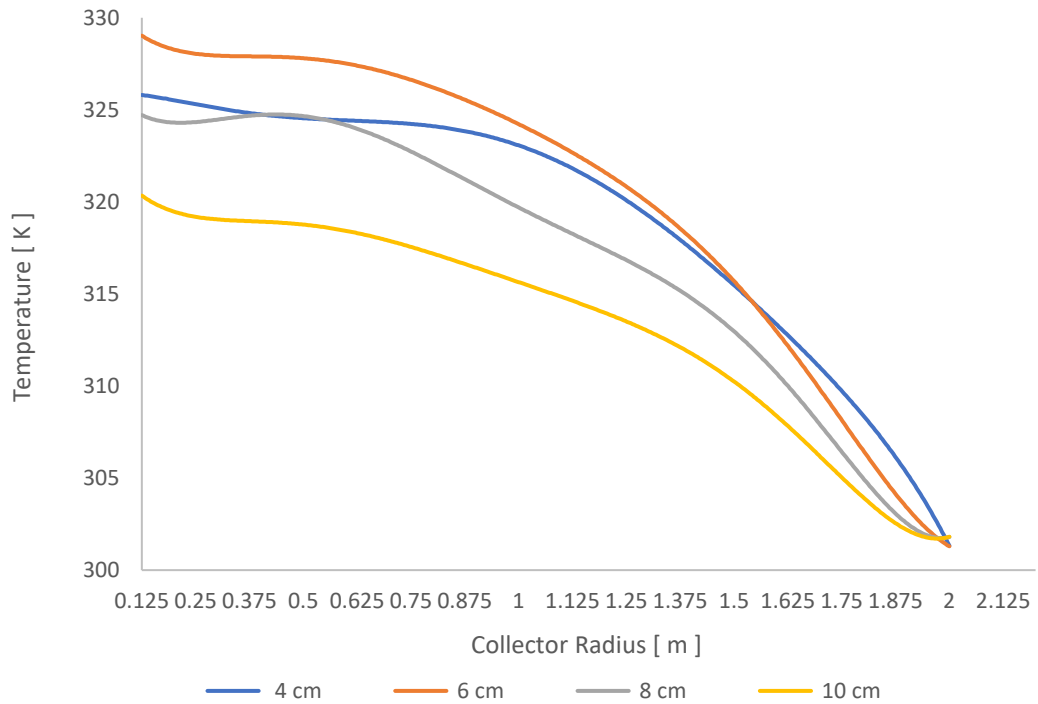
The other parameter which has effect on the performance of the SCPP is the height of the collector. In the following part, four different value are considered as the height of the SCPP’s collector 4, 6, 8 and 10 cm, as shown in Table 3.6.

The influence of change in height of the SCPP’s collector on the temperature of the flow is depicted in Figure 4.25. From these contours, it can be noted that, there are some changes present in temperature distribution through both the solar collector and the tower due to effect of changing height of collector. The height of solar collector effects significantly on the heated area under the solar collector and also on area at the entrance of the tower.



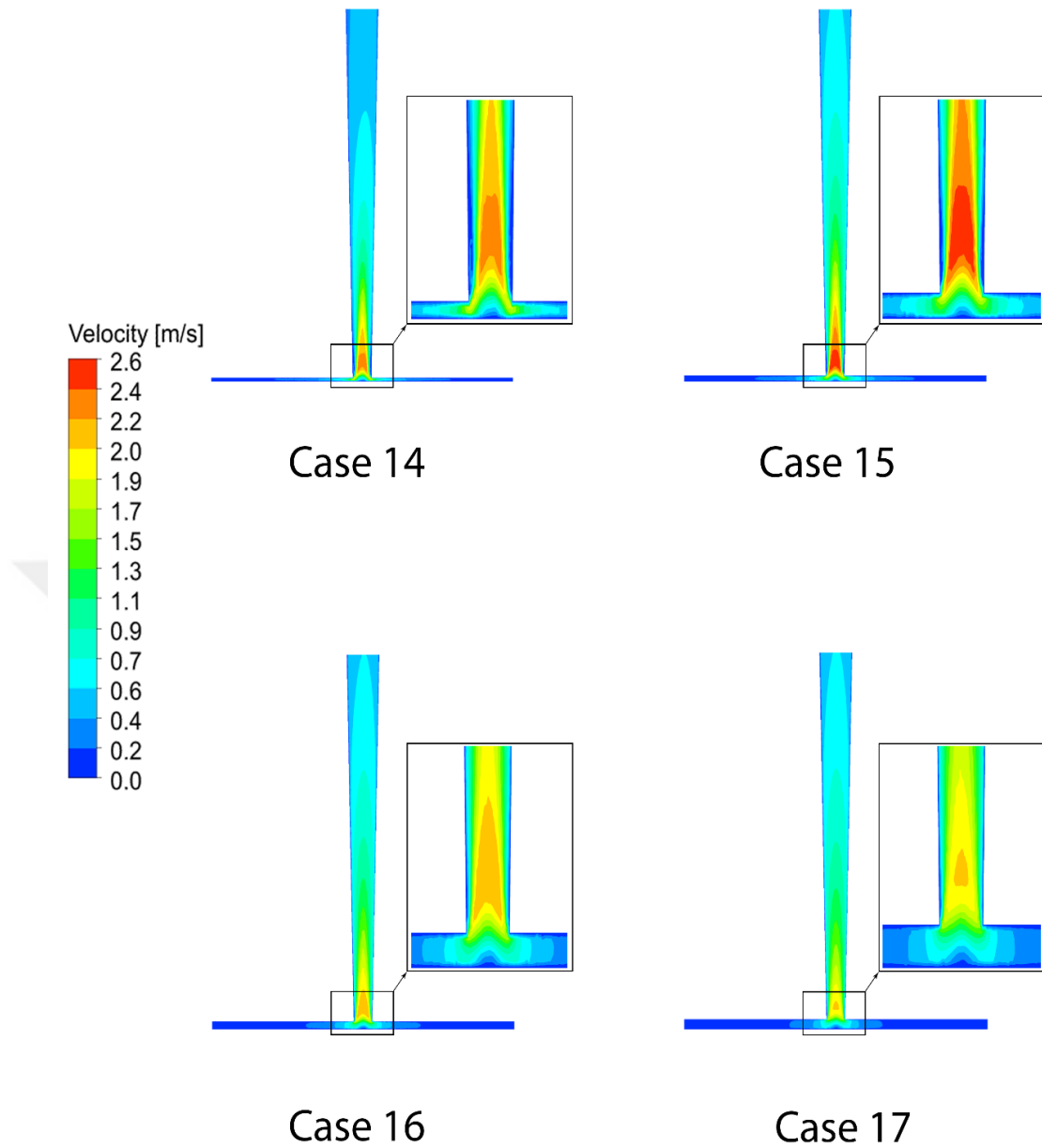
**Figure 4.25:** The simulation results for the air temperature distribution among various collector heights of the SCPP for cases 14-17 of Study 5.

Figure 4.26 represents the impact of changing SCPP's collector height on the air temperature profiles. From Figure 4.26 it has been observed that the temperature distribution is similar for all cases except for collector height equal to 4 cm (case 14). Also, the maximum air temperature differs from case to another and it reaches its maximum value at collector height equal to 6 cm (case 15).



**Figure 4.26:** The influence of SSCP’s collector height on its temperature profile for cases 14-17 of Study 5.

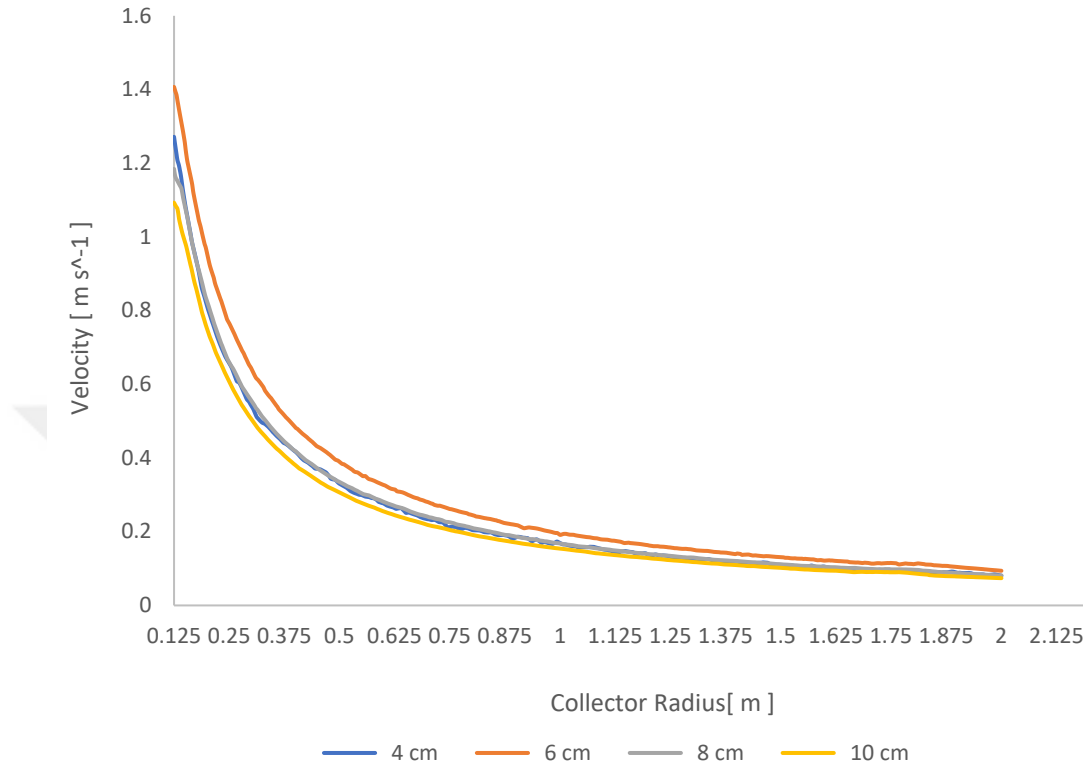
The impact of changing SSCP’s collector height on the air velocity is presented in Figure 4.27. According to the findings, there is no big changes in velocity distribution for collector height 6 cm (case 15), 8 cm (case 16) and 10 cm (case 17) but there is little difference at collector height equal to 4 cm (case 14). Furthermore, the area of the maximum velocity distribution which is located near the inlet of the tower differs with varying of the collector height.



**Figure 4.27:** The simulation results for air velocity distribution among various collector heights of the SCPP for cases 14-17 of Study 5.

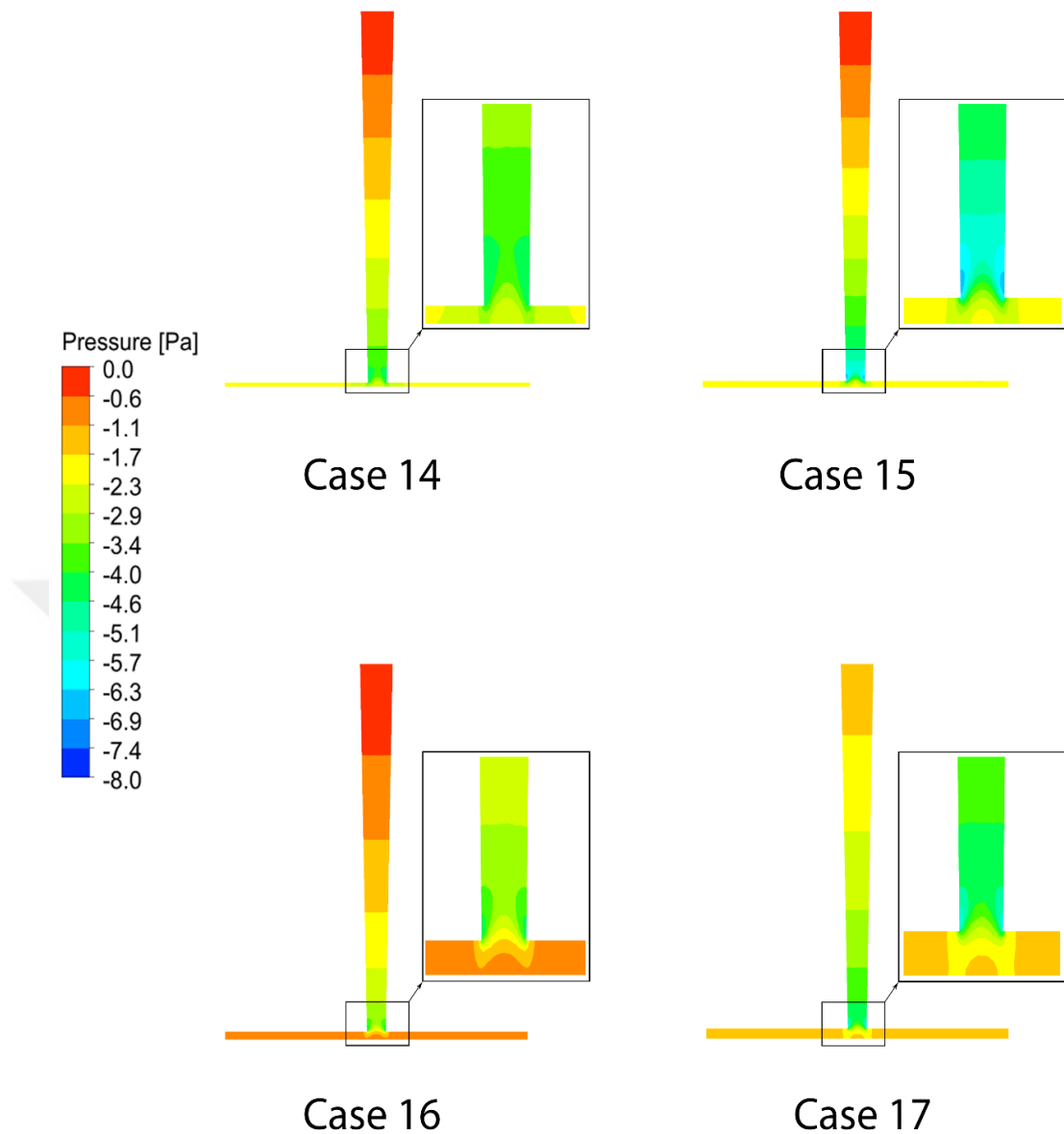
The impact of changing SCPP's collector height on the air velocity is presented in Figure 4.28. As depicted in Figure 28, the velocity profiles indicates that velocity is increasing with increasing collector height until reaching a specific height, than after that value, air velocity starts to drop until reaching minimum value at collector height equal to 10 cm (case 17). For all cases the curves of air velocity is similar, minimum

at the entrance of collector, maximum at end of the solar collector, near the chimney entrance. Due to this findings, the solar collector height has a significant impact on the performance of the solar chimney.



**Figure 4.28:** The influence of SSCP’s collector height on the air velocity profile for cases 14-17 of Study 5.

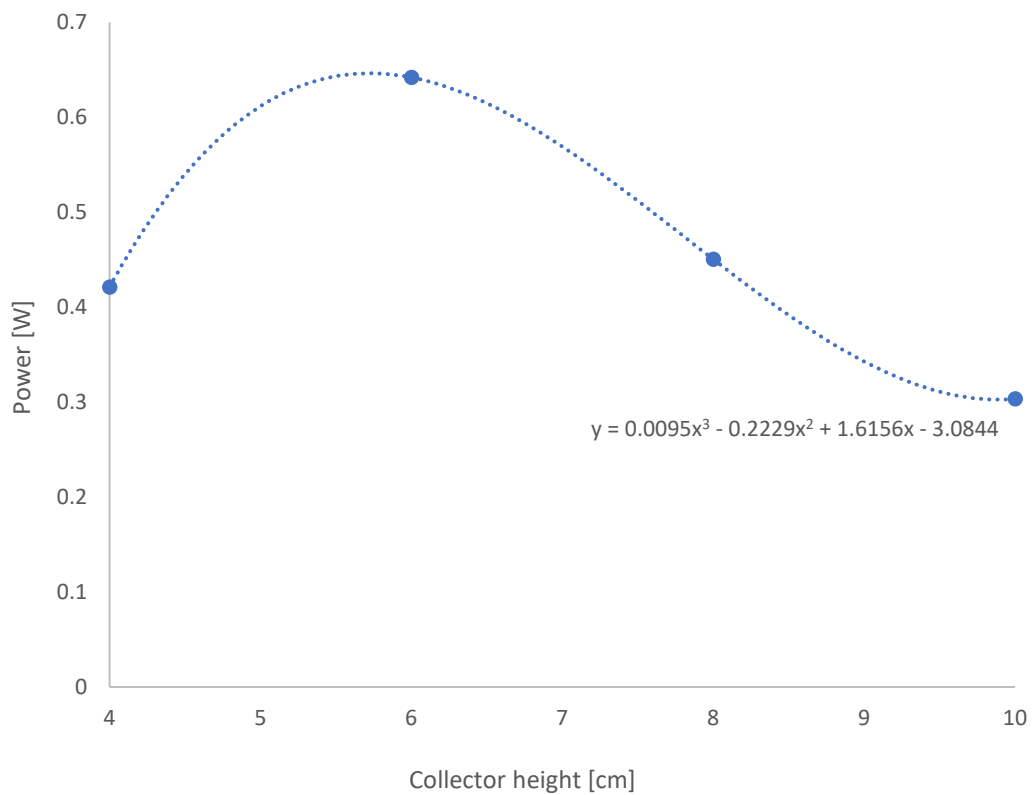
The impact of changing the SSCP collector’s height on the flow pressure is depicted in Figure 4.29. From the results, it has been observed that the maximum pressure value exist at outlet of the tower and less pressure value at inlet of the collector and it is almost uniform along the collector and changes along the tower. Moreover, the biggest pressure difference occurs at area situated at the base of the chimney near to end of the collector. Due to that pressure difference, the air flows from the base of the tower towards chimney exit. Furthermore, the value of the pressure difference is affected by changing collector height and it differs from height to another and it reach the highest value at solar collector height equal to 6 cm (case 15).



**Figure 4.29:** The simulation results for the static pressure distribution among various collector height for cases 14-17 of Study 5.

The influence of changing the height of the SCPP's collector on the temperature of the flow is depicted in Figure 4.30. According to the findings presented in the figure 4.30, the value of output power of SCPP can be affected by the change in the height of the solar collector. There is a best height where the value of output power reaches its highest level and further, it decreases by increasing the height of the solar collector. This leads to the importance of choosing an appropriate height for the solar collector

where the output power value reaches the highest when the height of the solar collector is equal to 6 cm (case 15).



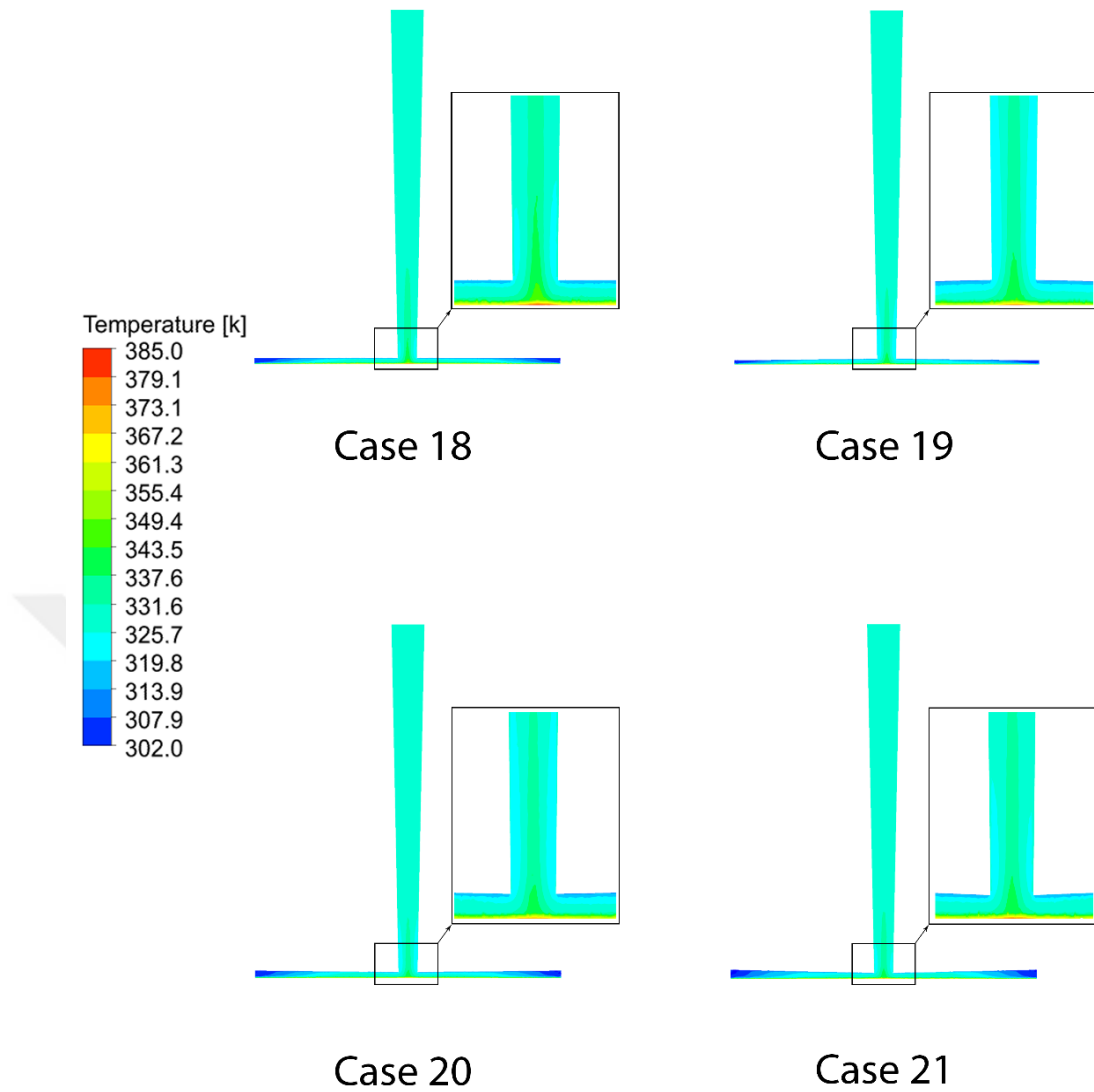
**Figure 4.30:** variation of power with respect to SCPP's collector height.

#### 4.7 Effects of Inclination angle of collector on SCPP Performance

In the following the third collector parameter which can effect on performance of SCPP is studied, which is the inclination angle of the solar collector. It is considered to be an effective one that can make change in the performance of the SCPP. As written in Table 3.7, the inclination angles of the solar collector are considered as 0, 0.5,-0.5 and -1, respectively.

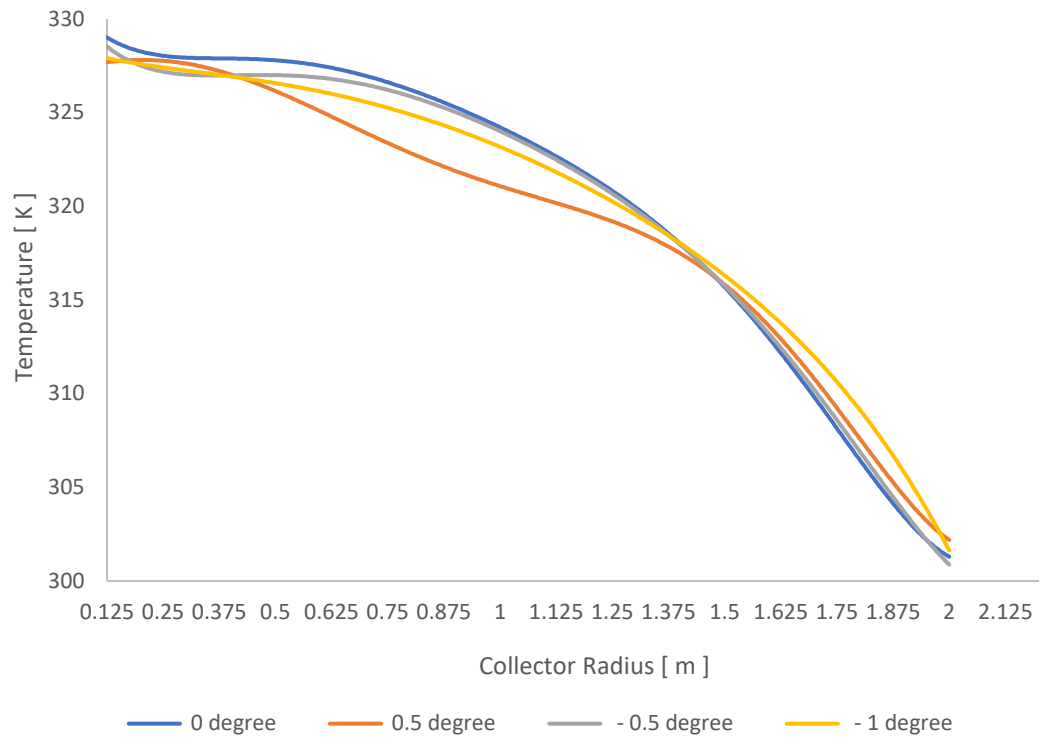
The changes in the temperature of the air flowing inside SCPP based on different inclination angles of the collector roof are presented in Figure 4.31. The findings indicate to presence of same temperature distribution inside the tower for all angles with little difference along the collector. Moreover, the positive and negative angles affected on the temperature distribution at area located in the entrance of the collector and also at area near to collector roof.





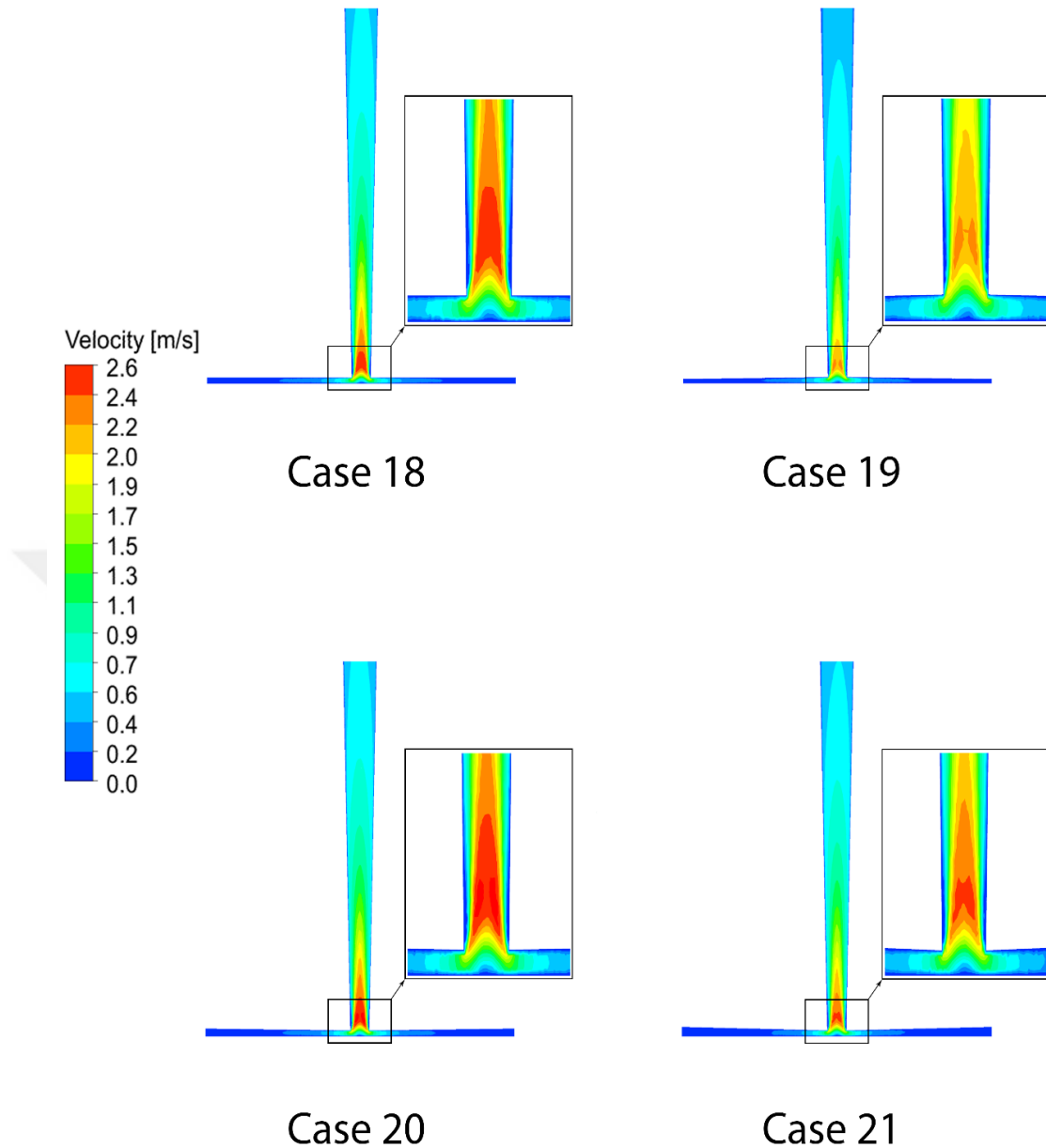
**Figure 4.31:** The simulation results for the air temperature distribution among various collector inclination angles of the SCPP for cases 18-21 of Study 6.

The distribution of air temperature inside SCPP for different inclination angles of the collector roof of the tower are depicted in Figure 4.32. The temperature profiles show similarity in curves expect case 19 which has reduction area at inlet of the collector and that reduction area leads to some changes in temperature profile. Furthermore, for cases 19, 20 and 21, the maximum temperature are almost same for all of them but the highest value of temperature compared to other angles belong to case 18, which has no inclination angle.



**Figure 4.32:** The influence of SCPP’s collector inclination angle on its temperature profile for cases 18-21 of Study 6.

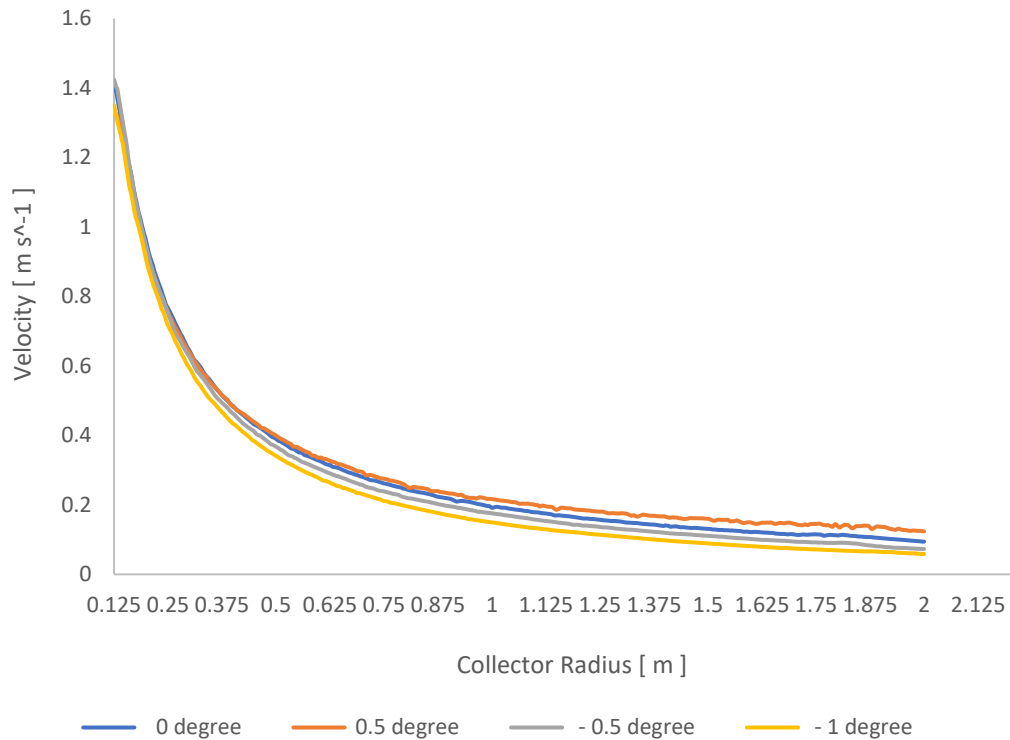
The distribution of air velocity based on different inclination angles of the SCPP’s collector in its contour is illustrated in Figure 4.33. Due to these findings, it is obvious that the area at entrance of tower is affected by changing the slope angle of the collector. Moreover, the temperature distribution along the collector vary with changing inclination angle of the collector and temperature at the end of the tower differs from case to another.



**Figure 4.33:** The simulation results for the flow velocity distribution among various collector inclination angles of the SCPP's or cases 18-21 of Study 6.

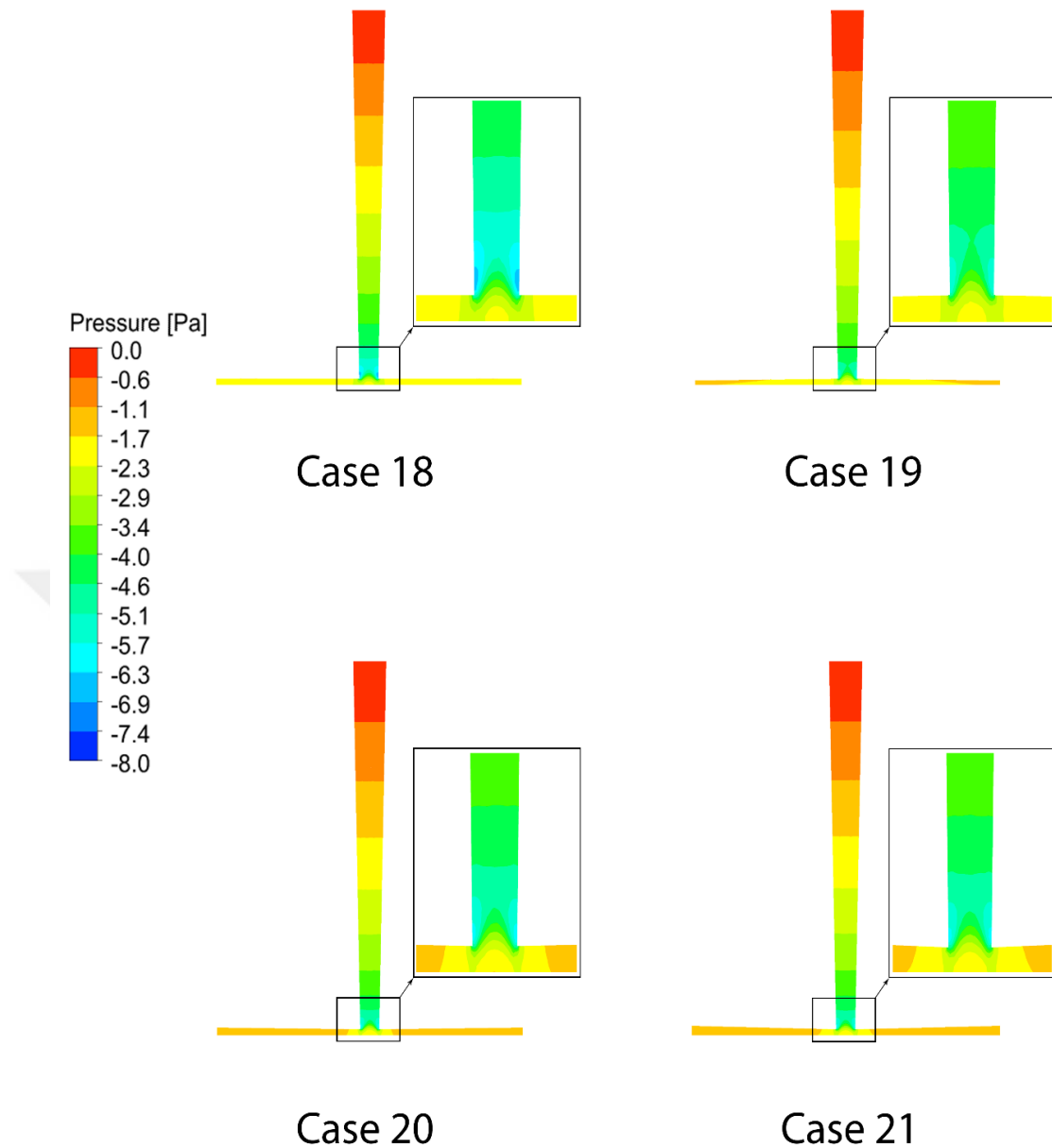
The distribution of the air velocity inside SCPP for different inclination angles of the SCPP's collector is displayed in Figure 4.34. The results indicate the existence of a difference in temperature profiles starting from entrance of the collector until reaching the end of. These changes belongs to impact of collector roof angles on velocity magnitude along the collector and it leads to differences in value of maximum velocity for each case and it reach to highest value at case (20) and minimum value at case (19).

According to above, the inclination angle of the SCPP's collector has an important effect on velocity magnitude of the airflow.



**Figure 4.34:** The influence of SCPP's collector inclination angle on its velocity profile for cases 18-21 of Study 6.

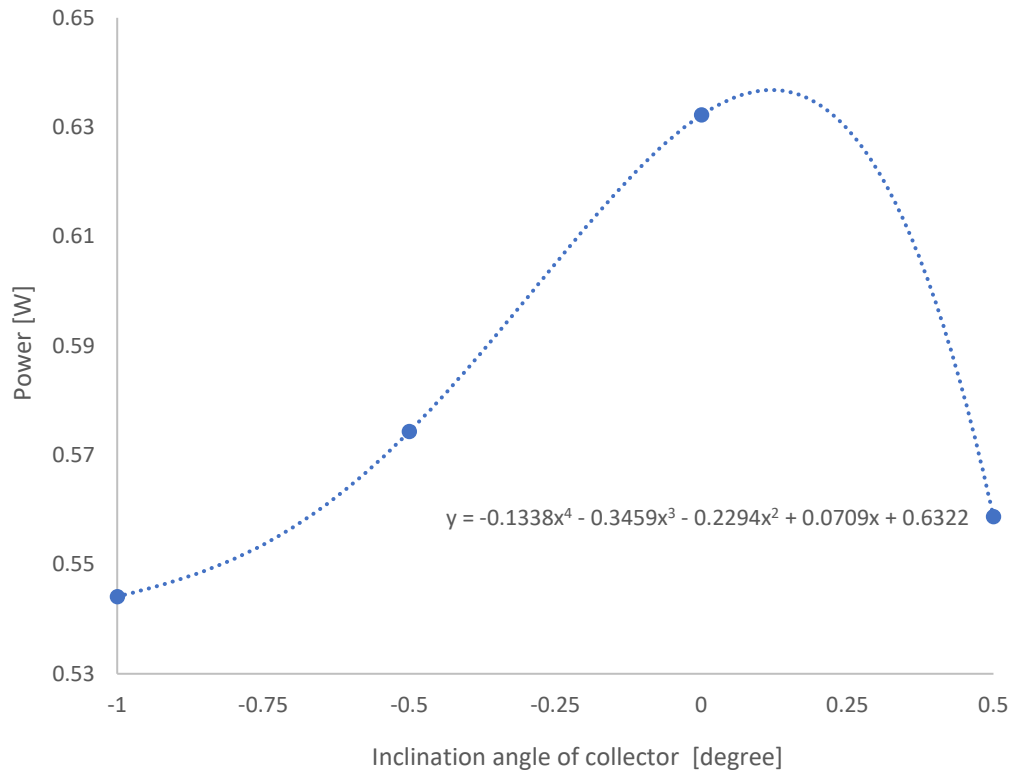
The influence of varying inclination angle of the SCPP's collector on flow pressure is presented in Figures 4.35. According to the results, the depression zone which is located at entrance of tower near to the tower wall varies with changing of inclination angle of the collector. The maximum depression zone happens at case 18 where maximum pressure difference also occurs there. Actually, the pressure difference which is responsible on the air velocity through the SCPP differs from angle to another and the minimum value of it exist at case 19. Furthermore, it has been noticed that the gradient of pressure along the tower is the same for all cases and the value of pressure reaches maximum at the exit of the tower.



**Figure 4.35:** The simulation results for the static pressure distribution among various collector inclination angles of SCPP's for cases 18-21 of Study 6.

The influence of changing the inclination angle of the collector on the output power of SCPP illustrated in Figure 4.36. The findings showed that the output power value is influenced by changing the inclination angle of the solar collector roof. In fact, the change in tilt angle has effects on increasing the value of the output power of the SCPP. Moreover, it was noted that the increase or decrease from the best value of the slope of the solar collector roof is accompanied by a decrease in the value of the output power. In addition, the inclination angle of the collector equal to 0 (case 18) is the best

choice where the output power reaches its maximum value. Furthermore, the results show the importance of the inclination angle of the solar collector roof for the performance and effectiveness of the solar chimney systems.



**Figure 4.36:** variation of power with respect to inclination angle of the S CPP collector.

## CHAPTER 5

### CONCLUSIONS AND FUTURE WORK

#### 5.1 Conclusions

With the increasing demand for renewable energy, especially solar energy, researchers have increased interest for effective renewable energy systems with higher efficiencies and output powers. One of these applications is the solar chimney power plant, which operates by the aid of the buoyancy force and the greenhouse effect and consists of three main elements which are the tower, solar collector and the turbine.

The purpose of this study is to find the best performance and maximum output power value of the solar chimney system by investigating the effect of changing the SCPP's parameters on performance and obtaining a better understanding of the nature of the impact of these parameters on the performance of SCPP.

During the studies done on the parameters that can have direct impact on the performance of the SCPP, the height, diameter and geometry of the SCPP's chimney and the height, diameter and the inclination angle of the SCPP's collector and the different configurations of the SCPP are considered.

According to the obtained results, the performance of the SCPP increases by increasing the height of the chimney till specific point of height. If the height increases more than that point, then the performance of the SCPP rises slightly. In this research four values are considered for as 3m (case 1), 1.5m (case 2), 2.5m (case 3) and 3.5m (case 4). According to the obtained results the best performance was achieved from the SCPP which has 3.5 (case 4) meter chimney height. Based on the simulation results for the proposed case, the pressure value is less than the other ones, while the velocity and temperature were higher than the others. It can be concluded that, there is a feasible height value which can be determined for a good cost-performance depending on numerical simulations and the trend of the power curve in Figure 4.6.

The other parameter which has been assessed to find the best condition for the SCPPs performance was the diameter of SCPP's chimney. The study of changing the diameter of the SCPPs' chimney shows that there is a best diameter value. By increasing the tower diameter the performance of the SCPP increases, but if the chimney diameter increase more than critical tower diameter (best value), then it has negative effect on the performance of the SCPPs. Simulations have been done for five different diameter value, 20 cm (case 5), 15 cm (case 6), 25 cm (case 7) and 35 cm (case 8). Based on the obtained results the performance of the studied SCPP with the 25 cm (case 7) diameter was better than the others.

Analyzing the geometry of the SCPP's tower can be considered as one of the best methods to find a way for increasing the efficiency of SCPP. The different structure of the chimney can make changes in the power and performance of SCPPs. In this research four structure of the SCPPs' chimneys are analyzed. The chimneys configurations which are analyzed are, standard chimney (case a), diverging chimney (case b), converging-diverging chimney (case c) and standard-diverging chimney (case d). According to the proposed simulation results, the diverging chimney (case b) has the best performance compared to the other ones as explained in the previous parts.

Besides the tower, the SCPPs' collector dimensions have effect on the performance of the SCPPs. In this research three features of the SCPPs' collectors which have direct influence on the efficiency are analyzed and simulated; the height, diameter and inclination angle of the collector. In the first step, five values are considered as the diameter of the studied SCPP's collector, 200 cm (case 9), 250 cm (case 10), 300 cm (case 11), 350 cm (case 12) and 400 cm (case 13). According to the obtained simulation results, the collector with 400 cm diameter (case 13), decreased the pressure and increased the flow velocity and temperature better than the other ones, which caused the improvement in the performance of the SCPP. Among the study, depending on the simulation results, it can be concluded that, as long as cost performance is considerable and there is enough space, the collector diameter value can be increased for a good performance.

Furthermore, the four values have been considered as the different heights of the SCPP collector for simulation, 4 cm (case 14), 6 cm (case 15), 8 cm (case 16) and 10 cm (case 17). According to the achieved results, the SCPP's with the collector that has 6



cm height (case 15), has found to have better performance compare to the others. In this case, the temperature of the flow was more than the other analyzed cases. The collector height has an important effect and there is a best point for the best performance, which can be found by numerical simulations. Moreover, the results of simulation of the inclination angle of the studied SCPP, shows that the collector with zero inclination angle (case 18) has better performance compare to the ones which had 0.5 (case 19), -0.5 (case 20) and -1 (case 21).

As a sum up, according to the simulation results, an best SCPP which is to be built as a future work for the studies, based on the considered ranges of changes in its structure should have the following features

- ❖ 3.5 m chimney height (case 4).
- ❖ 25 cm chimney diameter (case 7).
- ❖ Diverging chimney geometry (case b).
- ❖ 400 cm diameter of the collector (case 13).
- ❖ 6 cm height of the collector (case 15).
- ❖ The Zero inclination angle for the collector (case 18).

## 5.2 Recommendations for Future Work

- Finding the best divergence angle of the tower and making a study to calculate the variations of the output power and the efficiency of SCPP during the day and for several days during the year and study in details the impact of the variations of solar radiation values during the day on the output power values.
- Making an experimental work based on the best parameters which are obtained from the CFD numerical findings, and comparing the experimental results with the numerical results and examining how the results match each other. Also the

experimental prototype can contain a wind turbine and study the design of the turbine and its effect on performance of SCPP.

- Constructing of solar chimney power plant with hybridization techniques and study the effects of using these techniques on the performance of SCPP. Also energy storage systems can be used in the solar chimney power plant and it can be modified to get maximum power. Furthermore, other renewable energy systems can be used as a hybrid system and get benefit from using these systems to maximize the output power of SCPP.
- Performing comprehensive feasibility and economical studies on the cost of power production using large-scale solar chimney power plants, also working on reduce the cost of construction of these power plants and utilizing modern construction techniques to obtain higher efficiency and lower cost to build an effective solar chimney power plants.

## REFERENCES

- [1] Ghalamchi, M., Kasaeian, A., Ghalamchi, M., & Mirzahosseini, A. H. (2016). An experimental study on the thermal performance of a solar chimney with different dimensional parameters. *Renewable Energy*, 91, 477-483.
- [2] Schneider, S. H. (2001). What is 'dangerous' climate change?. *Nature*, 411(6833), 17.
- [3] Dhahri, A., & Omri, A. (2013). A review of solar chimney power generation technology. *International Journal of Engineering and Advanced Technology*, 2(3), 1-17.
- [4] Al-Kayiem, H. H., & Aja, O. C. (2016). Historic and recent progress in solar chimney power plant enhancing technologies. *Renewable and Sustainable Energy Reviews*, 58, 1269-1292.
- [5] T. Hamilton, *Mad Like Tesla: Underdog Inventors and Their Relentless Pursuit of Clean Energy*. ECW Press, pp.93-103, 2011.
- [6] W. Ley, *Engineers' dreams*. Viking Press, 1954.
- [7] Kasaeian, A. B., Molana, S., Rahmani, K., & Wen, D. (2017). A review on solar chimney systems. *Renewable and Sustainable Energy Reviews*, 67, 954-987.
- [8] Schlaich, J., Bergemann, R., Schiel, W., & Weinrebe, G. (2005). Design of commercial solar updraft tower systems—utilization of solar induced convective flows for power generation. *Journal of Solar Energy Engineering*, 127(1), 117-124.
- [9] Haaf, W., Friedrich, K., Mayr, G., & Schlaich, J. (1983). Solar chimneys part I: principle and construction of the pilot plant in Manzanares. *International Journal of Solar Energy*, 2(1), 3-20.

- [10] Haaf, W. (1984). Solar chimneys: part ii: preliminary test results from the Manzanares pilot plant. *International Journal of Sustainable Energy*, 2(2), 141-161.
- [11] Solar updraft tower – Wikipedia. [https://en.wikipedia.org/wiki/Solar\\_updraft\\_tower](https://en.wikipedia.org/wiki/Solar_updraft_tower) (Access Date: 19.08.2019).
- [12] Wolf, M. I. (2008). Solar updraft towers: their role in remote on-site generation.
- [13] Dai, Y. J., Huang, H. B., & Wang, R. Z. (2003). Case study of solar chimney power plants in Northwestern regions of China. *Renewable Energy*, 28(8), 1295-1304.
- [14] Nizetic, S., Ninic, N., & Klarin, B. (2008). Analysis and feasibility of implementing solar chimney power plants in the Mediterranean region. *Energy*, 33(11), 1680-1690.
- [15] Hamdan, M. O. (2011). Analysis of a solar chimney power plant in the Arabian Gulf region. *Renewable Energy*, 36(10), 2593-2598.
- [16] Larbi, S., Bouhdjar, A., & Chergui, T. (2010). Performance analysis of a solar chimney power plant in the southwestern region of Algeria. *Renewable and Sustainable Energy Reviews*, 14(1), 470-477.
- [17] Zhou, X., Wang, F., Fan, J., & Ochieng, R. M. (2010). Performance of solar chimney power plant in Qinghai-Tibet Plateau. *Renewable and Sustainable Energy Reviews*, 14(8), 2249-2255.
- [18] Najmi, M., Nazari, A., Mansouri, H., & Zahedi, G. (2012). Feasibility study on optimization of a typical solar chimney power plant. *Heat and Mass Transfer*, 48(3), 475-485.
- [19] Sangi, R. (2012). Performance evaluation of solar chimney power plants in Iran. *Renewable and Sustainable Energy Reviews*, 16(1), 704-710.
- [20] Asnaghi, A., & Ladjevardi, S. M. (2012). Solar chimney power plant performance in Iran. *Renewable and Sustainable Energy Reviews*, 16(5), 3383-3390.
- [21] Ayadi, A., Driss, Z., Bouabidi, A., Nasraoui, H., Bsisa, M., & Abid, M. S. (2018). A computational and an experimental study on the effect of the chimney height on the thermal characteristics of a solar chimney power plant. *Proceedings of the Institution*

of Mechanical Engineers, Part E: Journal of Process Mechanical Engineering, 232(4), 503-516.

[22] Zhou, X., Yang, J., Xiao, B., Hou, G., & Xing, F. (2009). Analysis of chimney height for solar chimney power plant. *Applied Thermal Engineering*, 29(1), 178-185.

[23] Kasaeian, A., Ghalamchi, M., & Ghalamchi, M. (2014). Simulation and optimization of geometric parameters of a solar chimney in Tehran. *Energy conversion and management*, 83, 28-34.

[24] Maia, C. B., Ferreira, A. G., Valle, R. M., & Cortez, M. F. (2009). Theoretical evaluation of the influence of geometric parameters and materials on the behavior of the airflow in a solar chimney. *Computers & Fluids*, 38(3), 625-636.

[25] Hu, S., Leung, D. Y., & Chan, J. C. (2017). Numerical modelling and comparison of the performance of diffuser-type solar chimneys for power generation. *Applied energy*, 204, 948-957.

[26] Bouabidi, A., Ayadi, A., Nasraoui, H., Driss, Z., & Abid, M. S. (2018). Study of solar chimney in Tunisia: Effect of the chimney configurations on the local flow characteristics. *Energy and Buildings*, 169, 27-38.

[27] Toghraie, D., Karami, A., Afrand, M., & Karimipour, A. (2018). Effects of geometric parameters on the performance of solar chimney power plants. *Energy*, 162, 1052-1061.

[28] Li, J. Y., Guo, P. H., & Wang, Y. (2012). Effects of collector radius and chimney height on power output of a solar chimney power plant with turbines. *Renewable Energy*, 47, 21-28.

[29] Hassan, A., Ali, M., & Waqas, A. (2018). Numerical investigation on performance of solar chimney power plant by varying collector slope and chimney diverging angle. *Energy*, 142, 411-425.

[30] Al-Dabbas, A. M. (2011). A performance analysis of solar chimney thermal power systems. *Thermal Science*, 15(3), 619-642.

[31] Zhou, X., Yang, J., Xiao, B., Hou, G., & Xing, F. (2009). Analysis of chimney height for solar chimney power plant. *Applied Thermal Engineering*, 29(1), 178-185.

- [32] Nizetic, S., & Klarin, B. (2010). A simplified analytical approach for evaluation of the optimal ratio of pressure drop across the turbine in solar chimney power plants. *Applied Energy*, 87(2), 587-591.
- [33] Kasaeian, A., Mahmoudi, A. R., Astarai, F. R., & Hejab, A. (2017). 3D simulation of solar chimney power plant considering turbine blades. *Energy Conversion and Management*, 147, 55-65.
- [34] Thakre, S. B., Bhuyar, L. B., Dahake, S. V., & Wankhade, P. (2013). Mathematical Correlations Developed For Solar Chimney Power Plant – A Critical Review. *Global Journal of Research In Engineering*.
- [35] Ming, T. (Ed.). (2016). *Solar chimney power plant generating technology*. Academic Press.
- [36] Cebeci, T., Shao, J. P., Kafyeke, F., & Laurendeau, E. (2005). *Computational fluid dynamics for engineers*. Springer Berlin Heidelberg.
- [37] Rao, J. S. (2017). *Simulation based engineering in fluid flow design*. Springer.
- [38] D'Auria, F. (Ed.). (2017). *Thermal-Hydraulics of Water Cooled Nuclear Reactors*. Woodhead Publishing.
- [39] Wilcox, D. C. (2008). Formulation of the kw turbulence model revisited. *AIAA journal*, 46(11), 2823-2838.
- [40] Menter, F. R. (1994). Two-equation eddy-viscosity turbulence models for engineering applications. *AIAA journal*, 32(8), 1598-1605.
- [41] Ayadi, A., Nasraoui, H., Bouabidi, A., Driss, Z., Bsis, M., & Abid, M. S. (2018). Effect of the turbulence model on the simulation of the air flow in a solar chimney. *International Journal of Thermal Sciences*, 130, 423-434.
- [42] FLUENT, ANSYS Fluent User Guide- FLUENT 18.2.
- [43] Bouabidi, A., Nasraoui, H., Ayadi, A., Driss, Z., & Abid, M. S. (2019). Numerical analysis of chimney diameter effect on the fluid flow and the heat transfer characteristics within the solar tower. *Energy Sources, Part A: Recovery, Utilization, and Environmental Effects*, 1-13.

- [44] Hu, S., Leung, D. Y., & Chan, J. C. (2017). Numerical modelling and comparison of the performance of diffuser-type solar chimneys for power generation. *Applied energy*, 204, 948-957.
- [45] Das, P., & Chandramohan, V. P. (2019). Computational study on the effect of collector cover inclination angle, absorber plate diameter and chimney height on flow and performance parameters of solar updraft tower (SUT) plant. *Energy*, 172, 366-379.
- [46] Ayadi, A., Bouabidi, A., Driss, Z., & Abid, M. S. (2018). Experimental and numerical analysis of the collector roof height effect on the solar chimney performance. *Renewable energy*, 115, 649-662.
- [47] Ayadi, A., Driss, Z., Bouabidi, A., & Abid, M. S. (2017). Experimental and numerical study of the impact of the collector roof inclination on the performance of a solar chimney power plant. *Energy and Buildings*, 139, 263-276.